ADDIS ABABA UNIVERSITY
SCHOOL OF GRADUATE STUDIES
DEPARTMENT OF EARTH SCIENCES

GIS – BASED GROUNDWATER VULNERABILITY MAPPING OF ATEBELA RIVER CATCHMENT, SEBETA AREA

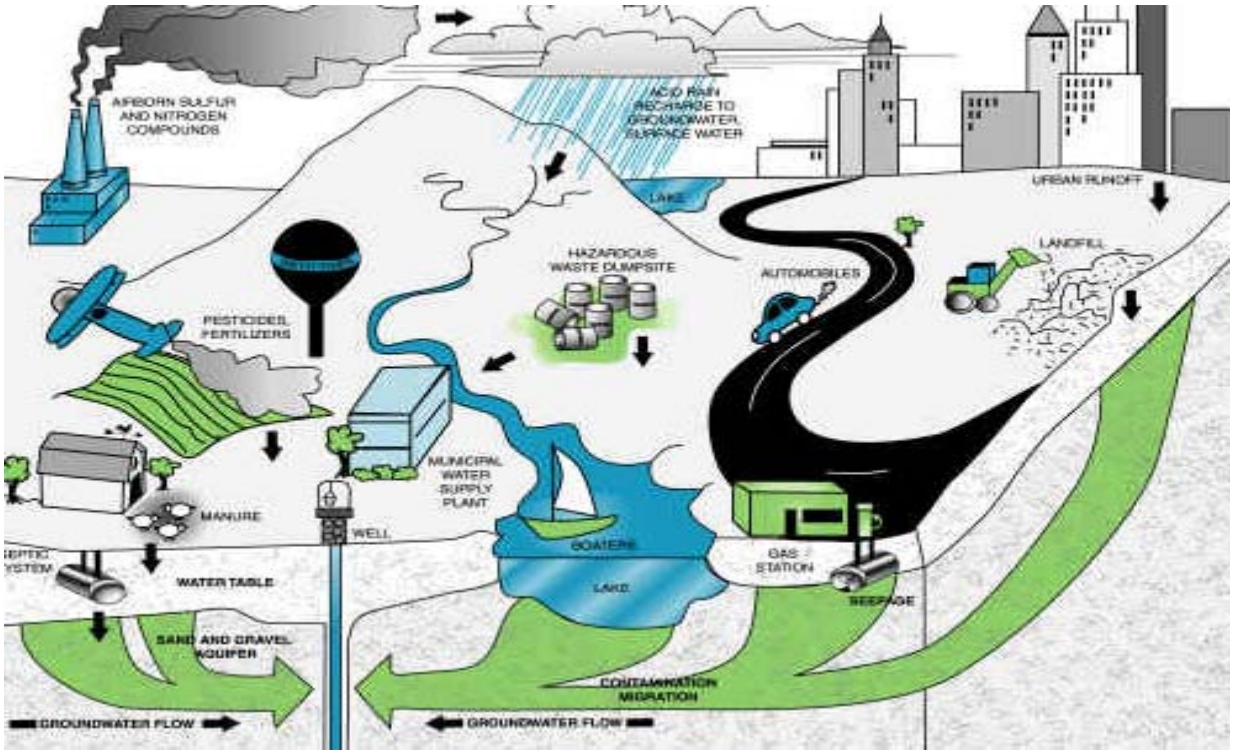

A THESIS SUBMITTED TO THE SCHOOL OF GRADUATE STUDIES IN PARTIAL FULFILIMENT FOR THE DEGREE OF MASTER OF SCIENCE IN HYDROGEOLOGY

BY

SOLOMON KENEA

JULY, 2007
ADDIS ABABA

DECLARATION

I, the undersigned, declare that this thesis is my original work, and has not been presented for a degree on any other university.

All sources of materials used for the thesis have been duly acknowledged.

SOLOMON KENEA

Signature_____

Place and date of submission: School of Graduate Studies, Addis Ababa University, July, 2007

The thesis has been submitted for examination with my approval as university advisor.

Tamiru Alemayehu (PhD) _____

This research work is dedicated to my family and those who are engaged in the protection of groundwater.

Solomon Kenea
2007

ABSTRACT

This research work which focuses on Atebela groundwater catchment found in Sebeta–Alemgena area applied the DRASTIC MODEL to the assessment of groundwater vulnerability to contamination. The area is characterized by recently expanding industrial activities around Sebeta town and modern and traditional agricultural practices all around which have polluting potential of the groundwater system. Both intrinsic vulnerability and specific vulnerability assessment and mapping are conducted in the objective of classifying vulnerable and non vulnerable areas, and to provide zoning for groundwater protection.

The mapping process involved GIS (ArcGIS 9.1 software) application and model builder extension in ERDAS 8.6 software. The specific vulnerability of groundwater to nitrate contamination and hazard centers was assessed and mapped. The vulnerability maps are presented in a clear and easily understandable format for the use by policy makers. These maps are useful to develop an appropriate legislative framework for the protection and sustainable use of the groundwater resources and for water pollution prevention of the groundwater of Atebela River catchment. Therefore, the vulnerability maps can be one tool that helps to achieve the Millennium Development Goals (“ensure environmental sustainability”).

Keywords: DRASTIC Model, intrinsic vulnerability, specific vulnerability, nitrate contamination, hazard centers, GIS mapping.

TABLE OF CONTENTS

Source of cover page design -
http://www.groundwater.org/gi/sourcesofgwcontam.html

LIST OF FIGURES

LIST OF TABLES

LIST OF SYMBOLS AND ACRONYMS

m	meter
l/s	liter per second
m/s	meter per second
mg/l	milligram per liter
pH	hydrogen ion activity
mm	millimeter
EC	electrical conductivity
TDS	total dissolved solids
R	recharge value
LU/LC	land use/land cover
UK-GWF	United Kingdom Groundwater Forum
WHO	World Health Organization
GIS	Geographic Information System
PPT	precipitation
PET	potential evapotranspiration
AET	actual evapotranspiration
SRO	surface runoff
ΔG	change in groundwater level or recharge
W	withdrawal
Q	discharge
K	runoff coefficient
SW	shallow wells
HDW	hand dug wells
DW	deep wells
SP	spring
MCM	million cubic meters
M. Max. T.	mean maximum temperature
M. Min. T.	mean minimum temperature
M. Mon. T.	mean monthly temperature
OBS	observatory
MDR	moderately deep rooted
DR	deep rooted
MF	moderately deep rated

LIST OF ANNEXES

ACKNOWLEDGMENT

In the first place, my gratitude goes to my advisor Dr. Tamiru Alemayehu, Addis Ababa University who was consistently following up and guiding me in every step of my work. His encouragements, comments and suggestions were important in giving strength and fulfillment to my mission of thesis writing. In addition, I would like to mention that it was impossible to accomplish it, if he had not provided me with important reading materials and field equipments.

I would like to appreciate Dr. Tarun Raghuvanshi, Addis Ababa University for his devotedness towards his students as a whole and in particular to me always cooperative and ready to help.

My sincere thanks go to my organization Woliso District Water Resources Office for allowing and sponsoring me to do my masters study and I am grateful to my colleagues for their encouragements. The Southwest Shewa Zone Water Resources Office deserves my admiration for the support and provision they have rendered me during my field work. I also thank the Oromia Water Resources Bureau for the financial support and allowing me to use the Water Analysis Laboratory. I am also indebted to the workers of Sebeta-Awas Water Resources Office for their support in field data collection.

I extend my gratefulness to Oromia Mineral Resources Development Agency for giving me geological information of the study area. My heartfelt thanks are to Water Works Design and Supervision Enterprise for providing me borehole data for my study area. The staffs of the Ministry of Water and the Ethiopian Meteorological Services Agency are appreciated for providing me with the required data. I would like to extend my thanks to my friend Meresa Kiros who gave me his thesis work in Dire Dawa which guided me in my research. My

special gratitude is to Dereje Nigussa for his help in the first steps to the field work.

I am always thankful to my father Kenea Aga, my mother Yenealem Wubneh, my sisters Meaza Kenea, Derartu Kenea and Bilise Kenea and my brother Adugna Kenea for their continued care and love, support and encouragement. I express my sincere thanks to my nephews Solomon Benti and Temesgen Benti and their families as a whole for their contribution to the success of my research work.

I am grateful to my classmates who are always willing to share their knowledge and experiences wholeheartedly, and their memories of good times spent together are remembered. I sincerely acknowledge my friend Biniam Teshale for his help in mapping my study area using GIS. My gratitude is to Aychelum Debebe for his encouragements and advices during my study.

My good friends Frehiwot Wubshet, Selamawit Hailu, Megersa Negera, Debela Yosef, Meseret Hailu, Kena Eba and Kebede Hailemariam who were consistently following up on me, supported me prayerfully being at my side during my studies and constantly encouraging me in the hardships I was facing deserve my heartfelt thanks.

Everyone who has in one way or the other contributed to the success of this research work is highly appreciated.

Lastly, I give all the glory and respect to my **LORD JESUS CHRIST** for everything.

CHAPTER I

1. INTRODUCTION

1.1 GENERAL

Groundwater is the safest in terms of quality, cheapest in terms of capturing, treating and piping and sustainable in terms of responding slowly to changes in rainfall conditions and being available during the summer and droughts as compared to surface water (UK-GWF, 2004). The quality of groundwater is usually very good under natural conditions. It does normally require much less treatment than river water to make it safe to drink. The soil and rocks through which the groundwater flows helps to remove pollutants. Since surface water is becoming highly susceptible to pollution and drying from time to time as the demand of water utilization for domestic, municipal, industrial, and irrigation has increased, the trend for production of groundwater for the same purposes is growing. As a result, the pressure on the utilization of groundwater has led to its vulnerability to depletion and contamination due to over-pumping and release of contaminants through several activities caused by human beings as well as natural factors. The problem stems partly from land-based development and industry and partly from over-pumping. Every factor, which is artificial, is directly or indirectly causing an impact on groundwater exploitation.

Clean groundwater is needed for more than drinking purposes. Agriculture depends heavily on groundwater for irrigation. Poor or contaminated groundwater could jeopardize crops and threaten the health of livestock. Clean groundwater is also essential to clean surface water, i.e. it supports rivers, lakes and wetlands, especially through drier months when there is little direct input from rainfall. Groundwater is connected to surface water in the hydrologic cycle, and some aquifers actually feed springs and rivers.

Groundwater pollution sources could be point source or diffuse source (Robins, 1998). Disposal of oils, solvents, chemical waste, leachate from waste disposal sites, herbicide use, could be some of the point sources of pollution, where as railways,

roads and airfields are line sources of pollution. Nitrate from agricultural practices and agriculture pesticides and urban pollution from leaking sewers, drains, etc are also diffuse sources of pollutions (Meresa Kiros, 2006).

Polluted or contaminated groundwater needs remediation for sustainable use but remedial techniques are costly and the application of the methods take a very long time until the quality of the groundwater is maintained. Instead, prevention of the susceptibility of groundwater to contamination is the best solution to the sustainable use of groundwater for drinking or other activities. Protection of groundwater from contamination requires knowledge and understanding of the aquifers vulnerability to contamination and the different geological factors that could either provide protective cover or facilitate contaminant transport. Therefore, groundwater vulnerability maps are an essential groundwater protection schemes and a valuable tool in environmental management.

1.2 PREVIOUS WORKS

There is no detail work done on groundwater to mention in the study area. Generally, published researches and scientific exercises within the study area could not be found posing a lack in detail and sub-detail information.

But the work of Deshu Mamo, 2004 on assessment of pollution of Sebeta River is one contribution. This study covers only a very small part of the catchment, about 10 km^2 and it strictly deals only with the pollution of the surface water and soils in and around Sebeta town.

The construction rock materials study project conducted by Oromia Mineral Resources Development Agency, written by Gelana Gadissa, 2005 with the title of Geology and Construction Rock Materials of Areas around Finfinne is one of the studies conducted in the study area and the surrounding.

Concerning the title of this particular research, only few works can be mentioned to be performed in the country. The first one is the work of Dereje Nigussa, 2003 the title of which is GIS Based Groundwater Vulnerability Assessment in Akaki River Catchment, Addis Ababa, Central Ethiopia. It has applied DRASTIC model and it deals more on the intrinsic vulnerability mapping of Addis Ababa.

The second work to mention is that of Tamiru Alemayehu et al. (2005), with the title of Hydrogeology, Water Quality and the Degree of Groundwater Vulnerability to Pollution in Addis Ababa, Ethiopia. This work has applied the DRASTIC model and has shown both the intrinsic vulnerability of the area and specific vulnerability assessment for population density and hazard centers such as industries and health centers.

Lastly, the work of Meresa Kiros (2006) goes beyond Addis Ababa i.e. Dire Dawa. His title is GIS-based Vulnerability and Hazard Mapping for the Protection of Dire Dawa Groundwater Basin, Ethiopia. He applied the European approach (PI and COP methods) to produce the intrinsic, specific and hazard vulnerability maps of Dire Dawa town. He has assessed the specific vulnerability of groundwater to contamination for nitrate.

1.3 STATEMENT OF THE PROBLEM

The research site, Sebeta – Alem Gena area, located at about 30km from Addis Ababa, is developing to an industrialized zone. The Regional Government of Oromia is operating targeting Sebeta Town and its surrounding as an investment center for industrial and agricultural development. Most of the activities carried out are a threat to the groundwater since the industries (tannery, alcohol factories, brewery, soap factory, etc) release the effluents into the rivers. In addition, the modern agricultural practices (including flower farming) with the application of fertilizers and pesticides are causes of groundwater pollution. Many boreholes are found within the study area especially in the towns of Sebeta and Alemgena. The combined effect of over-pumping of the groundwater with its contamination needs attention.

1.4 OBJECTIVES OF THE STUDY

Once groundwater is contaminated by chemical or biological materials, it is costly and time consuming to remediate it. However, it is possible to prevent groundwater before it is being contaminated and thereby improving the quality of groundwater by controlling the input of pollutants. Generally, the objective of this research work is to produce the groundwater vulnerability map of Atebela Catchment which can be used as a guide for the location of future developments in the area, in order to minimize the impact projected developments will have on the surrounding water resources.

Therefore, two types of vulnerability maps: Intrinsic Vulnerability and Specific Vulnerability map for nitrate of Atebela groundwater catchment using the DRASTIC model need to be produced in order to achieve the above objective. These maps can help:

- To identify and classify vulnerable and non vulnerable areas to groundwater contamination so as to provide zoning of the groundwater protection,
- To assess the specific vulnerability of the groundwater basin for nitrate contamination.
- To provide information for the groundwater resources management of the catchment.

1.5 METHODOLOGY OF THE STUDY

To attain the above-mentioned specific objectives the following methods or approaches are to be applied:

a. Literature review and analysis of previous works and data on the geology, meteorology, hydrology and hydrogeology of the study area,
b. Georeferencing all the available water resources (springs, streams and rivers; hand dug wells and boreholes),
c. Hydrochemical analysis and interpretation of the groundwater for the purpose of identifying the source of groundwater, flow direction and determining the flow velocity; isotope (tritium) analysis to provide evidence for active recharge,

d. Application of Remote Sensing (RS) and Geographic Information System (GIS) techniques and many other computer codes to make ease of bulk data management and facilitate the analysis, synthesis, and interpretation of the results.

The activities are classified into office and field works.

1.5.1 Office Works

- Collection and organization of previous works within and around the study area,
- Plotting all developed water schemes on 1:50,000 topographic maps,
- Interpretation of 1:50,000 topographic maps,
- Interpretation of 1:100,000 Landsat images in a regional and local scale,
- Understanding of the geologic and hydrogeologic setups of the catchment and the adjacent ones through observation of borehole logs from well completion reports, water well locating reports, pumping test reports, and water schemes inventory reports.

1.5.2 Field Works

- Observation and mapping of outcrops of different lithological units, interpreted and inferred geological structures in the study area,
- Observation and description of undeveloped water schemes,
- Georeferencing constructed water schemes,
- Collecting water samples for laboratory analyses from available water resources, and measuring in – situ field parameters of water samples,
- Lithological logging of hand dug wells which are not fitted with hand pumps,
- Observation of land use and land cover practices,
- Identification of perennial and intermittent streams,
- Mapping the different factories, industries, waste disposal sites; observing their effluents and conducting chemical tests.

CHAPTER II

2. METHODS OF GROUNDWATER VULNERABILITY ASSESSMENT

2.1 LITERATURE REVIEW

2.1.1 Groundwater Vulnerability Assessment Concept and Definition

The concept of groundwater vulnerability is based on the assumption that the physical environment may provide some degree of protection to groundwater against the natural and human impacts, especially with regard to contaminants entering the subsurface environment. The term 'vulnerability of groundwater to contamination' was introduced by French hydrogeologist J. Margat in the late 1960s. The idea of describing the degree of vulnerability of groundwater to contaminants as a function of hydrogeological conditions by means of maps was conceived to show that the protection provided by the natural environment varies at different locations (Vrba and Zaporozec, 1994).

The fundamental concept of groundwater vulnerability is that some land areas are more vulnerable to groundwater contamination than others. The ultimate goal of the vulnerability map is a subdivision of an area into several units showing the differential potential for a specified purpose and use. Results of vulnerability assessment are portrayed on a map showing various homogeneous areas called cells or polygon, which have different levels of vulnerability. Vulnerability maps only show relative vulnerability of certain areas to others, and do not represent absolute values (Vrba and Zaporozec, 1994).

Groundwater vulnerability to contamination was defined by the Committee on Techniques for Assessing Groundwater Vulnerability of the U.S. National Research Council (1993) as "the tendency or likelihood for contaminants to reach a specified position in the groundwater system after introduction at some location above the uppermost aquifer." But the Committee (1993) refined the definition later differentiating two general types of vulnerability: specific vulnerability (when assessment is contaminant specific) and intrinsic vulnerability (for any contamination in general).

"Intrinsic vulnerability" (Rao and Alley, 1993) defined by the time of travel of water from the point of contaminant entry to the reference location in the ground-water system.

Vowinkel and others (1996) defined vulnerability as sensitivity plus intensity, where 'intensity' is a measure of the source of contamination. This indicates that groundwater vulnerability is not only a function of the properties of the groundwater flow system (intrinsic susceptibility) but also of the proximity of contaminant sources, characteristics of the contaminant, and other factors that could potentially increase loads of specified contaminants to the aquifer and (or) their eventual delivery to a ground-water resource (Michael J. Focazio, et al, 2000).

The aim of vulnerability assessment as it is described by Bachmat and Collin (1987) is providing preliminary information and criteria for decision making concerning management of water resources and land use as related to groundwater quality control. Quantifying the assessment of vulnerability and displaying it in a fashion which makes it useful and convenient for actual application in the decision making processes is presented using vulnerability mapping. Kukuric (1999) developed vulnerability assessment software as a part of decision support system for groundwater pollution assessment from point source by integrating likelihood of release and pollution, contaminant severity, pathway activity and target exposure factors.

Basically there are two vulnerability assessment approaches; qualitative and quantitative approaches depending on local conditions and available data. Each of these approaches requires that adequate data be available on factors that affect groundwater vulnerability, such as soil properties, hydraulic properties, precipitation patterns, depth to groundwater, land use and land cover, and other characteristics of the area to be assessed. Different types and amounts of data are necessary depending on the specific assessment method used. The product of most vulnerability assessments to date has been a map depicting areas of relative vulnerability.

2.2.2 Groundwater Vulnerability Assessment Methods

Thus the preparation of aquifer vulnerability map is a key consideration and becomes a forecasting tool. Via the planning processes, it also acts as a prevention tool and an identifier of action priority list. Vulnerability mapping has been carried out in many countries in recent years and examination of these maps and descriptions of vulnerability in the scientific literature shows considerable variation from different perspectives. DRASTIC, GOD, SINTACS and currently European approach are some of the methods. Most of the assessment and mapping methods are GIS supported weighting and ranking of the component factors relevant to groundwater pollution according to their relative importance.

DRASTIC is a standardized system developed by US EPA for the evaluation of the groundwater pollution potential of any area in the United States of America (Aller et al, 1987). However, this method has been adopted in different countries considering local conditions for the protection of groundwater vulnerable zones to pollution. A valid point count system model (DRASTIC) was built up to assess aquifer vulnerability.

The name DRASTIC is taken from the initial letters of the hydrogeological factors defined that are used to evaluate the intrinsic vulnerability of aquifer systems. It attempts to quantify relative vulnerability by the summation of weighted indices for the following seven hydrogeological variables;

D= Depth to water,
R= net Recharge,
A= Aquifer media,
S = Soil media (texture)
T = Topography (slope)
I = Impact of lithology of Vadose zone
C = Hydraulic Conductivity of aquifer

Each factor is assigned a rating ranging from 1-10, according to the proportion of the degree of vulnerability. Then, the rating is multiplied by a weight to reflect the

importance of this factor to the vulnerability. The DRASIC index is made up of the sum of the products of rating and weights of the seven factors.

$$\textbf{DRASTIC index} = D_R D_W + R_R R_W + A_R A_W + S_R S_W + T_R T_W + I_R I_W + C_R C_W \text{ (Eq. 2.1)}$$

Where: R =Rating and W = Weight

The higher the DRASIC index is the greater the groundwater pollution potential and the lower is the less groundwater pollution potential according to the method. GOD relates primarily to vulnerability of ingress of pollutants to the saturated zone and not to lateral transport with in the zone (Foster, 1987). GOD considers groundwater occurrence, overall aquifer class in terms of grade of consolidation and lithological character and depth to groundwater table.

SINTACS (Civita and De Maio, 2000) is also similar to DRASTC method, but has four different weighting systems depending on the hydrogeological setting. The weighting system has been designed to illustrate the relative importance of normal, sever, seepage, karst and fissured parameters. Normal and sever reflect the density of human settlement and the intensity of land use, Seepage describes areas that are frequently flooded or swampy and karst feature is used for areas that are deeply karstified and fissured.

2.2 DRASTIC APPROACH

DRASTIC approach is one of the first point count system models developed for the U.S. Environmental Protection Agency in 1985 by Aller et al (1987) which considers a multiplier identified as an importance weight in addition to the rating given to every parameter. Each parameter is given a rating interval from 1 to 10, with two relative weight strings (varying from 1 to 5). The most significant parameters have weights of 5; the least significant, a weight of 1.

Once a DRASTIC index has been computed, it is possible to identify areas which are more likely to be susceptible to groundwater contamination relative to one another. The groundwater contamination potential is greater when the DRASTIC index is

higher. The DRASTIC index provides only a relative evaluation tool and is not designed to provide absolute answers (Vrba and Zaporozec, 1994).

The DRASTIC approach to mapping of groundwater vulnerability to contamination is based on the assumption that the physical environment may provide some degree of protection to groundwater with regard to contaminants entering the subsurface. The earth materials may act as natural filters to screen out certain contaminants. Water infiltrating at the land surface may be purified to some degree as it percolates through the soil and other fine grained materials in the unsaturated zone (Fig 2.1).

Vrba and Zaporozec (1994) explained that the degree of attenuation that occurs between the contaminant source and the aquifer determines the relative potential for groundwater contamination. The attenuation capacity, or ‘’purification capacity’’, of surface materials consists of the interactions of numerous physical, chemical, and biological processes in a soil-rock-groundwater system and is significantly determined by the solute transport mechanism as well as hydrogeological conditions (Golwer, 1983).

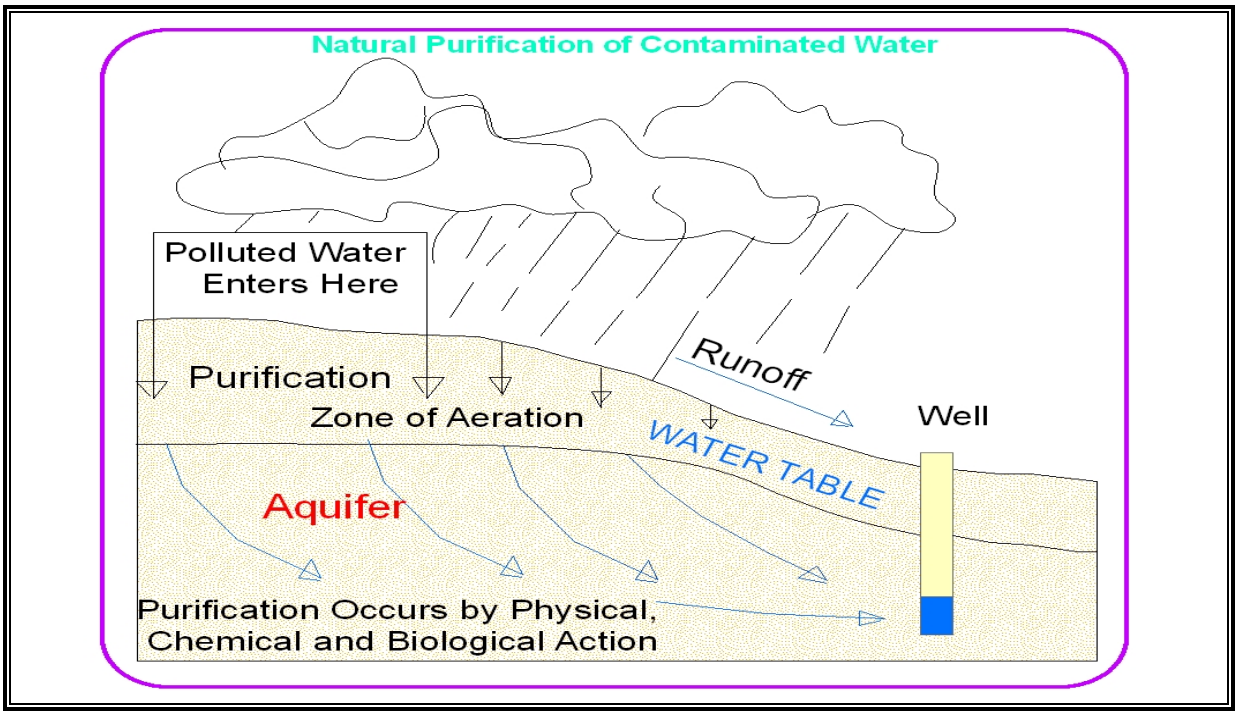

Fig 2.1 Natural purification of contaminated water

2.2.1 Intrinsic Vulnerability Assessment

According to Vrba and Zaporozec (1994), vulnerability maps cannot be produced without consideration of the individual factors that determine the homogeneity of the areas under study and the capacity for attenuating contaminants. The intrinsic (natural) vulnerability map is based on the assessment of various natural factors or attributes, such as soils, the unsaturated zone, aquifer properties, and recharge rate that enter into the determination of the vulnerability of groundwater.

When assessing groundwater vulnerability, the attributes or their parameters may be assigned different weights and rating according to their considered importance for the vulnerability assessment (Fig 2.2). Assessment of groundwater vulnerability is possible when the basic parameters of the attributes mentioned above are known.

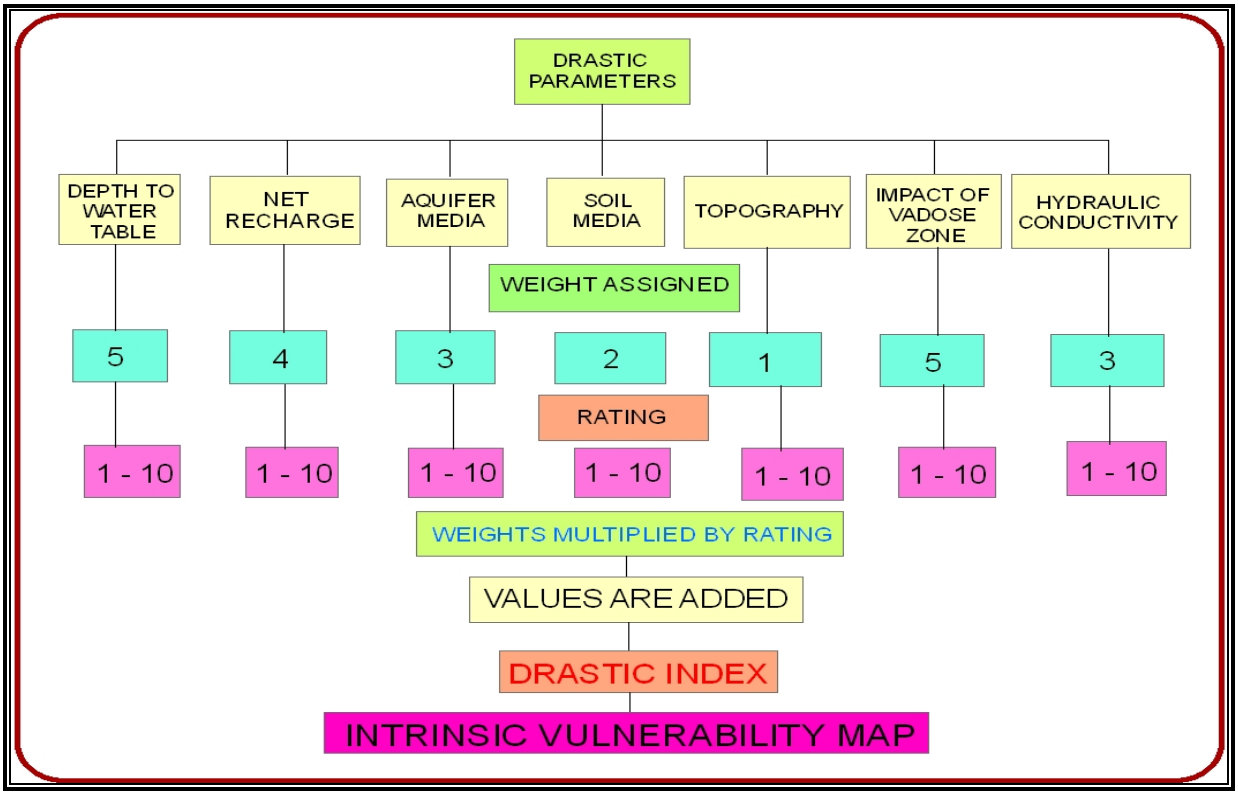

Fig 2.2 Weights and rating for the attributes of intrinsic vulnerability

2.2.1.1 Attributes of Primary Importance –

The principal attributes of intrinsic groundwater vulnerability include:

- Recharge,
- Soil properties, and
- Characteristics of the unsaturated and saturated zone.

a) Recharge (R)

Recharge is the amount of water passing through the unsaturated zone and into an aquifer during a specified period of time (Vrba and Zaporozec, 1994). It is usually expressed as annual net recharge. According to Aller et al (1987), net recharge is defined as the total quantity of water which is applied to ground surface and infiltrates to reach the aquifer. The amount and quality of recharge significantly affects the physical and chemical processes in the soil-rock-groundwater system. It should always be considered in the assessment of groundwater vulnerability.

Recharge may be evaluated on the basis of field measurement, derived from the water balance equation, or estimated with help of aerial photographs or satellite imagery and it also involves climatic data such as precipitation, air temperature, and evaporation, that significantly influence the amount of recharge (Vrba and Zaporozec, 1994).

b) The Soil (S)

Soil media refers to the upper most portion of the vadose zone characterized by significant biological activity. Soil has a significant impact on the amount of recharge which can infiltrate into the ground and hence on the ability of a contaminant to move vertically into the vadose zone (Aller et al, 1987). According to Vrba and Zaporozec, 1994, it is commonly regarded as one of the principal natural factors in the assessment of groundwater vulnerability.

The main soil parameters related to vulnerability include texture, structure, thickness, and content of organic matter and clay minerals. The soil has an important attenuation function (Zaporozec, 1985) and is a critical attribute when groundwater vulnerability to diffuse contamination sources is assessed.

The presence of fine-textured materials such as silts and clays can decrease relative soil permeabilities and restrict contaminant migration. Moreover, where the soil zone is fairly thick, the attenuation processes of filtration, biodegradation, sorption and volatilization may be quite significant. The pollution potential of a soil is largely affected by the type of clay present, the shrink/swell potential of that clay and the grain size of the soil. In general, the less the clay shrinks and swells and the smaller the grain size, the less the pollution potential (Aller et al, 1987).

Organic matter contained in the soil may also be an important factor particularly in the attenuation of pesticides. Organic matter is typically contained in the surface layer of the soil and composed of un-decayed plant and animal tissue, charcoal and various humic compounds. The organic content of the soil generally decreases with depth from the surface (Aller et al, 1987).

Vrba and Zaporozec (1994) explained that the soil's function as a natural protective filter in the retardation and degradation of contaminants can be damaged easily. The damage may lead to the loss of its control over groundwater quality. Therefore, the soil properties assessment needs to take into consideration whether the soil under study is in natural conditions or under stress from agricultural activities, etc.

c) The Unsaturated (Vadose) Zone

The vadose zone is defined as that zone above the water table which is unsaturated or discontinuously saturated (Aller et al, 1987). It is very important in the protection of groundwater especially in hilly and mountainous regions and in areas where the soil profile is not well developed. The character of the unsaturated zone and its potential attenuation capacity decisively determine the degree of groundwater vulnerability. Low

permeable rocks in this zone create a confining layer for the underlying aquifers and reduce significantly their vulnerability (Vrba and Zaporozec, 1994).

Some of the types of processes which may occur within the vadose zone are biodegradation, neutralization, mechanical filtration, chemical reaction, volatilization and dispersion. The amount of biodegradation and volatilization decreases with depth. The media also controls the path length and routing, thus affecting the time available for attenuation and the quantity of material encountered. The routing is strongly influenced by any fracturing present (Aller et al, 1987).

According to Vrba and Zaporozec (1994), the main parameters included in the assessment are the thickness, lithology, and vertical permeability. The thickness of the unsaturated zone depends on the position of the water table.

d) The Saturated Zone

The aquifer or the saturated zone is a heterogeneous system in which its vulnerability varies spatially and with depth. Vrba and Zaporozec, (1994) suggested that the definition of semiconfined, confined, and unconfined conditions is important and must always be considered when assessing aquifer vulnerability.

The main parameters for assessment of aquifer vulnerability include the aquifer nature and geometry, porosity, hydraulic conductivity, storage properties, transmissivity, and groundwater flow direction.

Aller et al (1987) mentioned that the route and path length which a contaminant must follow are governed by the flow system within the aquifer. Along with the hydraulic conductivity and gradient, the path length is an important control in determining the time available for attenuation processes such as sorption, reactivity and dispersion to occur. The also added that the aquifer medium also influences the amount of effective surface area of materials with which the contaminant may come in contact within the aquifer. The larger the grain size and the more the fractures or openings within the

aquifer, the higher the permeability and the lower the attenuation capacity of the saturated zone.

2.2.1.2 Attributes of secondary Importance –

The secondary attributes of intrinsic vulnerability assessment include topography, surface water, and the nature of the underlying unit of the aquifer. Vrba and Zaporozec (1994) explained that their importance for vulnerability varies with the area. Depending on the natural conditions, the importance may be greater in some areas such as flat recharge areas, bank infiltration from a surface water into shallow aquifer, groundwater contact with the underlying strata of high ion-exchange capacity; and smaller in others (steep-slope recharge areas, low level ion-exchange or sorption capacity of the underlying strata). An important attribute is topography, which influences recharge, soil development, and groundwater flow and velocity.

2.2.2 Specific Vulnerability Assessment

Groundwater vulnerability mapping has proven to be a valuable practical tool for land use planning and groundwater protection in many countries, in helping to avoid the contamination of water present beneath sensitive land. To achieve this objective, the DRASTIC approach has included additional criteria useful under certain conditions to compile specific resource or source vulnerability maps. These maps are more sophisticated and contain more information than intrinsic maps reflecting a more detailed potential migration picture of a particular contaminant.

Specific vulnerability of a groundwater system is mostly assessed in terms of the risk of the system becoming exposed to contaminant loading. In comparison with the assessment of natural vulnerability, which is based mostly on the static intrinsic parameters of the soil-rock-groundwater system, the dynamic and variable parameters are included in the assessment specific vulnerability (Vrba and Zaporozec, 1994).

In addition to intrinsic vulnerability assessment, the specific vulnerability mapping method works by combining the information about physical and chemical behaviors of

the contaminants and layers**.** Specific vulnerability takes into account the properties of a particular contaminant or group of contaminants in addition to the intrinsic vulnerability of the area. These parameters have been obtained from the scientific literature and they are different for each contaminant, but common for all field applications, (Zwahlen, 2003).

Vrba and Zaporozec (1994) explained that the important parameter in the assessment of specific groundwater vulnerability is the attenuation capacity of the soil, of the unsaturated zone, and of the aquifer with respect to properties of individual contaminants. Major attributes involved in assessing specific groundwater vulnerability include: land use (human impact) and population density. They mentioned that there is a fundamental difference between areas with land under stress (agriculture, industry, settlements, acid deposition) and areas where natural landscape with natural vegetation predominates (forests, uncultivated meadows, unpopulated mountainous regions). The more densely an area is populated, the greater the potential and real contaminant loads on the groundwater system.

Intrinsic vulnerability inadequately characterizes contaminant fate and transport since it accounts only for the inherent geological and hydrogeological setting of an area. It makes no allowance for the nature of the contaminants concerned. In addition to the intrinsic vulnerability of an area, specific vulnerability of groundwater to a particular contaminant or group of contaminants takes account the properties and related processes of contaminants.

- Intrinsic vulnerability maps generally display a worst case scenario and fail to take into account the positive effects deriving from specific contaminant properties such as retardation and degradation. This ignores the additional attenuation potential of contaminants under certain conditions and thus may overestimate the vulnerability of an area.
- Intrinsic vulnerability assessment cannot account for the diversity of processes undertaken in soil and subsoil layers and acts only as a general basis for each specific assessment where as, specific vulnerability assessment aims at

combining the effects of intrinsic and specific processes. Intrinsic vulnerability maps and databases provide intrinsic values.

- Specific vulnerability assessment deals with differences between particular contaminant behavior and their specific interaction with the host rock while intrinsic vulnerability assessment treats all substances as having similar transport behavior as that of water.

The vulnerability assessment conducted for the study area is presented in Chapter 8.

2.3 APPLICATION OF VULNERABILITY MAP

Groundwater vulnerability maps according to Vrba and Zaporozec (1994) are used for three main purposes planning, contamination assessment, and education.

2.3.1 Planning

The main value of vulnerability maps is that they can be used as an effective preliminary tool for planning, policy, and operational levels of the decision-making process concerning groundwater protection and management. They are valuable guides to planning and can help planners and regulators make informed, environmentally sound decisions regarding land use and protection of groundwater quality.

2.3.2 Contamination Assessment

Vulnerability maps are a good tool for groundwater professionals to make local and regional assessment of vulnerability potential, to identify areas susceptible to contamination, and to indicate the relative degree of concern and effort needed for more detailed assessment. They can help determine which areas may have groundwater problems and what types of site-specific data or studies are needed. In addition, they can be used for the design of monitoring networks and for the evaluation of contamination situations.

2.3.3 Education

Vulnerability maps are useful for educating and informing planners, regulators, and decision-makers about groundwater protection and contamination prevention. They can also be used to educate the public and policy makers about aquifers being part of a larger, interconnected ecological system affected by human activities. Further, they create public awareness about environmental protection.

CHAPTER III

3. BACKGROUND OF THE STUDY AREA

3.1 OVERVIEW OF GROUNDWATER POLLUTION IN ETHIOPIA

Similar to the globe, groundwater is the major source of drinking water in Ethiopia. More than 80% of the countries drinking water supply source is from groundwater. This includes more than 25 major cities in the country according to Kebede Tsehayu et al., (2004).

The issue of groundwater pollution has not been considered as a major problem in Ethiopia until recent times. Currently there is an ever-increasing demand of fertilizers and application of pesticides to enhance food production, expansion of settlements, widespread disposal of domestic and industrial effluents to the ground, increasing chemical diversity of potential groundwater pollutants manufactured, used and disposed of by mankind in recent decades. The expansion of settlements and industries in most cases are without proper sewer drainage system and poor waste disposal management. It is inevitable that these human intervention activities will pose pollution problem in the groundwater system. There are indicators that the groundwater system has started pollution in some big cities. Taye Alemayehu (1999) and Tamiru Alemayehu (2004) indicated the pollution of groundwater in Dire Dawa and Addis Ababa, respectively.

The groundwater pollution of Sebeta-Alemgena and its surrounding is a threat for the future sustainable domestic water supply of the area. High population intensity, industries, lack of proper sewers and waste disposal facilities, use of several open pit latrines, favorable geological, morphological and climatological conditions have facilitated groundwater pollution. Hence, groundwater vulnerability assessment for Atebela groundwater catchment and further mapping of the degree of vulnerability and potential contaminant sources is important for the area.

3.2 GENERAL FEATURES OF THE STUDY AREA

3.2.1 Location and Accessibility

Atebela River Catchment is part of the central landmass of Ethiopia, found in the Upper Awash Basin specifically situated on the northwestern shoulder of the Rift Escarpment. It is located at about 30 km southwest of Addis Ababa in Oromia Regional State, Southwest Shewa Zone, in the District of Alemgena. Two major all weather asphalt roads, namely the Addis Ababa – Jimma asphalt road and the Alemgena – Butajira asphalt road passes through the study area (Fig 3.1).

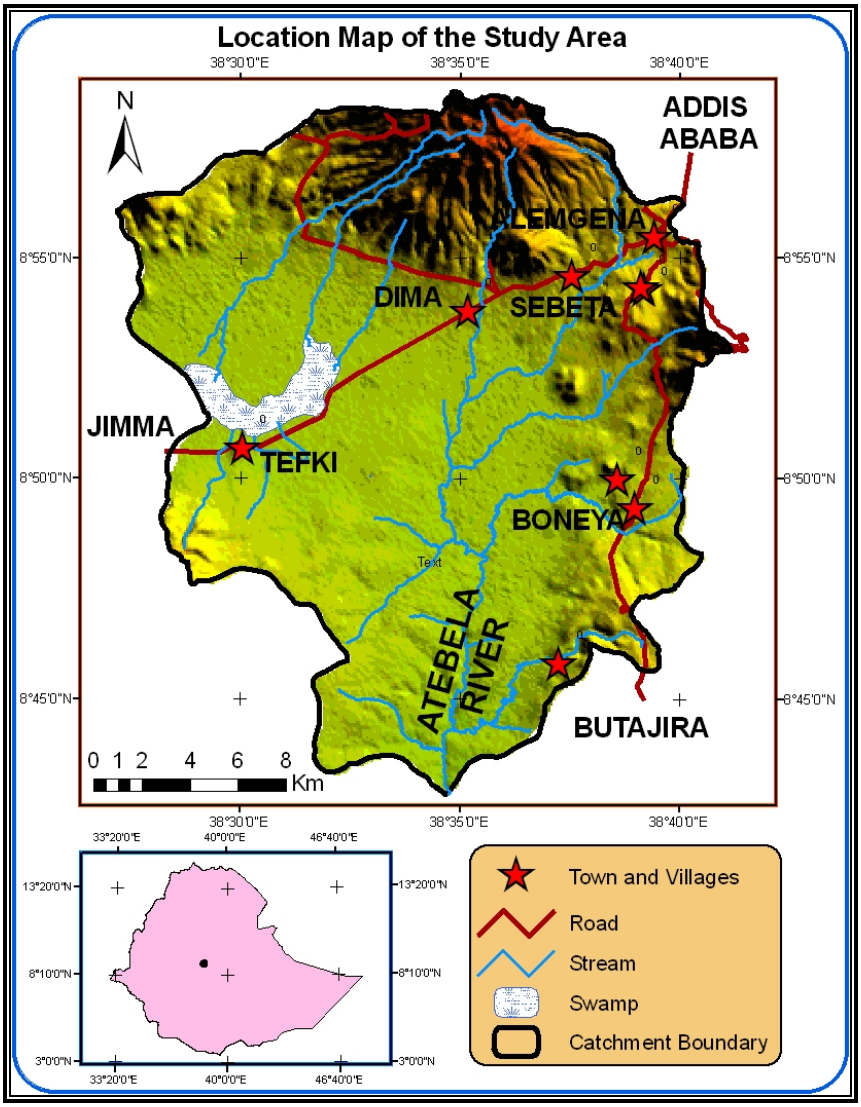

Fig 3.1 Location map of the study area

The area is specifically bounded by geographical coordinates of 38027'10'' - 38041'08'' E Longitude, and 8042'51'' - 8058'48'' N Latitude which covers a total of over 495.64 km2 area. It is bordered by Ilu District from the southwest, Holeta District from the north, Akaki District from the East, Addis Ababa from the northeast, and Kersa Kondaltiti District from the South.

As shown in Figure 3.2, the study area includes parts of 1:50,000 scale topographic sub-sheets of (0838 B3), (0838 B1), and (0838 A2). Major towns or villages that lie within the study area include Alemgena, Sebeta, Tefki and Dima. They are all found on the major asphalt roads.

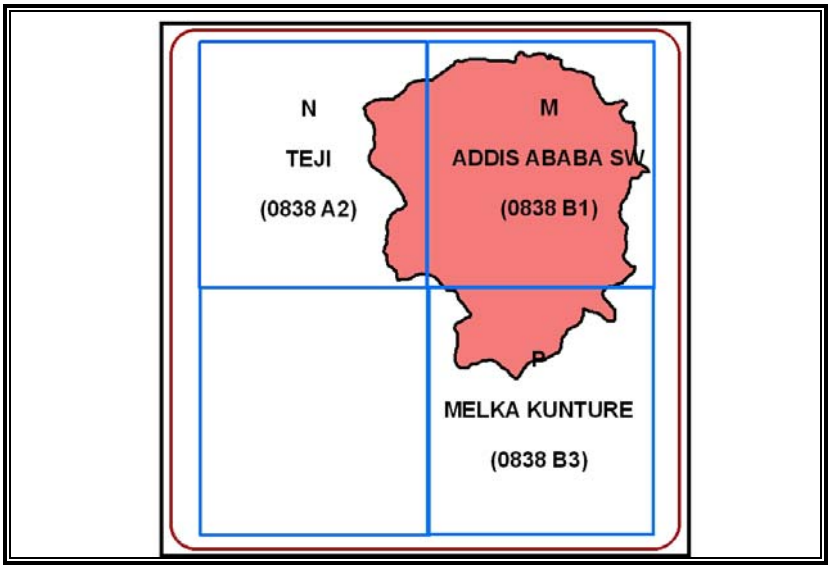

Fig 3.2 Diagram showing sub-sheets' layout of the study area

3.2.2 Climate

The climate of the area is predominantly humid to sub-humid with total annual rainfall of about 1043 mm, whereas the mean annual temperature is about 16.5 ^{0}C. The effect of orography on the climate is observed that it is on the wind ward side receiving the greatest amount of rainfall. The mountain of Wechecha is experiencing lower humidity during the hot season. The topography of the study area ranges from 2000 – 3380 m above the mean sea level.

3.2.3 Physiography and Drainage Pattern

The study area is characterized by very diverse spatial variation of topographic features. It ranges from very steep high mountains to flat plains with the general topography direction being from south towards the north. The mountainous areas are located in the northern and eastern parts of the study area with higher peaks of hills also found in the southwestern part around Tefki. The elevation ranges from 2362 m to a maximum of 3380 m on Mt. Wechecha. The altitude reaches a maximum of 3380 to 2000 m at the mouth of the river the slope ranges from 7 – 107 % (Fig. 3.3).

Most of the area is covered by flat land which extends from the foot of Wechecha and Daleti to the mouth of Atebela River and that also goes beyond Tefki town. It lies mainly on the southern, western and central part of the catchment at an altitude of 2000 – 2362 m with slopes of 0 – 7 %. The streams meander in this flat land especially in the southern part of the study area with gorges forming slope of 2 – 7 %.

The study area is found in two physiographic divisions. The first physiographic division is the plateau area which consists part of the Central Ethiopian Highland adjacent to the northwestern shoulder of the Rift Escarpment. It is part of extensive landmass of Tertiary Plateau Basalt (Trap Series). The mountain chain of Wechecha whose elevation peak of 3385 m is found in the plateau located along the Rift Margin area and elevation range in this study area varies from 2080 to 3380 m. The mountainous ridges of Wechecha to the north of the study area are covered by afforested eucalyptus and coniferous forest of Suba (Gelana Gadissa, 2005).

The second physiographic division is the Rift Escarpment which forms the major part of the study area (Fig 3.3). It is found following the North-western Shoulder of the Main Rift system. Young basaltic lava flows and jointed ignimbrite-sheets dominate geology of the areas under this physiographic division. Becho Plain, situated west of Mt. Wechecha, is included in this part where no significant topographic changes other than planar surfaces are exhibited. Elevation in this part of the study area varies from 2000 to 2080 m. The ridge of Daleti along the road to Butajira is covered by dense forest of smaller areal extent, and with lowering of elevation bushes, grass and

scattered trees of mostly man-made (coniferous, and eucalyptus trees) characterize the area. Most of the flatland areas within this physiographic division are agricultural land due to presence of fertile soil and favorable climatic conditions (Gelana Gadissa, 2005).

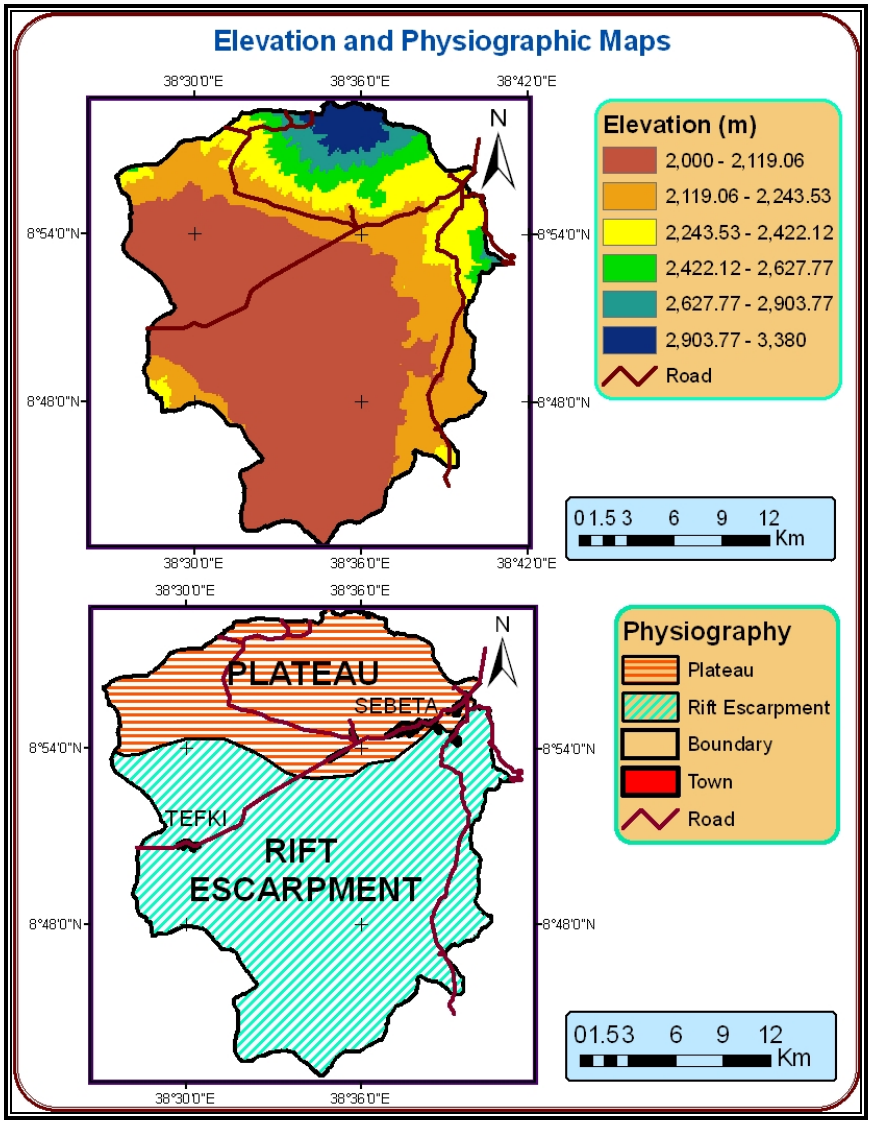

Fig 3.3 Topographic map of Atebela River catchment

The alluvial plain of the study area is an area of active deposition due to its subdued relief and consequently low stream gradients. Erosion gullies are common where steeper slopes occur.

The surface drainage of the study area is characterized by radial and parallel pattern on the hillside and foot of the Wechecha Mountain, respectively and rectangular and meandering pattern is observed in the southern part of the catchment. Streams that discharge from the northern and eastern part of the catchment including those in the southwest discharge into Atebela River while streams that flow from the west and northeast remain in the catchment forming swamp during the rainy season (Fig 3.4).

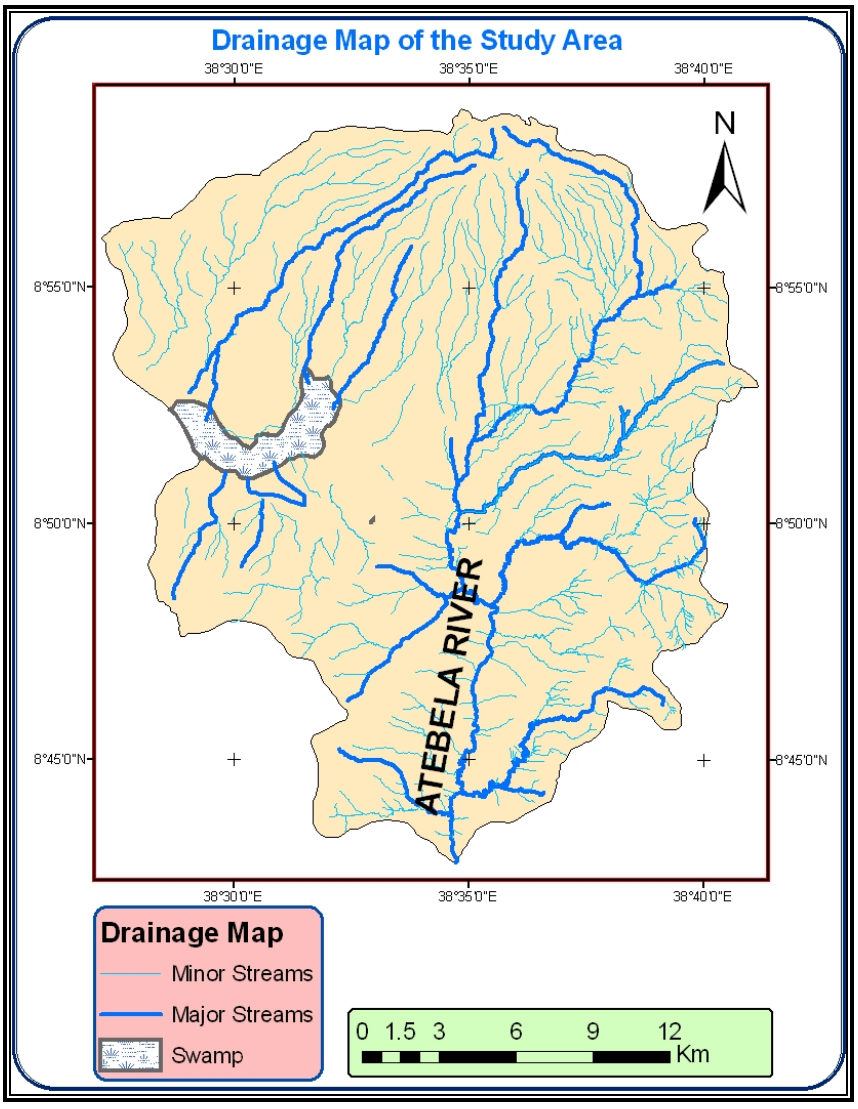

Fig 3.4 Drainage map of the study area

3.3 SOIL TYPE AND SOIL PROPERTIES

Soil is a dynamic natural body that involves external and internal soil forming processes acting on different geomorphic surfaces in relation to different soil forming factors such as parent materials, climate, relief/topography, organisms, and human influences over a period of time. These resulted in the formation of various soils in the study area.

Soil map available for of the study area is found on the study report of Becho Plain for which soil classification is based on air photo interpretation and description of soil auger borings and pits carried out according to FAO guidelines. Vertisols are the dominant soil class of the study area, and including all the upland plains, all the seasonal swamps, and most of the alluvial cover flood plains and terraces. They are black clays characterized by the dominance of the clay mineral, montmorillonite, which expands when wet and contracts when dry, giving rise to wide surface cracks. Accordingly, five soil groups are identified in the study area.

The first soil unit comprises of the gentle foot slopes of volcanic hills fringing the alluvial plain. The soils are eutric Vertisols which frequently have calcareous nodules at depth in the profile. They are susceptible to rill and gulley erosion on the prevailing slopes of 1.5 – 3.0%. In the study area, they are manifested starting from the northwest part at the foot of Mt. Wato Dalecha rounding along the foot of Wechecha and also along the road taking to Butajira. In addition, these soils are found at the southern part extending up to the foot of Mt. Debel then to Tefki.

The second type of soil comprises very gentle foot slopes of less than 1.5% gradient, which occur extensively to the north of the entire alluvial plain and also to the south of the road southwest of Tefki town. The eutric Vertisols are less susceptible to erosion on these slopes but are subject to periodic flooding by slow moving water.

The back swamp soil units are subject to the most prolonged flooding are characterized by stagni-calcic Vertisols with significant accumulation of calcium carbonate at depth.

Soil morphology is related to the appearance of the soil in the field in terms of depth, color, texture, structure, consistence, drainage and the presence or absence of stones, and carbonates.

The soil units have been grouped into the following classes for a generalized description of their soil morphology:

- Very shallow-to-shallow soils – these soils occur in the study area most prevalently in areas of steep slopes and are red to reddish brown in color. They are dominantly, in the southwestern, northern, eastern and southeastern hills/mountainous areas.
- Moderately deep to deep, poorly drained soils – these soils occur at receiving sites of runoff from the surrounding elevated terrain. They are heavy clay soils with a characteristic of montmorillonite dominated clay fraction which causes them to shrink and swell and occur in the vicinity of Tefki town.
- Alluvial soil – these soils are young soils that are often found on low-lying plains and near river stream courses. They constitute sand and gravel with varying thicknesses (Fig 3.5).

Different land/soil degradation types were encountered within the basin area. They are mainly evident as moderate to severe erosion, flooding and landslides. The main contributors for the phenomena are steep slopes, very little vegetation cover, indiscriminate use of the land, etc. All these situations aggravate (accelerate) the degradation processes. The textural map of the soil in the study area is shown in Fig 3.5.

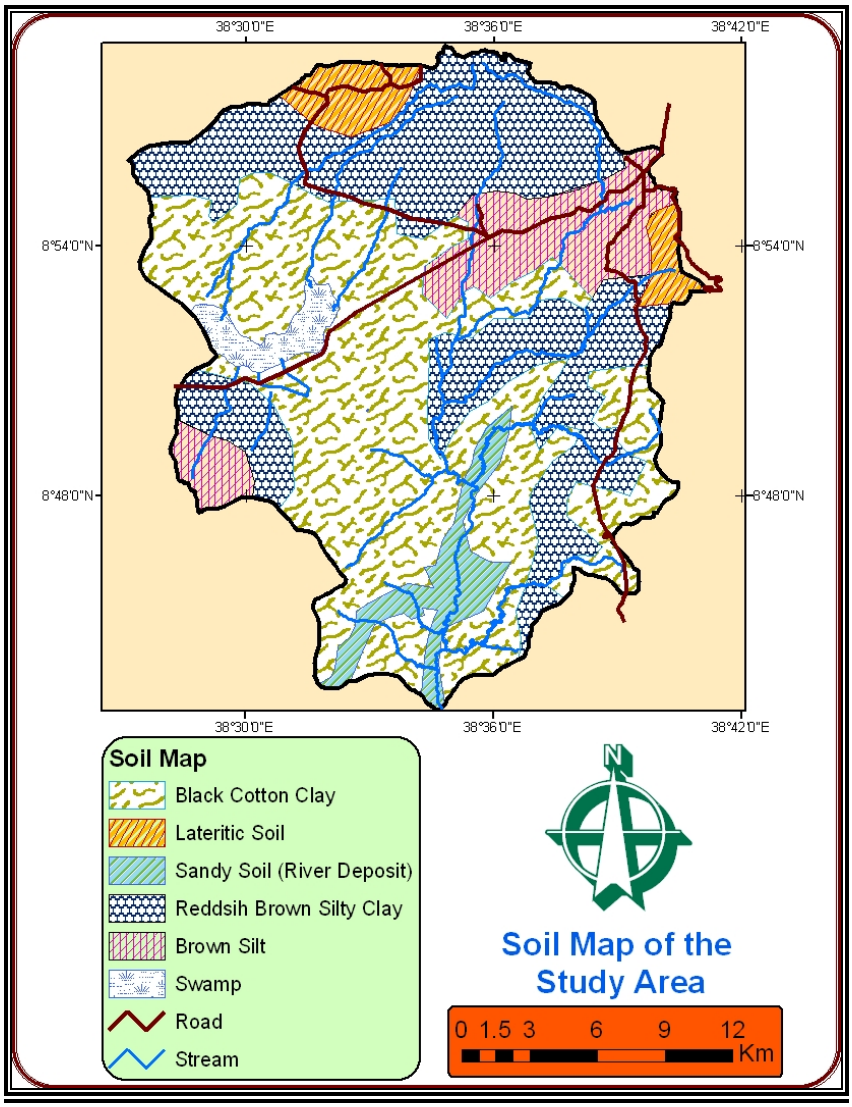

Fig 3.5 Soil map of the study area

3.4 LAND USE AND LAND COVERAGE

Land use map with a scale of 1:50,000 are available for the study area and seven types of land use / land cover types are identified. According to Gelana Gadissa (2005) study report of construction rock materials investigation, the land cover is classified as forest, bare rock, agriculture and grassland, swamp, bushes and shrubs, and built up areas (towns, all weather and asphalt roads, etc). The relative percentage of the land cover is given in Table 3.1.

The major classes are sub-divided into mapping units (Fig 3.6). The main purpose of this sub-division is to reduce the variation within a given land use/land cover types by breaking heterogeneous into more homogeneous land use/land cover types in relation with the hydrography of the basin.

Table 3.1 Spatial distribution of land use/land covers in the study area

Group	Major Classes	Area (km^2)	% Coverage
1	Forest	20.09	4.05
2	Bare rock	19.91	4.01
3	Cultivated and grassland	317.34	63.99
4	Bushes and shrubs	105.40	21.25
5	Swamp	13.51	2.72
6	Built up areas (Town + Asphalt Road)	19.66	3.96

(Source: Adapted from Gelana Gadissa, 2005)

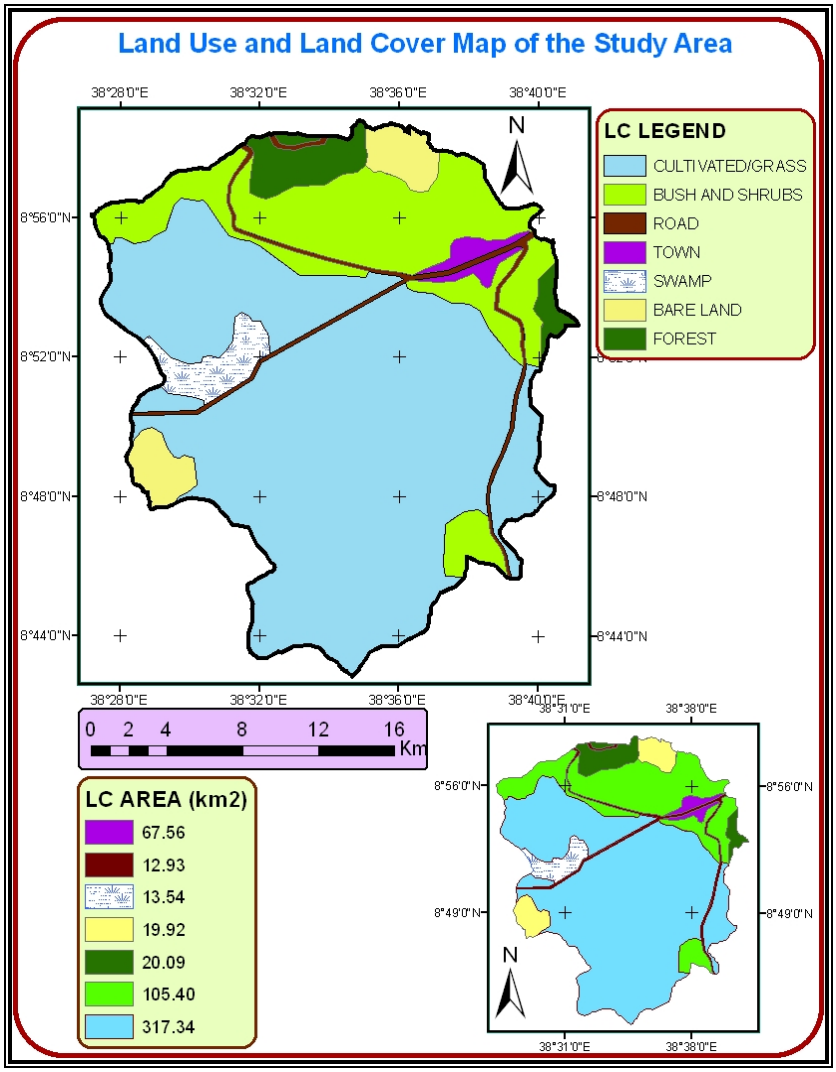

Fig 3.6 Land cover/land use map (Source: Gelana Gadissa, 2005)

CHAPTER IV

4. HYDROMETEOROLOGY

Meteorological data such as rainfall, temperature, wind speed, runoff, humidity and others collected from Ethiopian Meteorological Services Agency need to be analyzed in order to obtain recharge. Eight meteorological stations (Addis Ababa Observatory, Sebeta, Holeta, Melka Kunture, Boneya, Teji, Akaki and Insilale) are considered for the analysis.

4.1 EFFECTIVE ANNUAL ARIAL DEPTH OF PRECIPITATION

The three common methods namely, arithmetic mean, Thiessen Polygon and isohytal methods are involved for calculating or estimating effective depth of precipitation and the results are compared (see Annex 4 rainfall summary of the stations).

4.1.1 Arithmetic Mean Method

This method is appropriate for uniformly distributed rainfall gauge stations.

Table 4.1 Mean monthly areal depth of precipitation from arithmetic mean

STATIONS	JAN	FEB	MAR	APR	MAY	JUN	JUL	AUG	SEP	OCT	NOV	DEC	Total
Addis Ababa OBS	18.5	37.8	66.0	91.4	86.7	136.5	265.1	279.6	167.6	39.7	6.9	8.5	1204.5
Sebeta	15.2	63.6	80.5	108.7	105.0	186.7	328.4	369.9	140.9	39.9	8.7	6.5	1453.8
Holeta	13.6	43.8	59.2	76.3	64.1	103.6	213.6	244.1	125.0	17.9	4.1	7.8	973.1
Boneya	13.1	28.8	46.0	64.0	56.7	103.7	208.3	209.4	114.3	15.7	3.4	5.1	868.5
Awash Melka	15.0	26.1	60.2	69.7	59.3	100.5	230.7	214.9	86.3	22.5	2.7	3.6	891.3
Teji	17.6	36.1	54.3	78.8	70.9	121.3	221.3	215.7	97.5	24.2	5.6	5.7	948.8
Asgori	16.9	30.9	49.6	82.4	63.1	120.4	223.4	225.1	95.0	22.7	3.7	4.5	937.8
Akaki	14.2	29.0	63.0	84.6	72.7	121.7	260.8	268.9	127.9	23.8	3.9	3.0	1073.3
Insilale	17.8	25.8	50.0	69.8	56.3	104.7	199.5	193.8	95.2	21.5	8.7	2.8	846.0
Total	141.8	296.1	478.8	655.8	578.5	994.4	1951.6	2027.5	954.4	206.4	39.0	44.7	9197.0
Mean for all the stations	15.8	32.9	53.2	72.9	64.3	110.5	216.8	225.3	106.0	22.9	4.3	5.0	1021.9

Therefore, according to the arithmetic mean method, the effective depth of precipitation is 1021.89 mm.

4.1.2 Theissen Polygon Method

This method calculates the weighted average of each precipitation station in and near the catchments based on the following relationship:

$$PPT = (\sum(A_i)/A)*P_i,\ i = 1 - n$$

Where P_i is the precipitation of the i^{th} gauge,

A_i is the area of the specific polygon formed using the Theissen method corresponding to the precipitation P_i (Fig 4.1),

A is the total area of the catchment,

i refers to the i^{th} precipitation gauge, n is the number of the Theissen polygons.

Five meteorological stations namely Holeta, Sebeta, Boneya, Teji and Awash Melka are involved to calculate the areal depth of precipitation for the study area (Table 4.2 and Fig 4.1)

Table 4.2 Mean monthly areal depth of precipitation from Theissen Polygon

STATIONS	Area (Km^2)	JAN	FEB	MAR	APR	MAY	JUN	JUL	AUG	SEP	OCT	NOV	DEC	TOTAL
Sebeta	239.1	15.2	63.6	80.5	108.7	105.0	186.7	328.4	369.9	140.9	39.9	8.7	6.5	1453.8
Holeta	15.1	13.6	43.8	59.2	76.3	64.1	103.6	213.6	244.1	125.0	17.9	4.1	7.8	973.1
Boneya	149.8	13.1	28.8	46.0	64.0	56.7	103.7	208.3	209.4	114.3	15.7	3.4	5.1	868.5
Awash Melka	58.1	15.0	26.1	60.2	69.7	59.3	100.5	230.7	214.9	86.3	22.5	2.7	3.6	891.3
Teji	33.9	17.6	36.1	54.3	78.8	70.9	121.3	221.3	215.7	97.5	24.2	5.6	5.7	948.8
Weighted Avg.	**495.9**	**14.6**	**46.2**	**65.3**	**87.6**	**81.5**	**144.5**	**269.9**	**288.9**	**123.0**	**28.8**	**6.0**	**5.7**	**1162.0**

Total annual precipitation of the study area calculated using Theissen method is 1161.98 mm.

4.1.3 The Isohyte Method

This method is effective in areas which have very big topographic variation. For the study area, the elevation varies from 2000 m on the mouth of Atebela River to 3380 m on Mt. Wechecha with a total difference in elevation of more than 1300 m. One advantage of the method for determining catchment averages is that it allows the influence of physiographic parameters to be taken into account. These factors include elevation, slope, and distance from the coast and exposure to rain-bearing winds (Shaw, 1988). The formula applied is as follows:

$$P_A = \frac{\sum ((P_i + P_{i+1})/2) * A_i}{\sum A_i}$$

Where, P_i is the precipitation of the i^{th} rainfall contour,

A_i is the area bounded between consecutive rainfall contours (Fig 4.2),

i refers to the i^{th} rainfall contour

The method yields an annual mean precipitation of 1103.57 mm (Table 4.3).

Table 4.3 Mean annual precipitation from isohyte

Bounded Area	Area (Km^2)	RF Contour No.	Total Rainfall (mm)
I	20.74	1	1400
II	49.87	2	1300
III	54.14	3	1200
IV	83.43	4	1100
V	148.58	5	1000
VI	122.05	6	900
VII	17.37		
Total	496.18		1103.57

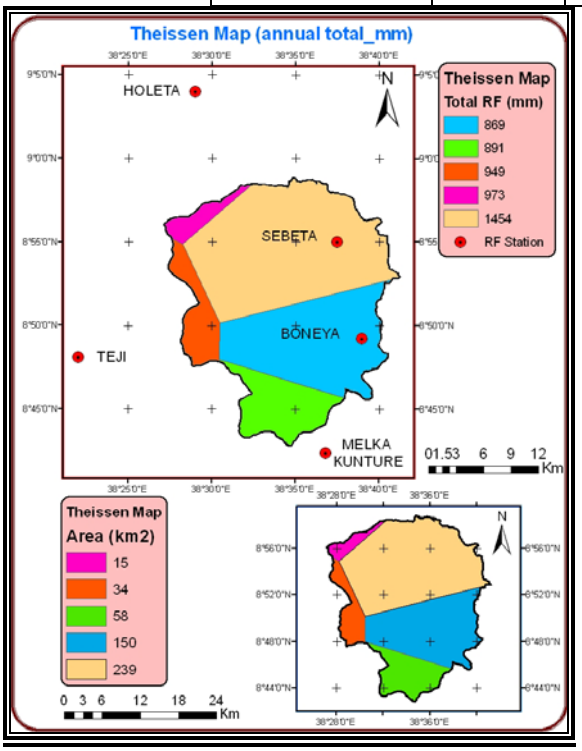

Fig 4.1 Theissen polygon map

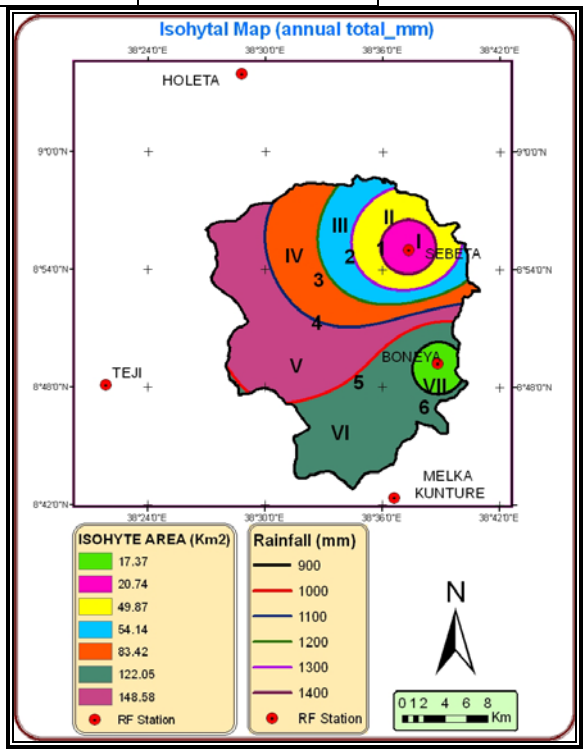

Fig 4.1 Isohytal map

The average precipitation amount calculated using the three methods is 1095.87 mm.

4.2 TEMPERATURE

The temperature of the water surface is important in that it governs the rate at which water molecules leave the surface and enter the overlying air. A change in water surface temperature may, therefore, have a profound short-term effect up on the rate of evaporation. For this research, the temperature data for Addis Ababa Observatory (at a UTM coordinate 0472616 m E longitude and 0998662 m N latitude), Asgori, Holeta and Tulubolo are used since there is no meteorological station in the study area that records temperature data (Table 4.4).

Table 4.4 Mean maximum and minimum temperatures of the study area for 31 years.

STATION	TYPE	MONTH OF THE YEAR												AVG
		JAN	FEB	MAR	APR	MAY	JUN	JUL	AUG	SEP	OCT	NOV	DEC	
Addis Ababa OBS	M. Max. T.	23.6	24.6	24.8	24.4	24.8	23.2	20.8	20.8	21.5	22.6	22.9	23.1	23.1
	M. Min. T.	9.0	10.3	11.6	12.1	12.4	11.5	11.3	11.5	11.3	10.2	8.7	8.2	10.7
	M. Mon. T.	16.3	17.4	18.2	18.3	18.6	17.4	16.1	16.2	16.4	16.4	15.8	15.7	16.9
Asgori	M. Max. T.	27.5	28.5	29.0	28.4	29.0	27.6	25.0	24.8	25.4	25.8	26.5	26.8	27.0
	M. Min. T.	7.1	7.6	9.0	10.2	9.4	9.7	10.7	11.0	9.9	6.0	4.6	4.9	8.3
	M. Mon. T.	17.3	18.0	19.0	19.3	19.2	18.7	17.8	17.9	17.7	15.9	15.5	15.8	17.7
Holeta	M. Max. T.	23.8	24.7	24.8	24.3	24.7	22.9	20.1	19.8	20.8	22.3	23.0	23.3	22.9
	M. Min. T.	3.4	5.1	7.3	8.3	8.0	7.9	9.4	9.5	8.0	4.9	2.0	1.6	6.3
	M. Mon. T.	13.6	14.9	16.1	16.3	16.4	15.4	14.8	14.7	14.4	13.6	12.5	12.5	14.6
Tulubolo	M. Max. T.	24.3	25.0	25.3	25.5	25.7	24.8	23.3	23.5	23.6	23.3	23.9	23.6	24.3
	M. Min. T.	8.6	8.7	9.7	9.9	9.6	9.8	9.8	9.8	9.3	9.0	8.5	8.3	9.2
	M. Mon. T.	16.4	16.9	17.5	17.7	17.6	17.3	16.6	16.6	16.5	16.2	16.2	15.9	16.8
Mean Monthly Temperature of all Stations		15.9	16.8	17.7	17.9	17.9	17.2	16.3	16.3	16.2	15.5	15.0	15.0	16.5

Therefore the mean monthly temperature of the study area is 16.5 ^{0}C.

The rainfall-temperature relation shows that rainy season is characterized by low temperature. The dry season on the other hand is characterized by high temperature (Fig 4.3).

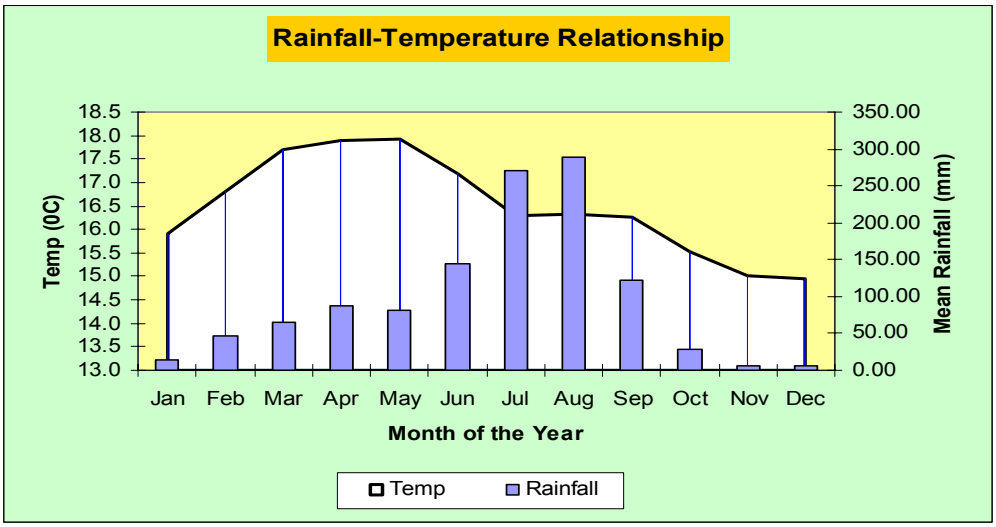

Fig 4.3 Relationship of temperature versus rainfall

4.3 RELATIVE HUMIDITY

Relative humidity for the stations of Addis Ababa and Holeta Research Center are used for the analysis since there is no data for this parameter in the study area. The measurement was conducted twice in a day; at 1200 and 1800. Mean monthly relative humidity is calculated as in the Table 4.5.

Table 4.5 Mean monthly relative humidity of the study area (%)

Station Name	MON. M. R. HUMIDITY	JAN	FEB	MAR	APR	MAY	JUN	JUL	AUG	SEP	OCT	NOV	DEC	AVG
ADDIS ABABA OBS	(1800)	40.93	38.67	42.50	47.97	47.50	61.03	73.63	74.77	66.73	46.67	41.45	40.18	51.84
	(1200)	41.83	40.83	43.53	46.63	43.67	54.43	66.40	67.60	59.40	41.93	38.77	38.28	48.61
	MEAN	41.38	39.75	43.02	47.30	45.58	57.73	70.02	71.18	63.07	44.30	40.11	39.23	50.22
HOLETA	(1800)	36.64	39.78	43.50	52.56	48.83	65.06	79.78	81.67	73.78	48.22	40.44	36.94	55.08
	(1200)	36.97	39.61	41.94	48.11	42.89	56.28	70.83	72.00	62.89	43.61	35.44	33.64	49.04
	MEAN	36.81	39.69	42.72	50.33	45.86	60.67	75.31	76.83	68.33	45.92	37.94	35.29	52.06
	AVERAGE HUMIDITY	**39.09**	**39.72**	**42.87**	**48.82**	**45.72**	**59.20**	**72.66**	**74.01**	**65.70**	**45.11**	**39.03**	**37.26**	**51.14**

So, the mean relative humidity of the study area is 51.14 %.

4.4 WIND SPEED

Evaporation from a free water surface is facilitated by the movement of air molecules (wind). The wind acts to remove the vapor in contact with the water surface to an area away from the site. In the same way, since the wind speed data for the study area is not available, the data for the Addis Ababa and Holeta station is used. Accordingly, the mean wind speed calculated for the study area is 0.61 m/s (Table 4.6).

Table 4.6 Mean monthly wind speed (m/s) above 2m from ground surface.

Station	JAN	FEB	MAR	APR	MAY	JUN	JUL	AUG	SEP	OCT	NOV	DEC	AVG (annual)
ADDIS ABABA OBS	0.72	0.73	0.82	0.83	0.75	0.45	0.37	0.34	0.45	0.79	0.77	0.73	0.65
HOLETA	0.63	0.66	0.73	0.69	0.70	0.48	0.40	0.39	0.43	0.54	0.58	0.60	0.57
MEAN WIND SPEED	0.68	0.70	0.77	0.76	0.73	0.46	0.39	0.36	0.44	0.66	0.68	0.67	0.61

The yearly wind speed pattern shown in Fig 4.4 in the same manner as temperature depicts that the wind speed is lowest in the rainy season. This might be the effect of orography lowering the speed of the wind blowing from the northwest.

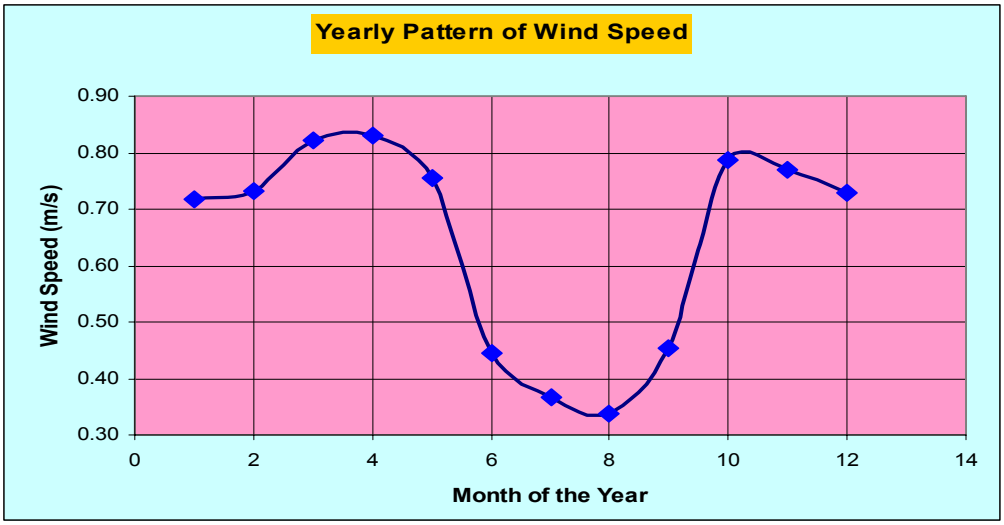

Fig 4.4 The yearly wind speed pattern of the study area

4.5 EVAPOTRANSPIRATION

A value of the actual evapotranspiration over a catchment is often obtained by first calculating the potential evaporation plus transpiration (PET), i.e. assuming unrestricted availability of water, and then modifying the answer by accounting for the actual soil moisture content.

4.5.1 Potential Evapotranspiration (PET)

Thornthwaite, 1948, conceptually defined potential evapotranspiration (PET) as the rate at which evapotranspiration would occur from an area completely and uniformly covered with growing vegetation which has access to an unlimited supply of soil water and without advection or heat storage effects. And according to Jensen et.al.,1990, operational definition, practically PET is defined by the method used to calculate it, and many methods have been proffered.

Jensen et al., 1990 suggested that the methods can be classified on the basis of their data requirements as temperature based, that uses only air temperature and some times day length; radiation based, that uses net radiation and air temperature; combination, based on the Penman combination equation which uses net radiation, air temperature, wind speed and relative humidity; and pan, that uses pan evaporation, some times with modifications depending on wind speed, temperature, and humidity. For this paper the Penman or Combination method and Thornthwaite method are applied to calculate the potential evapotranspiration as follows.

4.5.1.1 Penman or Combination Approach

According to Van Bavel, 1966, since Penman or Combination method gives satisfactory results and it has a theoretical foundation, and it requires meteorological inputs that are widely available or can be reasonably well estimated from available data, it has been adopted to quantify the PET of the study area.

The Penman or Combination approach to calculate PET is done using the following formula and steps, and the result of the calculation is presented below in Table 4.7.

$PET = ((\Delta/\gamma)\, H_T + E_{at}) / ((\Delta/\gamma) + 1)$

Δ = the slope of the curve of saturated vapor pressure plotted against temperature

γ = hygrometric constant (0.27mmHg/^{0}F)

$E_{at} = 0.35(0.5 + u_2/100)(e_a - e_d) = f(u)(e_a - e_d)$

e_a = the saturated vapor pressure at air temperature, T_a

e_d = the saturated vapor pressure at the dew point = $e_a * H_R/100$

$T_d = e_a - e_d$ = the saturation deficit

u_2 = mean wind speed at 2m above the surface, miles/day

E_a = energy for evaporation based on the air humidity and air temperature

$H_T = R_I(1-r) - R_0 = 0.75R_I - R_0$ is the net heat

R_I = incoming radiation, R_0 = outgoing radiation, r = albedo

$R_0 = \sigma Ta^4 (0.47 - 0.075\sqrt{e_d})\ (0.17 + 0.83n/N)$

σTa^4 = the theoretical black body radiation at T_a

T_a = mean air temperature for a month, ^{O}C

σ = the Stephan Boltzman Constant, = $5.67 * 10^{-8} Wm^{-2}/K^4$

Taking account of the increased albedo for vegetation and introducing the multiplying factor 0.95 to σTa^4 since vegetation does not radiate as a perfect black body, the following equation for H is used:

$H = 0.75R_a(0.18 + 0.55n/N) - 0.95\sigma Ta^4(0.10 + 0.9\, n/N) - (0.56 - 0.092\sqrt{e_d})$

$R_I(1-r) = 0.75R_a * f_a(n/N)$

$f_a(n/N) = 0.16 + 0.62n/N$ for latitudes south of $54_{1/2}^0$ N

R_a = solar radiation (fixed by latitude and season) = 10^0 considered for the study area

n = bright sunshine over the same period, h/day, H_T = the available heat

N = mean daily duration of maximum possible sunshine hours (North Latitudes) = 10^0 considered for the study area

Table 4.7 Mean annual PET obtained from Penman method

ELEMENTS	JAN	FEB	MAR	APR	MAY	JUN	JUL	AUG	SEP	OCT	NOV	DEC	(ANNUM)
T (^{0}C)	16.29	17.45	18.21	18.25	18.58	17.37	16.06	16.17	16.41	16.38	15.80	15.66	
n(Hrs)	8.3	8.3	7.3	6.7	6.9	4.9	3.2	3.3	4.8	7.9	9.2	9.1	
N (Hrs)	11.7	11.9	12	12.2	12.5	12.6	12.4	12.4	12.1	11.9	11.7	11.6	
n/N	0.708	0.695	0.611	0.548	0.551	0.387	0.255	0.265	0.398	0.662	0.784	0.785	
H_R (%)	39.09	39.72	42.87	48.82	45.72	59.20	72.66	74.01	65.70	45.11	39.03	37.26	
u_1 (m/s)	0.68	0.70	0.77	0.76	0.73	0.46	0.39	0.36	0.44	0.66	0.68	0.67	
u_2 (miles/h)	1.52	1.57	1.72	1.70	1.63	1.03	0.87	0.81	0.98	1.48	1.52	1.50	
e_a (mmHg)	13.95	14.96	15.6	15.7	16.03	14.88	13.65	16.79	14	13.89	13.42	13.3	
e_d	5.45	5.94	6.69	7.66	7.33	8.81	9.92	12.43	9.20	6.27	5.24	4.96	
Δ/γ	1.83	1.93	2	2.01	2.05	1.92	1.8	1.808	1.835	1.83	1.77	1.75	
R_a (mm/day)	14.6	15	15.2	14.7	13.9	13.4	13.6	14.3	14.9	15	14.6	14.3	
E_{at}	1.533	1.628	1.613	1.454	1.572	1.084	0.664	0.776	0.857	1.374	1.476	1.504	
R_l (1-r)	6.559	6.648	6.143	5.510	5.229	4.019	3.245	3.478	4.546	6.417	7.075	6.936	
R_0	3.03	2.95	2.60	2.29	2.34	1.68	1.22	1.10	1.66	2.74	3.28	3.34	
f_a (n/N)	0.599	0.591	0.539	0.500	0.502	0.400	0.318	0.324	0.407	0.570	0.646	0.647	
σTa^4 (mm/day)	13.58	13.76	13.92	13.96	13.97	13.83	13.66	13.66	13.65	13.51	13.41	13.41	
H_T	3.524	3.697	3.540	3.221	2.890	2.339	2.026	2.383	2.889	3.674	3.790	3.598	
PET (mm/day)	2.82	2.99	2.90	2.63	2.46	1.91	1.54	1.81	2.17	2.86	2.95	2.84	
PET (mm/month)	87.44	86.74	89.83	79.03	76.20	57.28	47.73	56.12	65.17	88.69	88.63	87.94	910.80

Therefore, the total annual PET of the catchment obtained using Penman or Combination method is 910.80 mm/year.

4.5.1.2 Thornthwaite Approach

The formula is based mainly on temperature with an adjustment being made for the number of day light hours. An estimate of the potential evapotranspiration, PET, (Table 4.8) calculated on a monthly basis, is given by:

$$PET_m = 16N_m(10\check{T}_m/I)^a \text{ mm}$$

$$I = \sum i_m = \sum(\check{T}_m/5)^{1.5}$$

Where,

$a = 6.7 \times 10^{-7}I^3 - 7.7 \times 10^{-5}I^2 + 1.8 \times 10^{-2}I + 0.49$ (to 3 significant digits) = 1.636

N_m (day light factors) – obtained by dividing the possible sunshine hours for the appropriate latitude by 12 (it is the monthly adjustment factor related to hours of daylight),

m = months in a year 1, 2, 3, ---, 12,

$\check{T}_m$ = monthly mean temperature, ^{0}C,

I = the heat index for the year = 71.921

Table 4.8 Mean annual PET obtained from Thornthwaite method

Element	Months of a Year												TOTAL
	JAN	FEB	MAR	APR	MAY	JUN	JUL	AUG	SEP	OCT	NOV	DEC	
$\check{T}_m$ (^{0}C)	15.9	16.8	17.7	17.9	17.9	17.2	16.3	16.3	16.2	15.5	15.0	15.0	
N	11.7	11.9	12	12.2	12.5	12.6	12.4	12.4	12.1	11.9	11.7	11.6	
N_m	0.975	0.992	1.000	1.017	1.042	1.050	1.033	1.033	1.008	0.992	0.975	0.967	
i_m	5.881	6.520	6.950	6.973	7.163	6.475	5.757	5.816	5.946	5.929	5.617	5.543	I = 71.921
PET_m	57.12	63.70	69.79	72.21	74.34	69.91	63.07	63.23	61.18	55.85	51.92	51.28	753.61

From the above two approaches, since the Thornthwaite method underestimates the PET the value obtained from Penman Combination method seems to be representative. As a result, for further analyses the catchment's annual PET is considered to be 910.80 mm.

4.5.2 Actual Evapotranspiration (AET) – Obtaining AET from PET

Actual evapotranspiration is used to describe the amount of evapotranspiration that occurs under field conditions (Thornthwaite, 1944). A Value of the actual evapotranspiration (AET) over a catchment is more often obtained by first calculating the potential evapotranspiration, i.e., assuming an unrestricted availability of water, and then modifying the results by accounting for the actual soil moisture content. When the vegetation is unable to abstract water from the soil, then actual evapotranspiration becomes less than potential. Thus, the relationship between AET and PET depends up on the soil moisture content. When the soil is saturated or when it is at its field capacity, PET = AET (Shaw, 1984).

4.5.2.1 Soil – Water Balance Method – Thornthwaite and Mather, 1957

The soil-water balance of the study area was conducted for the purpose of finding the actual evapotranspiration of the catchment. The approach strictly follows the one outlined by Thornthwaite and Mather, 1957. Values of the major components of the soil water balance are presented in Table 4.9.

Table 4.9 Soil-water balance method (Thornthwaite & Mather, 1957)

mm	JAN	FEB	MAR	APR	MAY	JUN	JUL	AUG	SEP	OCT	NOV	DEC	TOTAL
PPT (1)	14.63	46.21	65.26	87.59	81.47	144.55	269.87	288.88	123.02	28.79	6.02	5.70	1161.98
PET (2)	87.44	86.74	89.83	79.03	76.20	57.28	47.73	56.12	65.17	88.69	88.63	87.94	910.80
PPT-PET (3)	-72.81	-80.77	-64.49	-29.26	-16.43	36.84	264.93	578.04	229.44	-60.56	-87.28	-87.64	
ACPWL (4)	-297.55	-338.08	-362.65							-59.90	-142.50	-224.74	
	Moderately Deep Rooted Crops (AWCR = 150 mm)												
SM-1 (5)	21	16	13	21.56	26.83	114.10	150	150	150	101.00	58	33.5	
ΔSM-1 (6)	-13.5	-5.00	-3.00	8.56	5.27	87.27	35.90	0.00	0.00	-49.00	-43.00	-24.50	
AET-1 (7)	28.13	51.21	68.26	79.03	76.20	57.28	47.73	56.12	65.17	77.79	49.02	30.20	654.94
D-1 (8)	59.31	35.53	21.57	0.00	0.00	0.00	0.00	0.00	0.00	10.90	39.61	57.74	255.86
S-1 (9)	0	0	0	0	0	0	186.24	232.76	57.85	0	0	0	476.84
TARO-1 (10)	13.80	6.90	3.45	1.72	0.86	0.43	186.24	325.88	220.78	110.39	55.20	27.60	
RO-1 (11)	6.90	3.45	1.72	0.86	0.43	0.22	93.12	162.94	110.39	55.20	27.60	13.80	462.83
DET-1 (12)	6.90	3.45	1.72	0.86	0.43	0.22	93.12	162.94	110.39	55.20	27.60	13.80	
	Deep Rooted Crops (AWCR = 250 mm)												
SM-2 (5)	78	67	61.25	69.81	75.08	162.35	250	250	250	197.25	142.25	103.5	
ΔSM-2 (6)	-25.5	-11.00	-5.75	8.56	5.27	87.27	87.65	0.00	0.00	-52.75	-55.00	-38.75	
AET-2 (7)	40.13	57.21	71.01	79.03	76.20	57.28	47.73	56.12	65.17	81.54	61.02	44.45	692.44
D-2 (8)	47.31	29.53	18.82	0.00	0.00	0.00	0.00	0.00	0.00	7.15	27.61	43.49	218.36
S-2 (9)	0	0	0	0	0	0	134.49	232.76	57.85	0	0	0	425.09
TARO-2 (10)	12.99	6.50	3.25	1.62	0.81	0.41	134.49	300.00	207.85	103.92	51.96	25.98	
RO-2 (11)	6.50	3.25	1.62	0.81	0.41	0.20	67.25	150.00	103.92	51.96	25.98	12.99	411.90
DET-2 (12)	6.50	3.25	1.62	0.81	0.41	0.20	67.25	150.00	103.92	51.96	25.98	12.99	
	Mature Forest (AWCR = 400 mm)												
SM-3 (5)	195	175	160	168.56	173.83	261.10	400	400	400	370	300	260	
ΔSM-3 (6)	-65	-20.00	-15.00	8.56	5.27	87.27	138.90	0.00	0.00	-30.00	-70.00	-40.00	
AET-3 (7)	79.63	66.21	80.26	79.03	76.20	57.28	47.73	56.12	65.17	58.79	76.02	45.70	742.44
D-3 (8)	7.81	20.53	9.57	0.00	0.00	0.00	0.00	0.00	0.00	29.90	12.61	42.24	168.36
S-3 (9)	0	0	0	0	0	0	83.24	232.76	57.85	0	0	0	373.84
TARO-3 (10)	12.19	6.09	3.05	1.52	0.76	0.38	83.24	274.38	195.03	97.52	48.76	24.38	
RO-3 (11)	6.09	3.05	1.52	0.76	0.38	0.19	41.62	137.19	97.52	48.76	24.38	12.19	361.46
DET-3 (12)	6.09	3.05	1.52	0.76	0.38	0.19	41.62	137.19	97.52	48.76	24.38	12.19	

Descriptions and approaches to computation of each of the main components that basically influence the balance are presented below.

The mean monthly precipitation (PPT) values obtained from Theissen Polygon method is presented in the first raw of Table 4.9.

The mean potential evapotranspiration (PET) calculated using the Penman Approach is listed in raw 2.

Changes in the balance of the precipitation and meteorologic demand of each month is computed and presented in raw 3, following the computation, the accumulated

potential water loss which is obtained by adding meteorologic demands (the negative values of P-PET) of consecutive months are listed in raw 4.

The available water capacity of the soil is obtained from a table developed by Thornthwaite and Mather, 1957. The above table provides AET calculated data for three vegetation types, i.e. for moderately deep rooted (MDR) crops having a rooting depth of 0.50 m grown on a clay soil texture with available water capacity of the root zone of 150 mm, for deep rooted (DR) crops having a rooting depth of 1.00 m grown on a clay loam soil texture with available water capacity of the root zone of 250 mm, and for a mature forest (MF) grown on a clay loam soil texture having a rooting depth of 1.60 m with available water capacity of the root zone of 400 mm. The AET obtained from the different types of vegetation are weighted for the area coverage of different land covers. Table 4.10 presents the contribution of each land cover to the different crops.

Table 4.10 Area of land cover and their proportion for vegetation type

LC/LU	Area (km^2)	% of Total	MDR		DR		MF		Area Covered
			% MDR	Area MDR	% DR	Area DR	% MF	Area DR	
Forest	20.09	4.05	0	0	0	0	80	16.072	16.07
Asphalt Road	12.92	2.61	0	0	0	0	0	0	0.00
Town	6.74	1.36	0	0	0	0	0	0	0.00
Bush and Shrubs	105.40	21.25	10	10.54	65	68.51	10	10.54	89.59
Swamp	13.51	2.72	20	2.70	15	2.0265	0	0	4.73
Cultivated/Grassland	317.34	63.99	70	222.14	10	31.73	10	31.734	285.61
Bare Land	19.91	4.01	0	0	10	1.991	00	0	1.99
Total	495.91	100.00	100	**235.38**	100	**104.26**	100	**58.35**	**397.99**

Cover Type	**MDR**	**DR**	**MF**	**Total**
% Area of LC from total	47.46	21.02	11.77	80.25

Using the graph of water retained in the soil against an accumulated potential water loss, and the available water capacity for the soil, the amount of water that will be retained by the soil (soil moisture, SM) calculated for each month is listed in raw 5.

The change in the soil moisture during the month is obtained by deducting the soil moisture of the month under consideration from the soil moisture of the preceding month. These values are entered in raw 6.

The actual evapotranspiration equals the potential rate during the months when the precipitation exceeds potential evapotranspiration. This is because the rain water is considered to be easily available to the plant even if the soil moisture of the whole root zone is not raised to the available water capacity. At times when the potential evapotranspiration exceeds the precipitation amount the actual evapotranspiration will be equal to the sum of precipitation and the amount of soil moisture withdrawn from storage.

The soil moisture deficit is calculated easily by subtracting the actual evapotranspiration from the potential. The moisture surplus (amount of water that can not be stored), which is attained after the soil moisture reaches its field capacity, is obtained by subtracting the change in soil moisture from values of (P-PET).

The total amount of water available for run off is simply equal to the amount of soil moisture surplus for the first month, but its value for the superseding months could be obtained by adding the surplus of the month and the detained amount of water in the preceding month because this detained water is thought to be readily available for run off for the coming month. These values are listed in row 10 of table.

Based on the bold assumptions of Thornthwaite and Mather, 1957, 50% of the surplus water that is available for run off in any month actually runs off, the rest 50% of the surplus is detained in the subsoil, groundwater and channels of the catchment and is available for runoff during the next month.

Finally, the actual evapotranspiration obtained from the three vegetation types are weighted based on their proportional area coverage from the general land cover map of the study area. In addition, the runoff is averaged for the three and the graph of annual water balance is presented in Table 4.11.

Table 4.11 Weighted actual evapotranspiration for the study area

	Jan	Feb	Mar	Apr	May	Jun	Jul	Aug	Sep	Oct	Nov	Dec	Total
PPT	14.63	46.21	65.26	87.59	81.47	144.55	269.87	288.88	123.02	28.79	6.02	5.70	1161.98
PET (mm/mon)	87.44	86.74	89.83	79.03	76.2	57.28	47.73	56.12	65.17	88.69	88.63	87.94	910.8
AET (weighted)	48.97	58.21	73.17	79.03	76.20	57.28	47.73	56.12	65.17	72.71	62.02	40.12	696.61
RO avg.	6.50	3.25	1.62	0.81	0.41	0.20	67.33	150.04	103.94	51.97	25.99	12.99	412.06

Based on the data from Table 4.11, the monthly water balance of the study area is shown in Fig 4.5 and the calculated runoff is plotted in Fig 4.6.

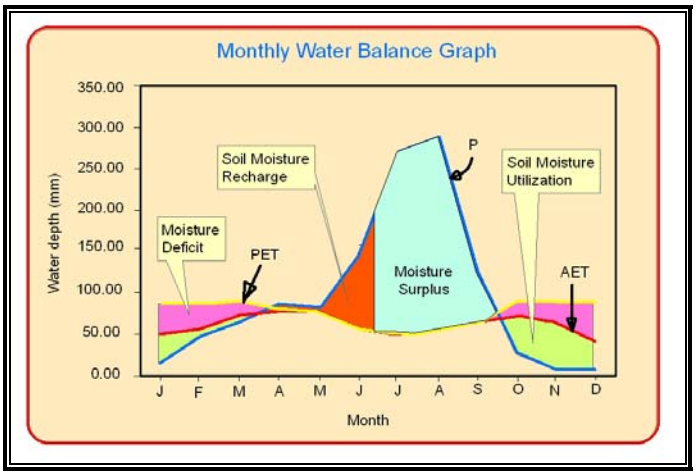

Fig 4.5 Annual soil-water balance of the study area

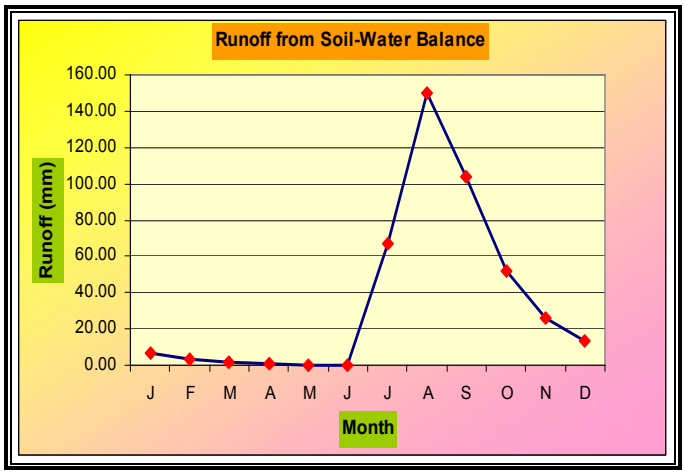

Fig 4.6 Runoff plot from soil-water balance of the study area

4.5.2.2 Water Balance of the Study Area

The main objectives of balancing the hydrologic components of the study area lie in identifying the annual groundwater recharge and the actual evapotranspiration of the area. In order to bring these objectives into effect, two water balance approaches, which have generally the same ground but presented in different forms, have been applied.

Based on soil-water balance approach of Thornthwaite and Mather, 1957 which helps to quantify the annual actual evapotranspiration of the area on the basis of the potential evapotranspiration already computed by using empirical formulae is applied

to estimate the annual recharge. The annual groundwater recharge using the general water balance equation for the catchment is estimated as follows:

$$\mathbf{PPT = AET + SRO \pm \Delta G + W}$$

Where SRO (= 322.73 mm) is the sum of the surface runoff for the months that precipitation exceeds the actual evapotranspiration obtained using the soil-water balance. As for the withdrawal, W, an average pumping rate of 3 l/s is considered based on the number of wells (60) available in the study area and it is approximated to 11.47 mm/year.

$$\Delta G = PPT - AET - SRO - W$$
$$= 1161.98 \text{ mm} - 696.61 \text{ mm} - 322.73 \text{ mm} - 11.47 \text{ mm}$$
$$= 131.17 \text{ mm/annum}$$

Accordingly, the total annual recharge into the groundwater system of the catchment is estimated to be 65 Million m^3.

4.6 OBTAINING STREAM FLOW DATA FOR ATEBELA RIVER

Atebela River does not have a stream gauge at its mouth. Generally two approaches have been adopted and integrated to obtain the likely discharge data of the river: scaling up the stream flow values from the gauge to the size of the drainage area of the project stream and runoff coefficient.

4.6.1 Scaling Up

Scaling up is made by calculating the proportionality (Drainage-Area Ratio) between the project site drainage area and the drainage area of the gauged catchment. The conditions considered for the estimation of the discharge are similarity in topography, climate patterns, soil characteristics, land-use and land cover.

The discharge data at the mouth of Atebela River is extrapolated from the discharge value obtained using Time-plot for Holeta River after analysis of river discharge data collected from the Ministry of Water Resources at GPS location of 0445883 E, 1004205 N on the basis of drainage area ratio:

$$\mathbf{Q_A = (A_H/A_A)\ Q_H}$$

Where,

A_H is the drainage area of Holeta River, 111 km^2

A_A is total drainage area of Atebela River catchment, 300.94 km^2

Q_H is steam flow in m^3/s of Holeta River, 5.62 m^3/s

Q_A is the discharge in m^3/s at the mouth of Atebela River.

Although the study involves a catchment area of 495.91 km^2, the actual area covered by the drainage of the Atebela River is 300.94 km^2. The rest of the streams flow to form swamp around Tefki town during the rainy season. Therefore, the discharge at the mouth of Atebela River using the above appraoch is 2.07 m^3/s.

4.7.2 Runoff Coefficient

The runoff coefficient is calculated using the assumption that runoff is a certain factor of the precipitation. Therefore, the runoff which is equal to 5.616 m^3/s (or 357.8 mm/year) obtained from the discharge data of Holeta River for the year 2004 using the Time-plot (Fig 4.7) divided by the total annual rainfall for Holeta is:

$$\mathbf{K = R_H\ (mm)/P_H\ (mm)}$$
$$= 357.8/973.13$$
$$= 0.367$$

Applying the runoff coefficient to the study area, the total discharge at the mouth of Atebela River is calculated to be 402.2 mm (or 6.31 m^3/s) using average precipitation of 1095.87 mm for the study area.

Discharge data collected at the mouth of Atebela River for three days at 10:30 am using flow meter is used to confirm the runoff amount. But, this does not consider the amount of discharge from effluents into Atebela River. The discharges are taken from June 08 – 10, 2007 (Annex 5). Accordingly, the discharge obtained using the runoff coefficient seems to exaggerate the value since it does not consider most of the factors influencing the runoff.

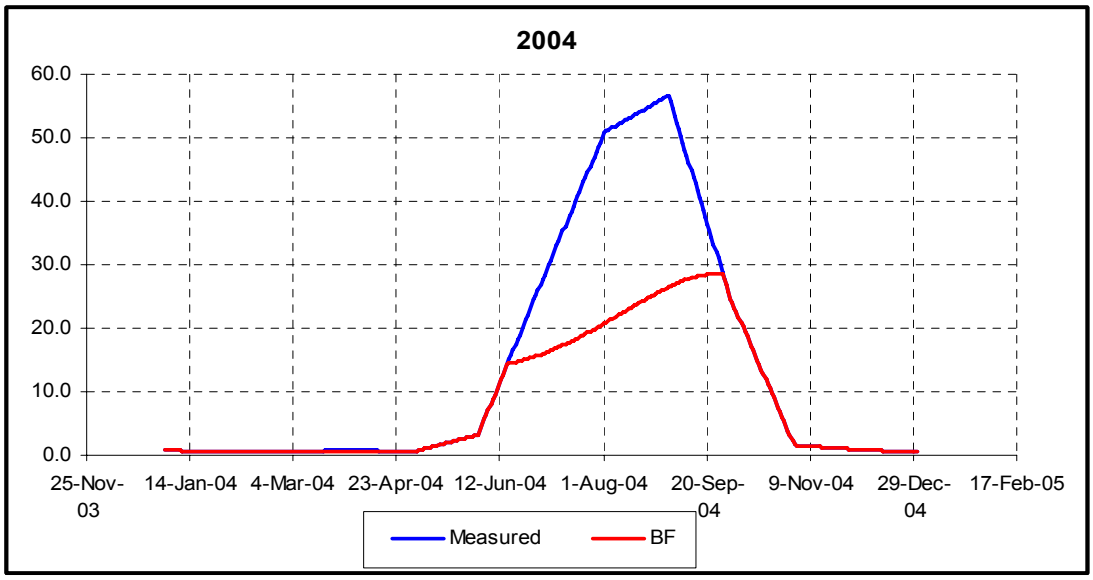

Fig 4.7 Base flow-runoff separations using Time-plot of Holeta River (2004)

CHAPTER V

5. GEOLOGY AND HYDROGEOLOGY

5.1 GEOLOGY

5.1.1 Regional Geology

The regional geological description of the study area is adapted from the report of Construction Rock Materials Study Project in Areas around Finfinne, Adama, and Ambo, presented by Oromia Mineral Resources Development Agency as prepared by Gelana Gadissa (2005). The study area is found in the central part of Ethiopia on the northwestern margin of the Rift Escarpment.

The regional geological setting of the area consists of one major rock group, namely Rift/Post-Rift Volcanic Products and Sediments (Fig 5.1). The Rift/Post-Rift Volcanics and Sediments, mostly confined to the zone of the Main East African Rift System generally stretching in the northeast direction across the area, comprise a rather complex geology with diverse rock units of basic to acidic composition. These are results of series of different volcano-tectonic activities in the Quaternary Period.

Details of the regional geology, as extracted from previous workers' reports (mainly from a compilation work of GEODEV–AFREDS (1999)), are provided in the following subsections.

5.1.1.1 Post Rift Volcanics and Sediments

5.1.1.1.1 Nazret Group

The name Nazret Group (Nn) was assigned to a thick succession of stratoid silicics of the Rift Valley floor with some occurring along Rift margins and adjacent plateau (Kazmin & Seifemichael Berhe, 1978, 1981; Kazmin et al., 1979). The stratoid silicics consist of rocks such as fiamme ignimbrites, pumice, ash, trachyte and rhyolite flows and domes with rare intercalations of basalt flows. In the Rift floor they reach a

thickness up to 250 m or more, and tend to thin towards the escarpment. On the plateau margins they range in thickness from 1 to 30 m.

The map unit had been assigned different local names by different authors. Mohr (1971) included the Nazret Group in his “Twit Series” for the peralkaline silicics of central and southern Oromia which include not only acidic rocks of the Rift but also the Alaji Formation. Zanettin and Justin-Visentine (1974c) used the name Balchi Rhyolites that predominantly consisted of tuffs and rhyolite. Juch (1975) called the same unit Pliocene Silicics a misfit for the actual age range of the unit. Later Meyer et al. (1975) introduced the name Nazret Series, which was later, replaced by Nazret Group (Kazmin & Seifemichael Berhe, 1978).

An area of maximum thickness of the silicic rocks occurs in the central part of the Rift. The thickness decreases sharply from the center of the Rift due north and south. In the study area the Nazret silicics appear beneath the younger volcanics (Juch, 1978).

5.1.1.1.2 Afar Group

a) Chilalo Formation

Several large trachytic volcanoes occur along both the eastern and western outer margins of the Rift Escarpment (Seifemichael Berhe & Kazmin, 1978; Kazmin 1979; Kazmin et al., 1981). These groups of complex shield volcanoes which developed on both sides of the Rift shoulders and margins of the Rift were described as Chilalo Trachytes, Chilalo & Bada Trachytes, Chilalo volcanics. They are Pliocene in age and are later named as Chilalo Formation (Mengesha et.al., 1996). Complex central volcanoes such as Chilalo, Bada, Kaka, Enkolo, Gara Gumbi, Asebot, Afdam, Bosete, Gash, Megal and other smaller volcanoes in the vicinity of Addis Ababa are well known volcanic centers. Kazmin et al. (1981) identified two clear volcanic units in a number of these complex volcanoes including Chilalo, Bada and Kubsa volcanoes. The lower unit consists of peralkaline ignimbrite and trachyte intercalations. The trachytes show clear flow structures. Highly porphyritic, dark grey trachyte with phenocrysts of sanadine represents the major rock types. Rhyolites are the first

products of the Chilalo Volcano followed by trachytes, whereas basalts followed by trachy basalts and trachytes are the products of the Beda Volcano. These flows are synchronous with younger ignimbrites of the Nazret Group, and partly inter-finger with them, making it part of the Nazret Group.

To date the following K-Ar ages are available: for the Wochecha 4.5 MY (Miller & Mohr, 1966), for Yerer 3.5 MY (Morton & Rex., 1979), for Chilalo 3.5 MY (Kuntz et al., 1975) and for Menagesha 3.0 MY (Morton & Rex., 1979). A relatively recent age of 1.4MY was reported by Di Paola (1976) for mugearitic flow on the western slope of Chilalo volcano, suggesting that some of the volcanic activity has probably continued into the Pleistocene. Di Paola (1972) has related the origin of these volcanoes to the opening of the Main Rift System of the area. The formation of these volcanoes coincided with the important stage of the opening of the Rift which is around 4 to 4.5 MY even though the Rift started opening much earlier (Kazmin et al., 1981). This rifting corresponds to the peak of the silicic volcanism in the Rift (Morbidelli et al., 1975; Kazmin et al. 1981.

b) Bishoftu Formation

An area in east Shewa Zone, south and southeast of Addis Ababa, is covered by Pliocene to Pleistocene alkali basalt and trachyte lava flows with well preserved scoria cones. They occur on the western escarpment of the Main Rift System and were named as Bishoftu Basalts (Zanettin and Justine-Visentin 1974), which considered them as younger than 2 MY old. These basalts are later named as Bishoftu Formation (Mengesha et al., 1996). Field investigation (Kazmin et al., 1981) has proved that these flows originated partly form at least the large Pliocene basaltic and trachytic volcanoes such as Yerer, Wechecha, Furi, etc. This proposition was similarly supported by age similarity of 2-8 MY on the basalt between the towns of Akaki and Bishoftu, southwest of Yerer Mountain (Morton, 1979).

5.1.1.1.3 Wonji Group

In the Main Rift System, in east Shewa and adjacent zones, Meyer et al. (1975) named Wonji Series to the volcanic succession younger than 1.6 MY and lying along or close to the Wonji Fault Belt (Mohr, 1967). It was pointed out that the latest volcanism in the Rift is related to crustal extensions along the axial zone of the Wonji Fault Belt (Mohr, 1967a; Meyer et al., 1975; Gibson, 1970; Dakin and Gibson, 1971). Although some volcanic activities occur outside the Wonji Fault Belt, bulk of the Pleistocene to recent volcanic activity is controlled by this tectonic feature. The Wonji Group includes the entire Rift volcanics formed after the last major event of rifting.

One of the major complexes that has been identified within the Wonji Group in the vicinity of the study area (Kazmin and Seifemichael Berhe, 1978; Kazmin et al., 1981) is fissural basaltic eruptions - sub recent and / recent fissural basalt flows. The recent fissure basalts are mainly concentrated along the Wonji Fault Belt, and also occur in western margin of the rift (Kazmin and Seifemichael Berhe, 1978; Kazmin et al., 1981). The flows are controlled by extensional fractures and exhibit fresh surface that took place during the historical period. Relatively older basalt flows synchronous with early stages of formation of the pantelleritic volcanoes are fissural products whereas the youngest are of central type eruption. Lines of well-preserved scoraceous cones follow fractures in the Wonji Fault Belt, which cut across the pantelleritic volcanoes. Recent flows followed low topographic features, or followed over the fault escarpments as shown on Fig 5.1 along the road to Butajira in the vicinity of the study area.

5.1.1.1.4 Alluvial and Lacustrine Deposits

a) Lacustrine Deposits

Although sinking of the main Rift System was dominantly accompanied by volcanic activity, sedimentation was also an integral part of the Rift formation. In the Rift, Quaternary sediments and mostly of lacustrine origin are intercalated with Pliocene to Pleistocene ignimbrites both in the Rift floor and Rift shoulders. The oldest sediments

are lacustuine diatomites, tuffaceous clays and silts interbedded with basal ignimbrites of the Nazret Group. These sediments are named Chorora Formation (Sickenburg Schonfeld 1975) and the age ranges between 9 and 7 MY (not show on the accompanying map due to scale).

The current Lakes that spread over the entire Rift Valley are remnants of once larger lakes, which used to cover major part of the developing rift floor. Pleistocene-Holocene lacustrine sediments are known in the central and southern part of the Rift in East Shewa Zone and were deposited in the huge ancestral lake whose level before 3500 to 2100 years used to be 100 meters higher than its level (Kazmin et al., 1981).

b) Alluvial Deposits

Quaternary sediments of fluvial origin are widely spread all over the area. Only the larger, more continuous areas of Quaternary deposits are shown on the map (Fig 5.1). Alluvial deposits are mostly recent, but it may include older Pleistocene sediments. Alluvial sediments cover an extensive area of western part of Ethiopia in West Wellega Zone and along the upper reaches of the Gibe River. Alluvial sediments also occur along the Tinishu Gibe River course. The alluvial sediments are mainly represented by sand, silt and clay.

5.1.1.2 Rift Structure

The Main Rift System in Ethiopia as part of the East African Rift System is a fault-bounded depression which extends from northern Afar to south up to Borena in Oromia. It generally trends SW-NE forming an elbow shape. The Rift splits the country almost into two equal parts, east and west. In the north it displays fanlike feature descending into the Afar Depression. The structural trend of the Main Ethiopian Rift continues up to the point of the Triple Junction, near Lake Abe, where the East African, Red Sea and the Gulf of Aden Rifts meet.

Rift Escarpment rises up to 1500 m above the Rift Floor. North of the latitude of Finfinne, both eastern and western escarpments are approximately at the same

altitude, and both have rather complicated structure. A major normal fault with considerable down throw can be traced at the foothills of the escarpment. In the lower slopes antithetic faults predominate separating blocks tilted down towards the Rift Floor. In the upper part of the escarpment there are several normal faults with rift ward downthrows of several hundred meters. This type of structure can be clearly seen in the eastern escarpment west of Mechara.

At the latitude of Addis Ababa, the Rift Valley appears to be crossed by a major east west transverse lineament and south of this the structure of the western and eastern escarpments is different. The Western Escarpment is generally higher in elevation and steeper than the Eastern Plateau. The western escarpment consists of three to five steps, either horizontal or slightly tilted away from the rift and separated by normal faults. West of Butajira, the escarpment is formed by a single fault of about 1000 m displacement.

5.1.1.3 Transverse Faults

Several transverse faults cross the Main Rift System (Kazmin et al., 1981; Kazmin & Seifemichael Berhe, 1978; Tadewos, 1995). They displace the escarpments and are also marked by clear alignment of volcanic centers along the faults. These faults trend predominantly NW or NNW, however, E-W faults are also common. Christiansen et al. (1975) indicated that the northwesterly trending fault line joining Ayelu and Amosa Volcanoes continues to the western escarpment of the Rift. This fault clearly displaces the segment of the Axial Wonji Fault Belt and is considered as a transform fault.

Mohr (1967a) recognized that at the latitude of Addis Ababa the Rift is crossed by a major E-W system of faults. They are marked by alignment of Pliocene trachytic volcanoes, such as Yerer, Wochecha and Menagesha.

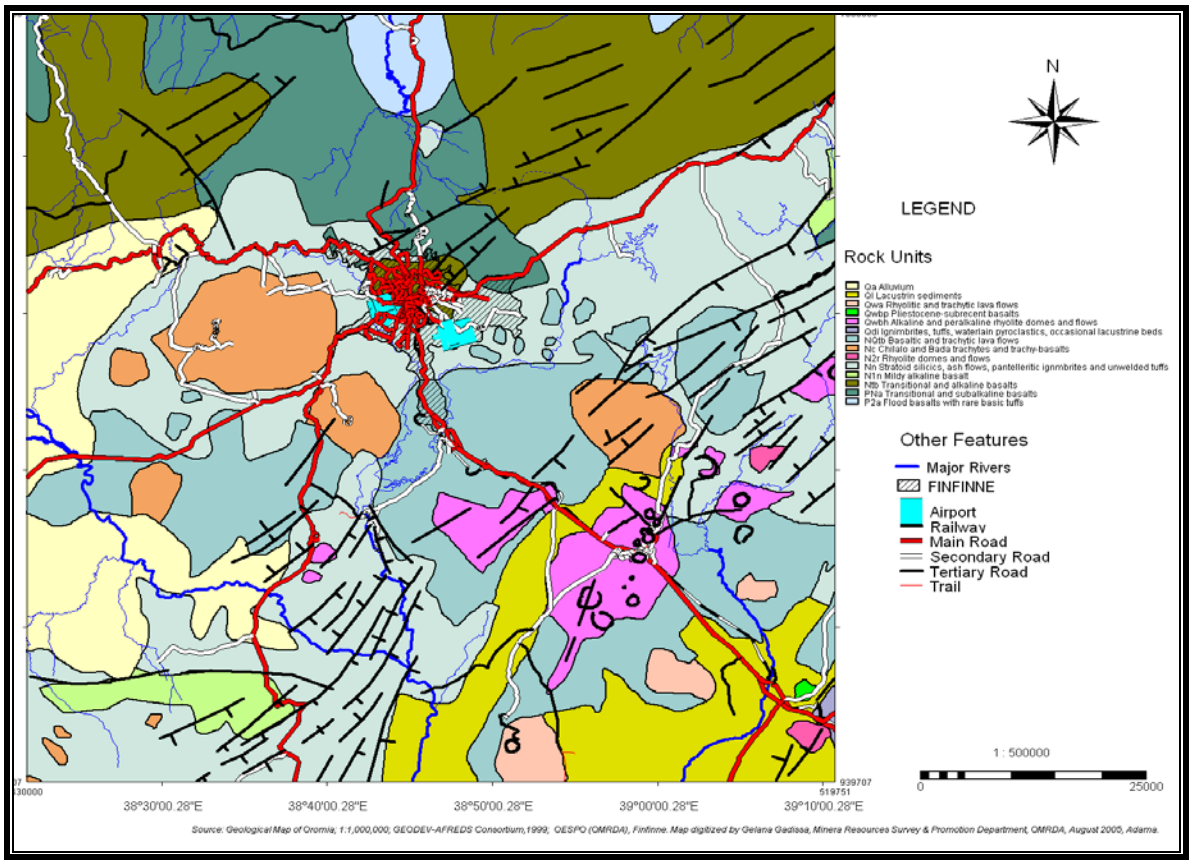

Fig 5.1 Regional geological map of the study area (from Gelana Gadissa, 2005)

5.1.2 Local Geology

5.1.2.1 Ignimbrite of the Nazret Group (Ngi)

Adama Group in general consists of fiamme ignimbrites of light greenish gray to reddish brown varieties, and unwelded tuffs. Rocks of this map unit usually occur one intercalating the other; the relatively thick deposit of unwelded tuffs and volcanic ash are most of the time blanketed by ignimbrite sheets of up to about 30 m thick in areas close to the rift margin of Northwestern Main Rift System, mainly in the vicinity of Addis Ababa and NE wards from the city; the whole system generally becomes thicker towards the Rift Axis (Fig 5.2).

It is unconformably overlies faulted blocks of Plateau Basalt Formations of Tertiary Volcanics in areas along the Rift Shoulder, and partly over the Entoto Silicics in the

vicinity of Addis Ababa. Younger volcanic products of the Rift Volcanics, mostly the younger basalts and trachyte flows, in areas of their occurrence covered the unit.

5.1.2.2 Trachyte Formation of the Wechecha Group (Qwt)

Large trachyitic volcano of Wechecha occurs along the rift escarpment close to the rift margin north of Sebeta town. This unit is also found southwest of the study area south of Tefki town. In addition, it is found along the road to Butajira. Gelana Gadissa (2005) explained that this volcano is of trachyte formation and generally forms mountain ranges and domes/plugs, with highly rugged surface characterizing the larger volcano of Wechecha. Wechecha Group is generally younger than Rocks of Nazret Group, as products of the former overlie the later unit. It in turn is overlain by products of younger volcanisms. Total thickness of the unit is more than 1000 m in the larger of volcano of Wechecha.

Wechecha Group (Qwt) in few cases has intercalations of rhyolites and ignimbrite, and rarely unwelded tuffs. The trachyte formations of Wechecha grade from more trachytic to rhyolites as one goes from base of the mountain to its top where a number of volcanic necks and plugs occur at the vents (Gelana Gadissa, 2005). Detail rock sampling and laboratory analysis was conducted by Gelana Gadisa (2005). The rock generally is porphyritic with large euhedral phenocrysts of feldspars. Some of the other minerals observed are biotite, pyroxene, iron oxide and plagioclase. It some times consist rocks of andesitic flows and/or associated tuff intercalations. Jointing due to cooling of the magma, and complex flow fold structure commonly occur in the rocks (Fig 5.2).

5.1.2.3 Rhyolite Flow of the Bilbilo Group (Qwr)

Rhyolitic flows occur mainly in the southeastern part of the study area. These include rhyolitic flows in Geja area. Most of these central volcanoes have little associated flows of the unit around the domes and cones. Similarity in many aspects of the associated rocks and the relation they have with the rest of the map units identified in this study led the authors to group the unit in to one category of Bilbilo Group (Qwr).

The rhyolitic rock of Bilbilo Group (Qwr) overlies and/or cut through older formations of namely the Nazret Group. Sometimes it is covered by recent basalt flows and scoria. It consists of rhyolitic rocks with cryptocrystalline to fine grained brittle rocks that have reddish to white color play in fresh and almost light brownish grey to white soft material when weathered. Sometimes it is difficult to distinguish the rock from equivalent units of various tuffs (trachyitic crystal tuff, andesitic crystal tuff, rhyolitic tuff, ignimbrites, etc.), perhaps, due to the effect of weathering – devitrification (Fig 5.2).

5.1.2.4 Recent Basalt Flows (Qb)

Recent basalt flows which are closely associated to the scoria cones occur mostly in the area along the road to Butajira and the central part of the catchment. The recent basalt flows occur found erupted through localized fractures across the mountain ridges of Wechecha, Furi, Entoto, etc., located along the rift shoulder. In these particular cases, the basalts flowed down the topography over the Mountain flanks and all the older units in areas of its occurrence (along its floor of eruption).

The basalt commonly occurs in boulder forms perhaps due to smaller volume of the lava, and thus has a limited thickness (less than 20m) and smaller extent. In areas of ancient depressions and stream valleys, the basalt has a relatively thick and more massive deposit with a tendency to develop columnar joint structures. The rock consists of porphyritic and rarely aphyric olivine basalt with olivine and some times plagioclase phenocrysts. The unit is more of basic, rarely andesitic, and usually scoraceous type (Fig 5.2).

5.1.2.5 Quaternary (Alluvium) Deposit (Qa)

Quaternary sediments of fluvial origin take the biggest portion of the study area and the surrounding neighboring catchments. The alluvial deposits are recent sediments occurring in areas of flood plains and river terraces. It covers wide area of the Flood Plain of Awash in Becho district. The Alluvium Deposit (Qa) consists mainly of sand, silt and clay (Fig 5.2).

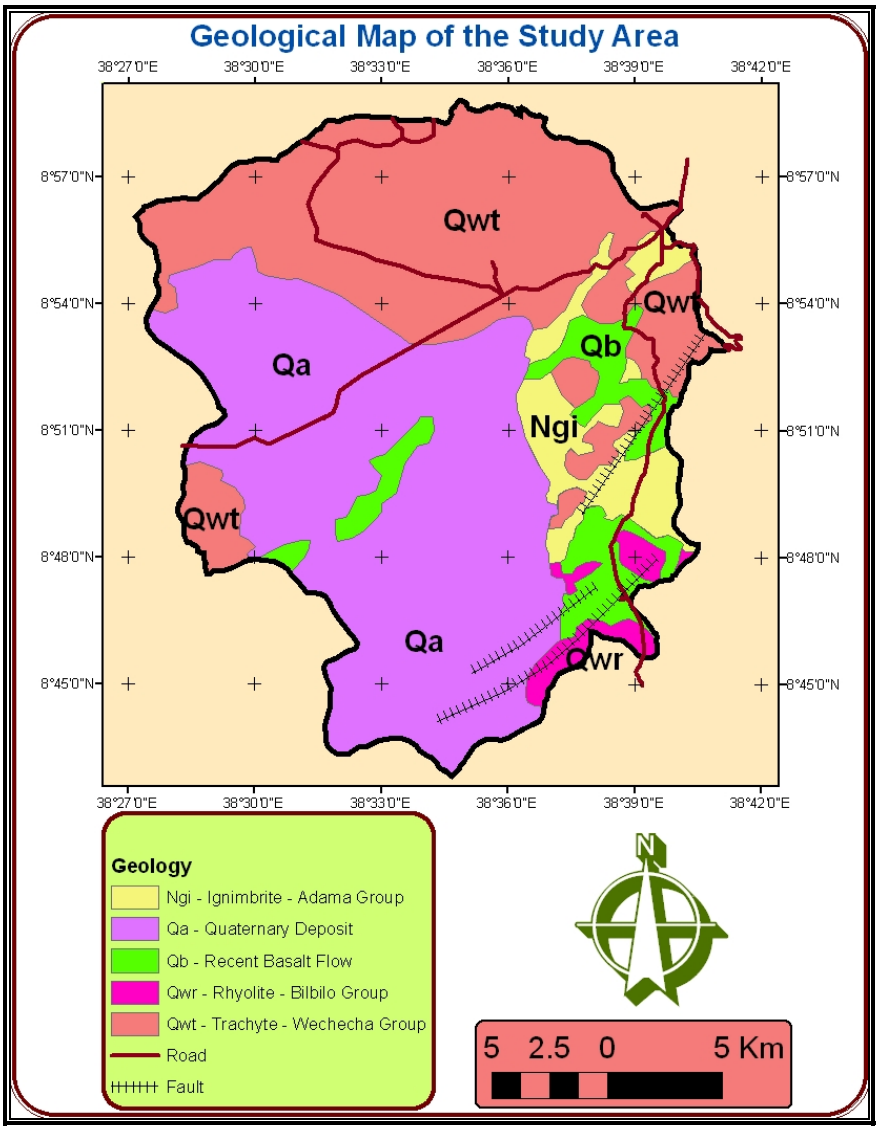

Fig 5.2 Geological map of the study area (after Gelana Gadissa, 2005)

5.2 HYDROGEOLOGY

The main hydrogeologic units in the study area are extrusive volcanics, pyroclastic units and alluvial deposits. The various rock units are subjected to varying degrees of secondary activities such as weathering, erosion and deposition. Some of the relatively hard formations are undergone fracturing, faulting and jointing.

The groundwater system of the area is inferred from water point data (Fig 5.3) and it could be classified into the deep groundwater system found on the eastern and northern hillside and plateau groundwater system characterizing most of the flat land and the shallow groundwater system.

5.2.1 The Deep Groundwater System

The deep groundwater system extends northern, eastern and southeastern part of Sebeta town. Ignimbrite is a dominant formation in the central part and trachyte in the northern. The groundwater system in the elevated area is characterized by springs of higher yields. High yield springs (up to 5 l/s) are measured in the basalt formation affected by faults. Table 5.1 shows the productivity of each geological unit in the system.

The groundwater of high yield is obtained by drilling more than 150 m in this part of the study area; especially for areas characterized by trachyte and ignimbrite and very shallow groundwater is possible only in the weathered part of the rocks.

Table 5.1 Productivity of the geological formation in deep aquifers

Aquifer	**Areal Extent**	**Aquifer Type**	**Yield (l/s**		**Productivity**
			Range	**Mean**	
Basalt	Localized	Faulted	5 – 10	5	Moderate
Trachyte	Extensive	Faulted and depression springs	0.6 – 3	1.8	Low
Ignimbrite	Extensive	Weathered and jointed			Low

5.2.2 The Shallow Groundwater System

It extends from Sebeta north-central to the mouth of Atebela River and from the slope break in the east to Tefki Town in the west. The area is considered to be high groundwater potential. The total groundwater recharge of the catchment based on the recharge calculated using the soil-water balance of Thornthwaite and Mather, 1957 is

estimated to be 65 Million m^3/year. The hydrogeological situation of each layer in the catchment is described in Table 5.2.

Table 5.2 Productivity of the geological formation in shallow aquifers

Aquifer	Areal Extent	Aquifer Type	Yield (l/s)		Productivity
			Range	Mean	
Alluvial	Extensive				Low
Basalt	Localized	Faulted	5 – 10	5	Moderate
Trachyte	Extensive	Faulted	0.6 – 3	1.8	Low

5.2.2.1 Alluvial Aquifers

Alluvial aquifers include the upper aquifer system of the flat portion of the Atebela catchment which extends mostly from the north-central to the south direction. They are composed of clay, silt, sand, gravel and rock fragment deposits. They are also manifest along the river banks. Shallow groundwater is the characteristic of these aquifers in which the saturated thickness ranges from 2 to 8 m. Groundwater depth varies from 6 to 16 m. The groundwater occurrence is limited to river channels and depressions where relatively thicker deposits are created.

5.2.2.2 Ignimbritic Aquifers

Ignimbritic aquifers are found underneath the alluvial aquifers in which the top part is weathered yielding water for hand dug wells in the flat part of the catchment. The depth of water strike in this case ranges from 8 – 14 m. On the other hand, they form deep aquifers of confined nature in the relatively elevated eastern part of the study area.

5.2.2.3 Basalt Aquifers

Basalt aquifers are found underneath the ignimbrite in most of the study area. They are the most productive aquifers but are relatively small in area extent; they yield

water for shallow wells of depth 60 to 70 m. The vesicular basalt and scoria are also found in some localities around Sebeta-Alemgena and along the road to Butajira.

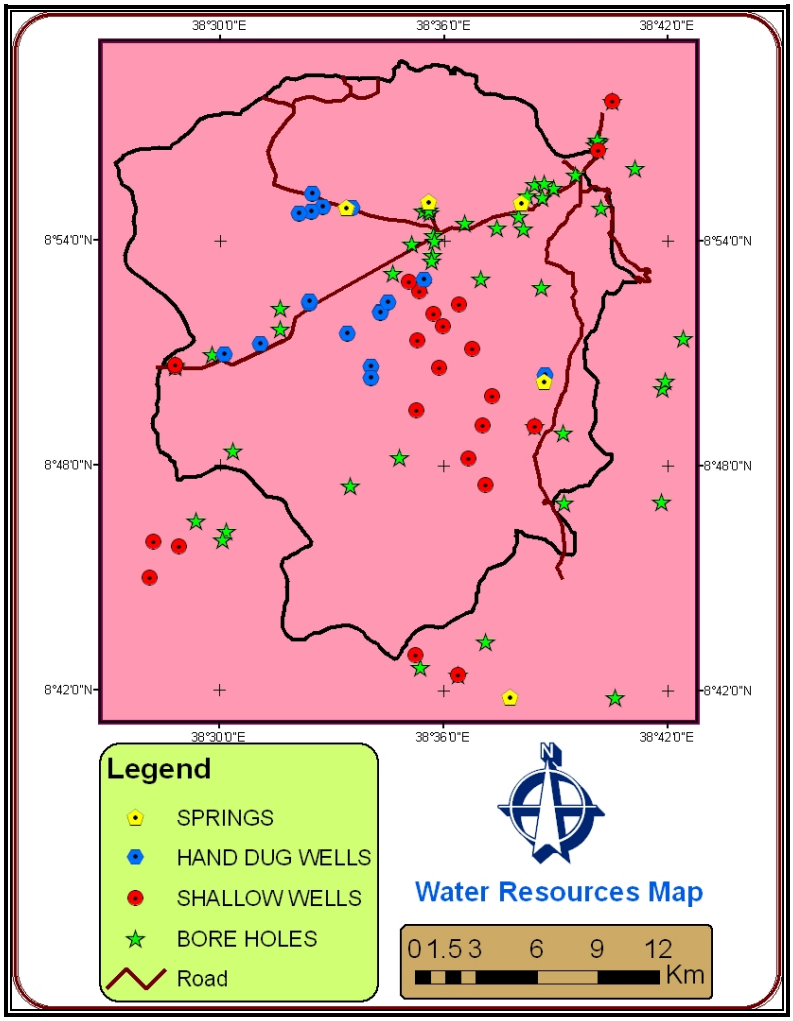

Fig 5.3 Water point map of the study area

Secondary processes play a significant role in the localization and controlling of the groundwater systems of the catchment. This can be observed from the lithological logs of boreholes drilled within and the surroundings of the catchment. Around 20 boreholes to a maximum depth of 183 m and a minimum of 39 m are bored in and very near to the study area. The major water bearing formations in all of the boreholes are weathered and fractured ignimbrites, weathered and fractured basalts, sediments associated with unwelded tuff and trachytes and rhyolites (Fig 5.4 and Fig 5.5).

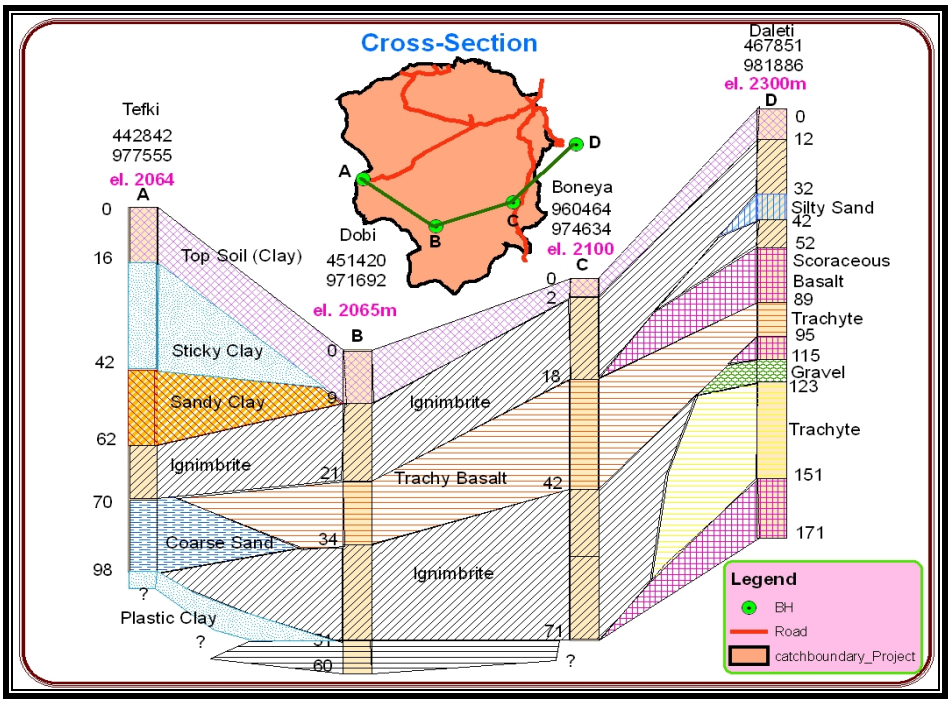

Fig 5.4 Cross-section along line connecting boreholes (not to scale)

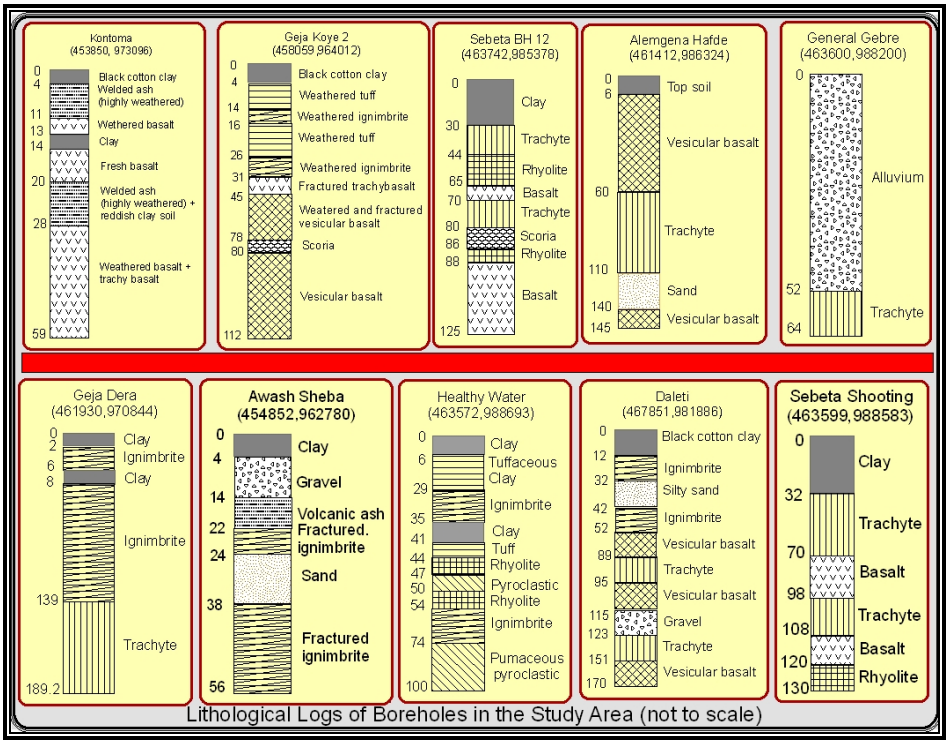

Fig 5.5 Lithological logs of boreholes in and surrounding the study area

5.2.3 Groundwater Flow

Groundwater movement i.e. its direction and velocity controls the transport of contaminants. The elevation of the water level from boreholes is used to map the general groundwater flow direction in the study area.

The groundwater flow direction in the study area is worked for shallow groundwater of unconfined aquifer and it is generally from north to south. The flow lines converge to the south. The movement is controlled by the topography, and in the swampy area the flow converges to center from the north and northeast direction as it is the same with surface water movement (Fig 5.6).

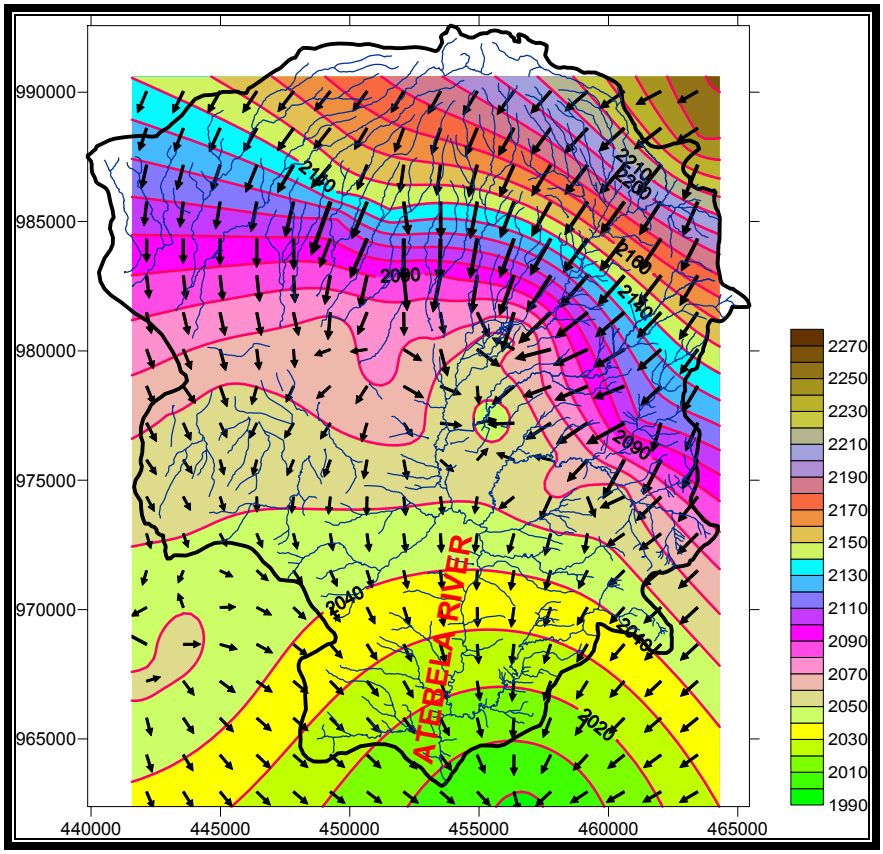

Fig 5.6 Shallow groundwater flow direction

The hydrogeological map of the study area is presented in Fig 5.7. It is prepared by utilization of borehole data (lithological logs, well yield, water level, and groundwater chemistry) and geological map of the study area. The well yields of the boreholes in

the study area vary between 38 l/s at Awash Sheba Flower south (56 m deep) end of the study area characterized by gravel deposit, fractured ignimbrite and sand deposit and 0.75 l/s around Tefki characterized by weathered jointed ignimbrite. High yield is found in vesicular basalt as observed from lithological log of Alemgena Hafde and this is grouped into high permeability aquifer class together with the fractured and weathered basalt, gravel. The fractured and weathered ignimbrite and weathered trachy basalt are mapped as intermediate permeability aquifer class and this class yields discharge in the range of 2 – 4 l/s. The third class of aquifer is the low permeability aquifer which yields 1 – 2 l/s and it constitutes weathered trachyte and rhyolite (Fig 5.7).

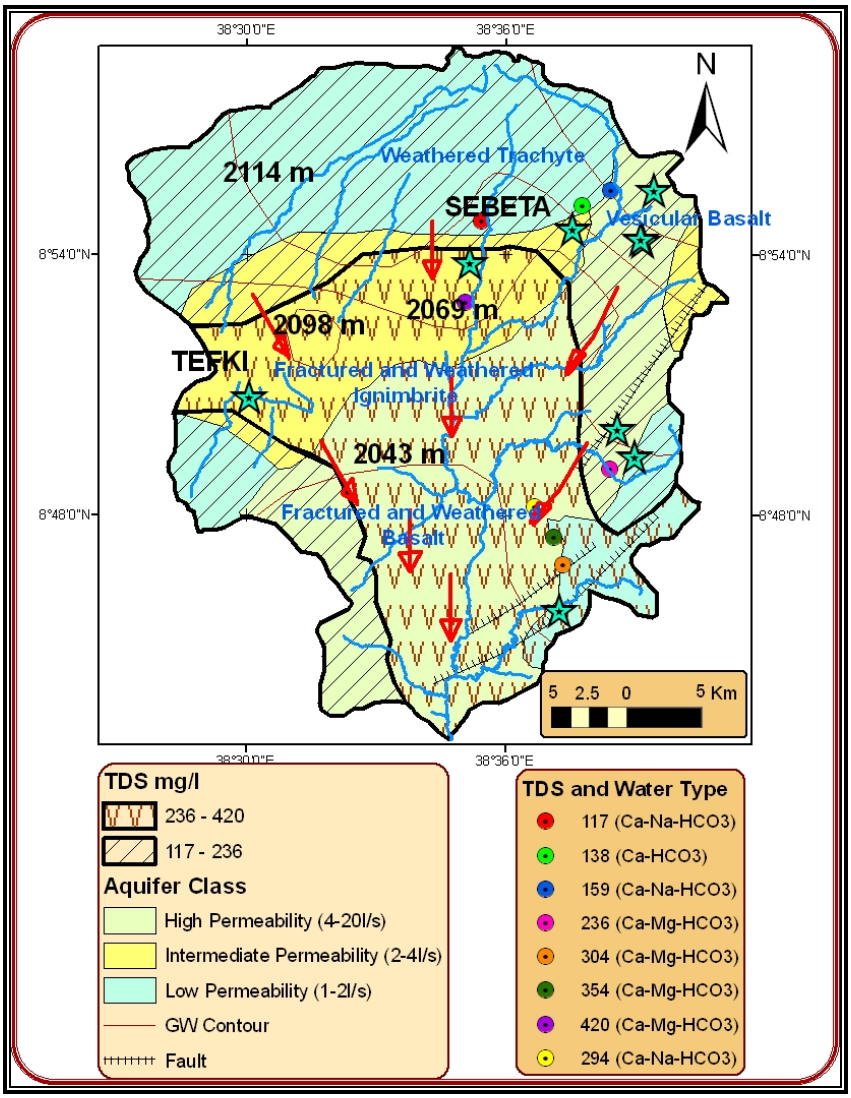

Fig 5.7 Hydrogeological map of the study area

The TDS is also grouped into two and mapped based on the borehole data with highest characterizing the central and southern part of the catchment. The lowest TDS values (117–236 mg/l) are characterizing the trachyte and rhyolite aquifers. The water type on the other hand shows Ca-HCO_3 or Ca-Na-HCO_3 on the low permeability aquifer while it is Ca-Mg-HCO_3 on the high permeability and intermediate permeability aquifers (Fig 5.7).

CHAPTER VI

6. HYDROCHEMISTRY

Hydrochemical information can be used to interpret the origin and mode of groundwater recharge, refine estimates of time scales of recharge and groundwater flow, decipher reactive processes, provide paleo-hydrological information, and calibrate groundwater flow models. Hydrochemistry can assist in understanding the evolution of water chemistry (quality), to examine natural base line conditions against which human impacts can be recognized and to take a look at some ways in which the protection and management of groundwater resources can be achieved.

Sample collection is done from hand dug wells and springs, and utilization of previously analyzed water chemistry data from boreholes and shallow wells as well as springs are done in order to avoid redundancy in sampling (Annex 2 and Annex 3). In-situ parameters such as pH, TDS and Temperature have been collected for the sake of crosschecking the laboratory results after proper calibration of pH and TDS meters.

Presentation of the results using Piper and Schoeller has been made to facilitate the interpretation and analyses. Trend and concentration analyses have been made by mapping a number of variables separately, such as EC (TDS), pH, Cl^-, N_a^+, Ca^{2+} and Mg^{2+} that greatly help interpret flow paths, recharging and discharging zones, local, intermediate and regional flow systems in the study area.

6.1 PHYSICAL PARAMETERS

6.1.1 pH

The pH of an aqueous system is a measure of the acid-base equilibrium achieved by various dissolved compounds. It is controlled by inter-related chemical reactions that produce or consume hydrogen ions and the geomedia. In most natural waters it is controlled by the CO_2^- - HCO_3^- - CO_3^- equilibrium system (WHO, 1984). Biochemical processes are also among the factors that control the pH-levels of natural waters. The

groundwater from the different sources in the study area has pH values ranging from about 6 to 7.9 and is associated with the high bicarbonate contents of the water. The pH levels of the shallow groundwater including those sampled for the hand dug wells increase to the west as these are the most feasible areas for shallow groundwater exploration. In the same way, the deep groundwater has its pH increasing towards the west and south. In either case, the pH levels tend to increase toward south and west parts of the study area which are the discharging zones.

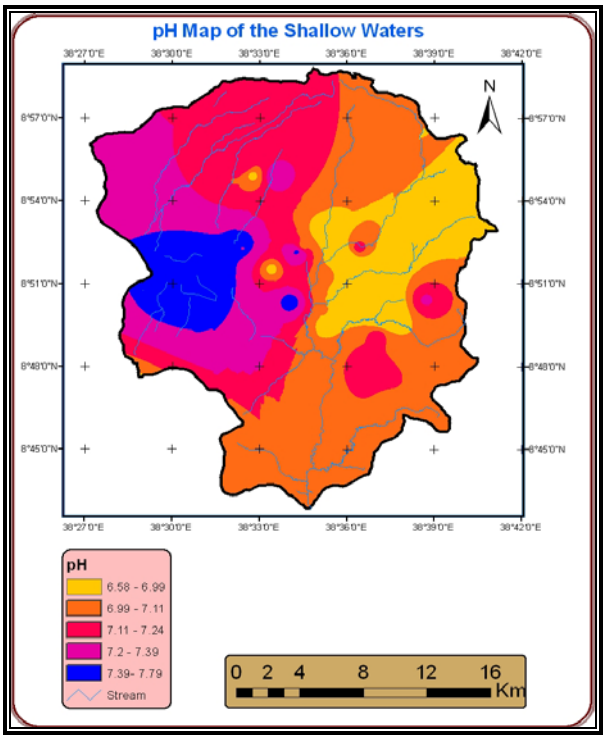

Fig 6.1 pH map of shallow groundwater

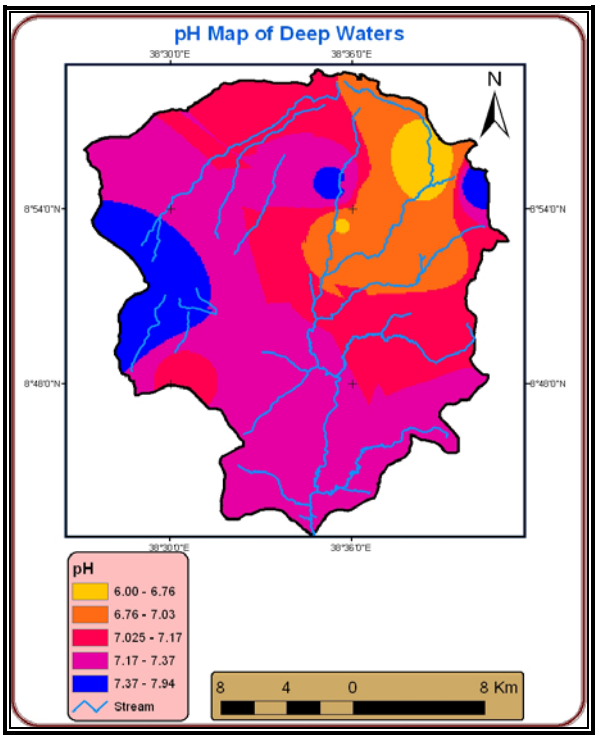

Fig 6.2 pH map of deep groundwater

6.1.2 Electrical Conductivity (EC) and Total Dissolved Solids (TDS)

The presence of charged ionic species in solution makes a solution conductive. As ion concentrations increase, conductance of the solution increases; therefore, the conductance measurement provides an indication of ion concentration.

It is apparent that the relationship between electrical conductivity and ionic concentration of water is direct, and most of the data set fit a straight-line regression closely (correlation coefficient = 0.65).

EC vs. TDS graph for the four types of water sources, namely, shallow wells, springs, hand dug wells and deep wells show no significant difference. The hand dug wells have shown high TDS which could indicate the susceptibility of the groundwater to external application of materials through different mechanisms which involve contamination. But the deep waters have higher TDS than the shallow waters which may indicate a relatively longer residence time (rock interaction). As for the springs, the available data don't show a good relationship between the two parameters, may be due to technical errors in data collection.

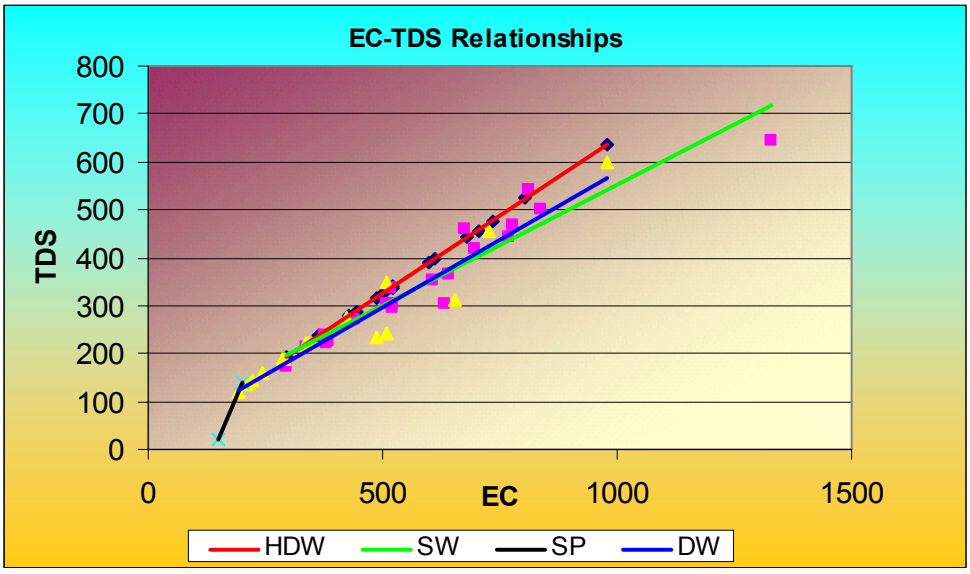

Fig 6.3 EC – TDS curve for the various water sources

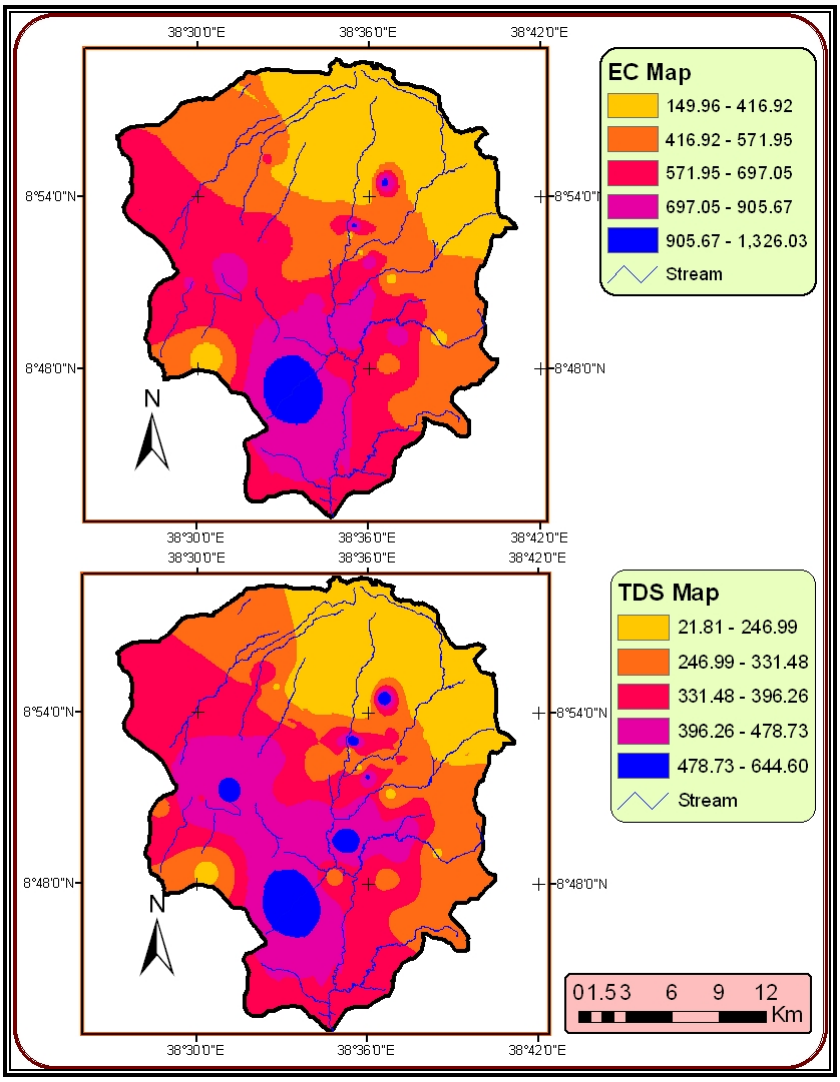

Fig 6.4 EC and TDS map of the study area

A 2D interpolated map of the EC values from all the water sources show an increase towards the south and the center of the catchment i.e. EC values are getting higher and higher towards the discharging zones and their values are generally lower in the recharging zones at the southwest, north and east. The trend shows the general increase of both parameters in the direction of groundwater flow (Fig 6.4).

6.2 CHEMICAL PARAMETERS

6.2.1 Ca^{2+}, Mg^{2+}, HCO^{3-} and Na^{+} Maps

The well chemistry data is mapped separately for the different ions. The Ca^{2+} map shows low values (0.18-43.28 mg/l) characterizing the northeastern and western part of the catchment. It is observed to increase to the south and the maximum value ranges between 87.75-121.68 mg/l. The evolution of Mg^{2+} on the other hand shows an increase towards the west and central while low values are characterizing the northeast and the southwest. As for Na+, the trend shows entirely low values on the north, south and eastern part of the catchment and it is observed to evolve to the west. The HCO_3^- ion on the other hand evolves towards the south and central part of the catchment (Fig 6.5).

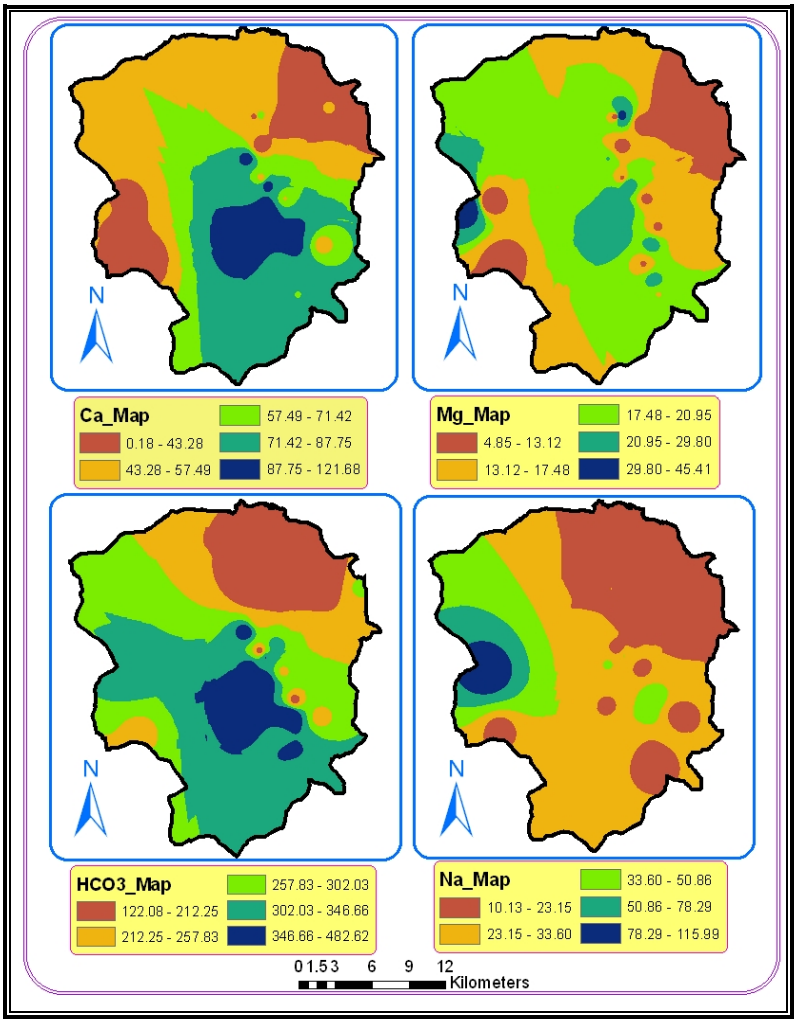

Fig 6.5 Ca^{2+}, Mg^{2+}, HCO^{3-} and Na^{+} Maps

The opposite direction of evolution of the Ca^{2+} and Na+ ions may indicate cation exchange. Cation exchange is a reaction in which the calcium and magnesium in the water are exchanged for sodium that is adsorbed to aquifer solids such as clay minerals, resulting in higher sodium concentrations (Hem, 1985).

The increasing trend in the Ca^{2+} ions concentration down the discharging zone (look at the Ca^{2+} evolution map) may be highly attributed to the effect of the geo-media in that some of the minerals forming rhyolites and trachytes (such as plagioclase feldspar and amphiboles) bear significant amount of Ca. On the other hand, the typically lower concentrations in Na+, HCO_3^- and Ca^{2+} near recharge sources is the low residence time which increases as groundwater flows away from the source of recharge.

6.2.2 NO_3^-, PO_4^{3-}, SO_4^{2-} and NH_3^- Maps

Maps of NO_3^-, PO_4^{3-}, SO_4^{2-} and NH_4^+ are Fig 6.6. The nitrate, mapped for the groundwater chemistry data available boreholes shows increase towards the south and it decreases towards the west. The PO_4^{3-} and NH_4^+ maps however show a different trend in which they lower in concentration towards the south. The SO_4^{2-} map on the other hand is generally increasing to the west and central part of the catchment.

The increasing trend of nitrate towards the south can be attributed to anthropogenic effect such as application of agricultural fertilizers and infiltration of river water into the groundwater through stream beds.

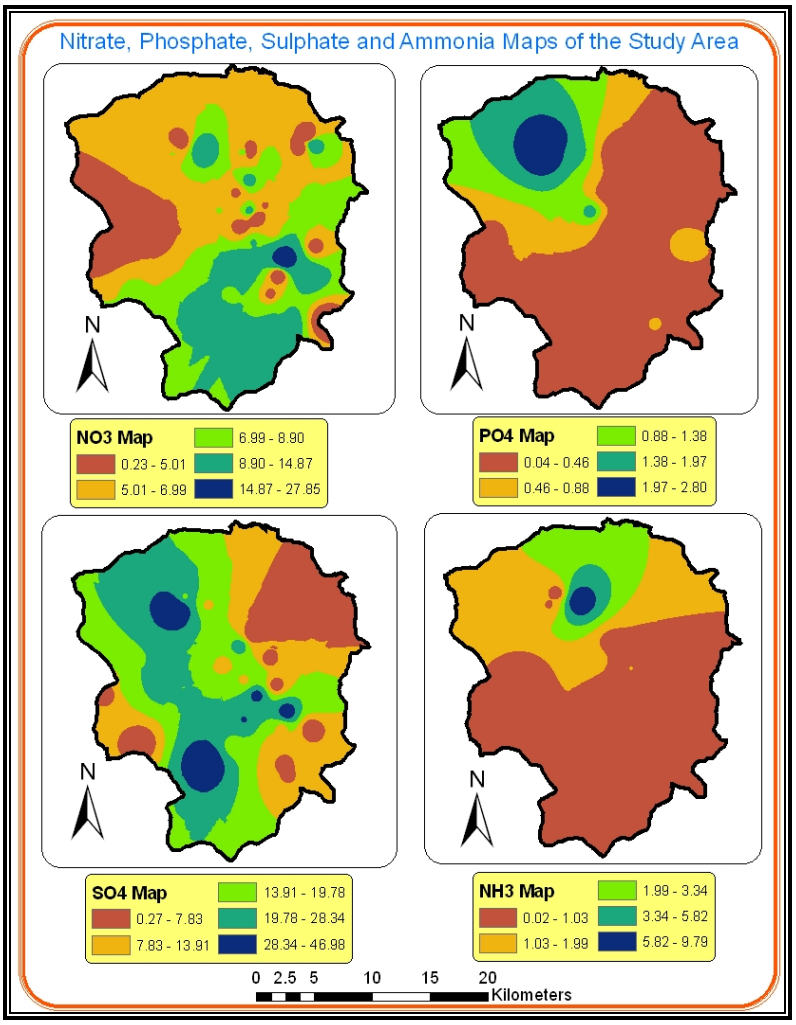

Fig 6.6 NO_3^-, PO_4^{3-}, SO_4^{2-} and NH_3^- Maps

6.2.3 Graphical Presentations

Most of the graphical methods are designed to simultaneously represent the total dissolved solid concentration and the relative proportions of certain major ionic species (Hem, 989) and all the graphical methods use a limited number of parameters, usually the available data, unlike the statistical methods that can utilize all the available parameters.

Piper Diagram

The piper diagram displays the relative concentrations of the major cations and anions on two separate tri-linear plots, together with a central diamond plot where the points

from the two tri-linear plots are projected. The central diamond-shaped field (quadrilateral field) is used to show overall chemical character of the water.

The piper plot for the study area is done for all water sources (boreholes, hand dug wells, springs and shallow wells) and it shows that the majority of the water samples are of calcium-magnesium-bicarbonate type of waters of borehole water samples are of calcium-bicarbonate.

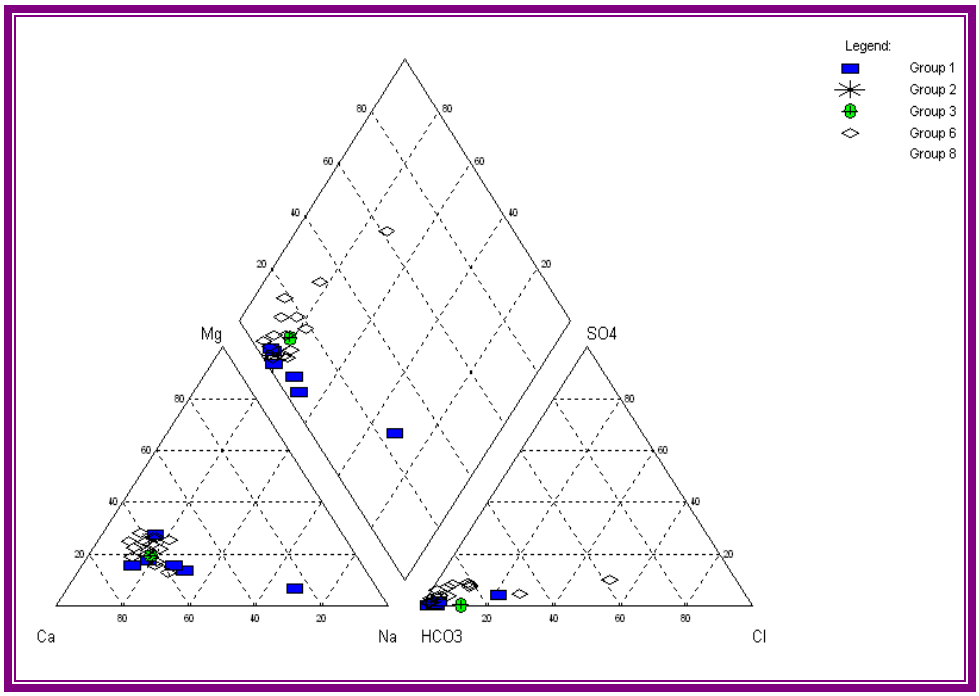

Fig 6.5 Piper plot of all sources (Group 1 – **BH**, Group 2 – **HDW**, Group 3 – **SP**, Group 6 – **SW**)

The groundwater chemistry data are plotted with piper diagram for the boreholes and shallow wells as shown in Fig 6.6 and 6.7. The boreholes are calcium bicarbonate type while the shallow wells are calcium-magnesium-bicarbonate type.

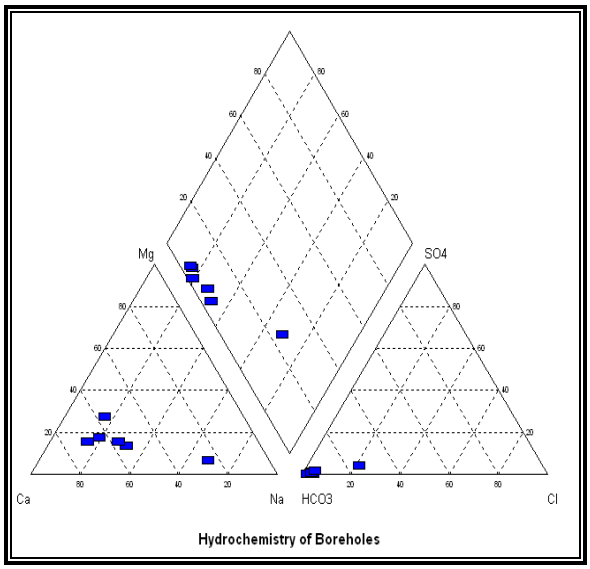

Fig 6.6 Piper plot of Boreholes

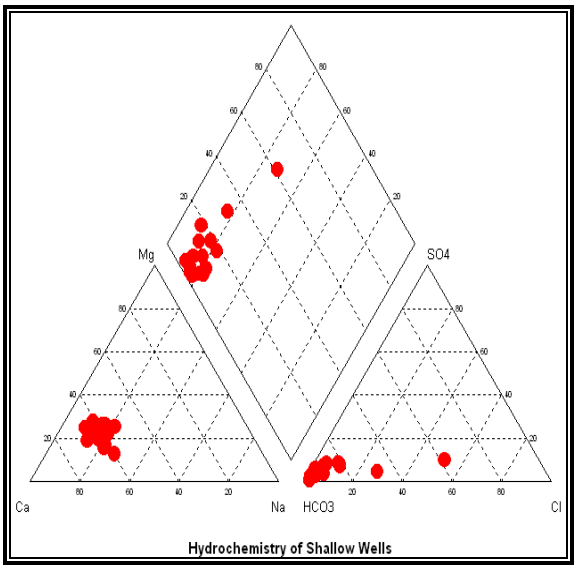

Fig 6.7 Piper plot of shallow wells

CHAPTER VII

7. SOURCES OF POLLUTION IN THE STUDY AREA

As observed from the number of available boreholes in the study area, the groundwater of the area is highly exploited for water supply of the towns, industries, factories, for rural water supply and in some cases for small scale irrigation by hand dug wells and springs. There are big projects of flower farming which involve groundwater exploitation. Groundwater is the sole source for public water supply.

The groundwater of area is intensively exploited and polluted. Currently, approximately more than 60 boreholes (highly concentrated in Sebeta town) and a large number of dug wells exploit about 65 MCM per year for an average 3 l/s pumping per borehole. The pollution from on-site sanitation (human waste) is extreme due to pathways to the hydrogeologic system created from poor design and construction of boreholes and dug wells and their deterioration. Two types of contamination sources of the groundwater of the catchment multiple point source contamination of pit latrines and septic tanks and line sources of contamination along the stream beds. The pollution is highly aggravated since the town has no sewerage conveyance and waste treatment plant.

The sources of pollution to groundwater originate from discharge of domestic and municipal solid and liquid wastes, industrial wastes or certain agricultural activities (Rao, 1996; Manahan, 1991). Deshu Mammo (2004) conducted study on the pollution of Sebeta River, which is the tributary of Atebela River and some of the explanations presented and analysis conducted (bacteriological and others) below are based on his data.

7.1 INDUSTRIAL POLLUTION

According to Deshu Mammo (2004), in the study area, there area many industrial sources of pollution mostly restricted to the town of Sebeta and Alemgena. As

presented in Fig 7.1, these include alcohol factories (National Alcohol Factory and Balezaf Alcohol Factory), Soap Factory, tannery (Blue Nile Tannery). Except for the Blue Nile Tannery all the other factories do not have treatment plant and they release their untreated waste effluents into Sebeta River which discharges into Atebela River.

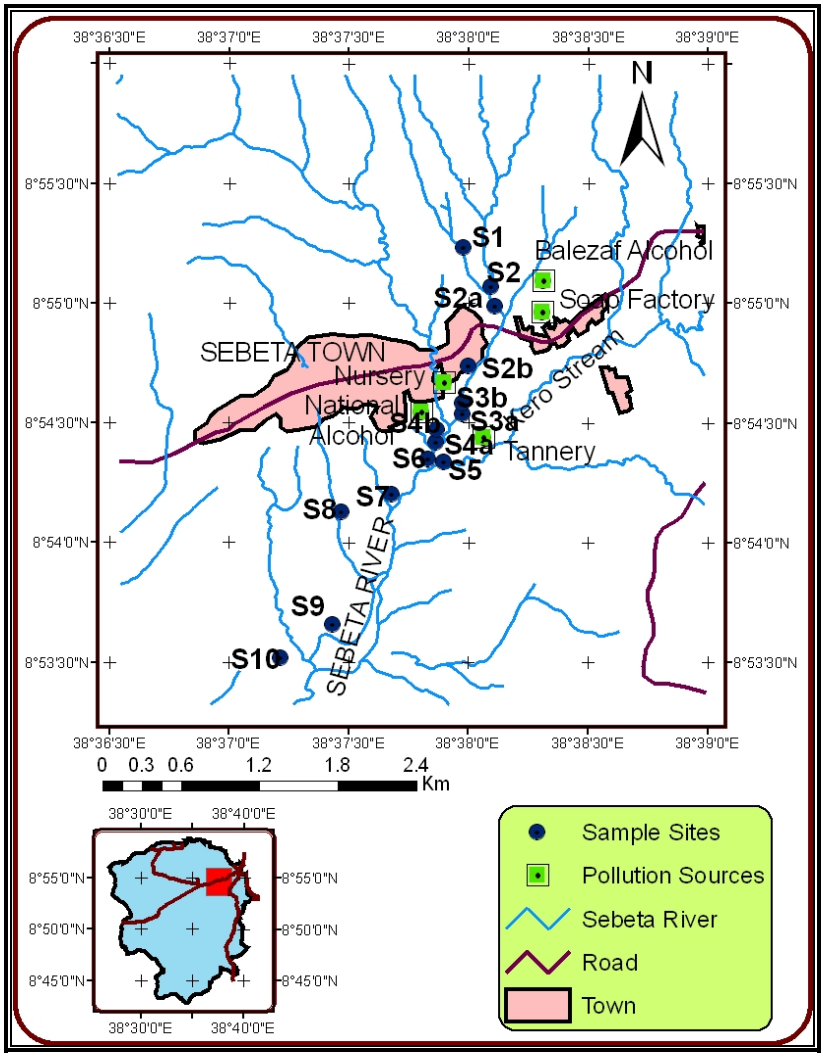

Fig 7.1 Sample sites for pollutants analysis (after Deshu Mammo, 2005)

Deshu Mammo (2004) explained that diverted water from Sebeta River for the purpose of traditional irrigation by the local farmers carried industrial residue which is dumped on the farmland and heavy metals are also observed from soil samples analyzed at a geographic coordinates of (0459100,0984100) and (0458650,0983100). These heavy metals include chromium and lead, and the highest concentration of Cr in the sediment is recorded at station 10. Qero stream is mentioned to have large

concentration of Cr (Fig 7.2). Some of the other heavy metals analyzed in the river water and the soil by Deshu Mammo (2004) are Pb and Zn. The Pb in the soil is observed to be higher than in the water (Annex 10). The metals found in the soil can find their way into the groundwater due to the favorable geologic condition (weathered and jointed ignimbrite on the stream beds and granular materials forming the banks).

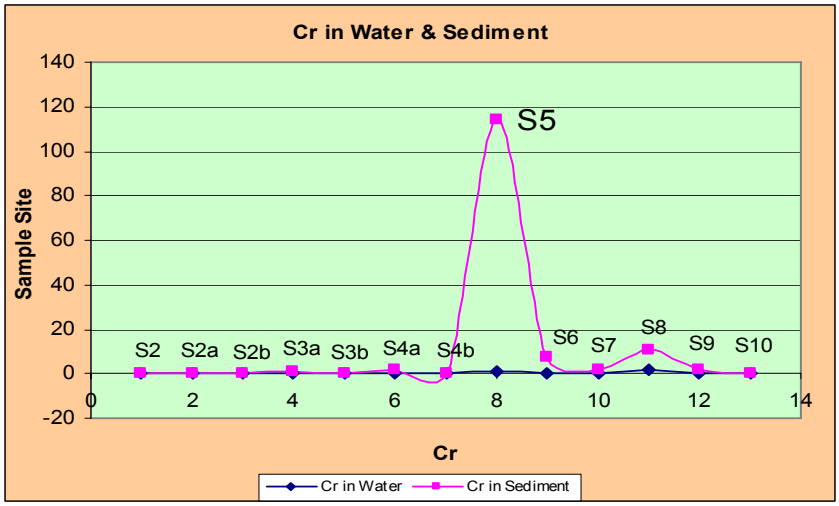

Fig 7.2 Cr evolution in the water and sediment

7.2 MUNICIPAL WASTE

This type of waste is described together with domestic waste. It is waste type generated from commercial establishments and residential activities. They occur in different forms such as water borne waste from households including sewage, rubbish, human and animal remains as well as chemical and laboratory wastes (Rao, 1996; Ogbanna et al., 2002).

Wastes from this group of pollutant source are causes of various diseases such typhoid fever, diarrhea, cholera, hookworm infestation, since waste damp sites are unsanitary and they harbor flies, rats, and other disease vectors (Tesfaye Berhe, 1988; Ogbanna et al., 2002).

Domestic waste is the primary source of organic waste released into fresh water (Tesfaye Berhe, 1988). Pollution of rivers with organic matter results in destruction of

organisms due to an increase in organic load and the concomitant depletion of dissolved oxygen in water (Fig 7.3). The dying organisms accumulate pollutants like toxic heavy metals (Ogbanna et al., 2002).

Utilization of human excreta on cropped soils may lead to contamination of crop grown and groundwater with pathogenic helminthes, protozoa, bacteria and viruses.

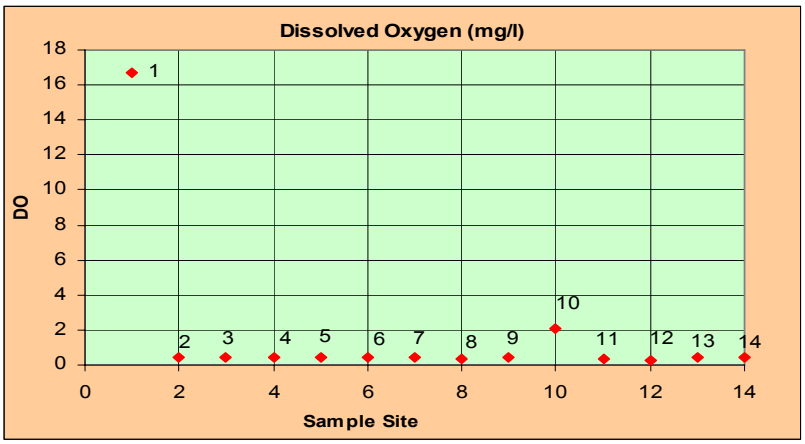

Fig 7.3 Dissolved oxygen evolution along Sebeta River

7.3 PETROL STATION

There is one petrol station in Sebeta Town which is found adjacent to Sebeta River. It is engaged in retail distribution of fuels, car washing and greasing services. Washing cars is done using high jet pressurized water that may contain washing solvents. This removes the chemicals (lubricants) used in greasing services in addition to the dirt. The liquid wastes from the station are discharge into the nearby drainage system.

The steel tankers holding the oil are buried in the soil which may leak it into the soil. Tamiru Alemayehu et al. (2005) mentioned that one of the problems associated with petrol stations is the absence of regular inspection of their storage tanks. It is severe in the rainy season and when the groundwater rises. In addition the pipelines are made of steel and they connect the storage tanker with distribution machines. The petrol station can be considered as a point pollutant source in the study area.

7.4 AGRICULTURAL POLLUTION

Although the community along the river side was practicing irrigation, currently modern irrigation is developing in addition to the traditional rain fed agriculture practiced by the community. The rain fed agriculture uses chemical fertilizers for teff and wheat production. The fertilizers applied on the hills are washed by rain and join streams or remain on the low lying and flat areas of the study area.

The modern irrigation practices include flower farming in green houses which is a recently started phenomenon in Ethiopia. It is considered to be one of the most important in the economic growth of the country. However, they are known for polluting the environment and especially the groundwater as they use chemicals in the production of flowers. There are about six floricultures in the study area. Although no detail investigation was conducted on their effluents in this particular research, they are known to apply chemicals for enrichment of the nutrition of the flowers. Different growth stages of the flowers require varying concentration of micronutrients (heavy metals such as iron, manganese, boron, zinc, copper and molybdenum).

CHAPTER VII

8. VULNERABILITY ASSESSMENT AND MAPPING

8.1 GENERAL APPROACH AND PROCEDURE OF THE RESEARCH

The DRASTIC model developed by U.S. Environmental protection Agency in 1987 has been adapted to carry out the vulnerability assessment and mapping for the study area. The acronym DRASTIC stands for D=Depth to water table, R=net recharge, A=Aquifer media, S=Soil media, T=Topography, I=Impact of vadose zone, and =hydraulic Conductivity. As explained in section 2.2.2, each parameter is given a rating interval from 1 to 10 and weights varying from 1 to 5. All the relevant data are organized and mapped using ArcGIS software (Fig 8.1).

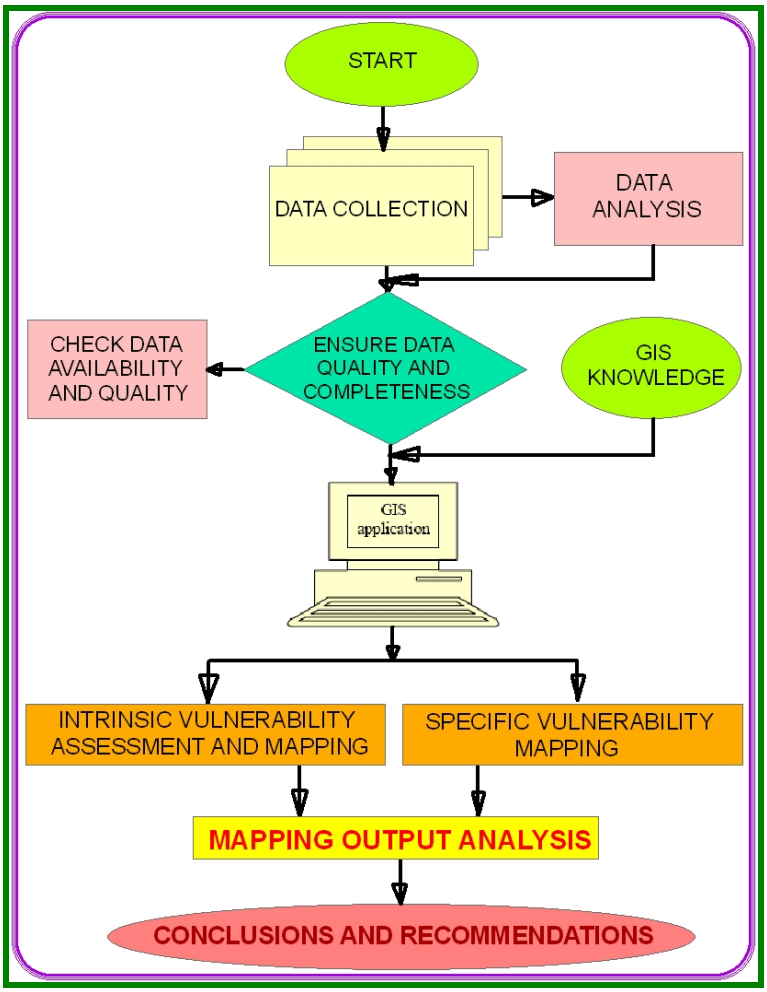

Fig 8.1 Flow chart showing organization and procedure of mapping

Table 8.1 DRASTIC ratings and weight strings

Parameters		Weight		Value Range		Rating
		Normal DRASTIC	Pesticide DRASTIC			
Depth to Water (m)		5	5	1.87 – 6.89 6.89 – 9.15 9.15 – 11.74 11.74 – 15.75 15.75 – 27.19		10 9 8 6 5
Net Recharge (mm)		4	4	73.45 – 83.95 83.95 – 89.20 89.20 – 97.07 97.07 – 107.56 107.56 – 118.05		1 3 6 8 9
Aquifer Media		3	3	Fractured and weathered basalt Fractured and weathered ignimbrite Sand and gravel deposit Weathered trachyte Fractured and weathered rhyolite		9 9 8 5 3
Soil Media	Soil texture	2	5	Clay Clay loam Sandy loam Silty loam Thin or absent	1 3 6 4 10	4
	Soil thickness	2	5	0.04 - 2.29 2.29 - 3.60 3.60 - 5.28 5.28 - 6.00 6.00 - 8.60 8.60 - 10.53 10.53 - 16.46 16.46 - 29.85	10 9 8 6 5 4 2 1	7 10
Topography (%)		1	3	0 – 4.62 4.62 - 13.84 13.84 – 26.43 26.43 – 44.89 44.89 – 106.98	10 9 5 3 1	10 9 5 3 1
Impact of the Vadose Zone Media	Vadose media	5	4	Basalt, trachyte, ignimbrite Gravel Ignimbrite, tuff, clay Trachyte Vesicular basalt	6 8 4 4 9	2 5 6 8
	Vadose Thickness	5	4	7.01 – 10.87 10.87 – 13.29 13.29 – 17.46 17.46 – 24.59 24.59 – 34.00	2 4 6 8 10	9
Hydraulic Conductivity (m/s)		3	2	$(0.007 – 0.01) \times 10^{-5}$ $(0.01 – 1.03) \times 10^{-5}$ $(1.03 – 1.29) \times 10^{-5}$ $(1.29 – 6.46) \times 10^{-5}$		1 8 8 10

Intrinsic vulnerability mapping and specific vulnerability mapping have been carried out using DRASTIC model. In the case of specific vulnerability mapping, nitrate was taken as a contaminant and hazard centers are also considered as one attribute.

The sources of the rating and weight strings for the analysis of the different parameters are Aller et al (1987). The ratings and weights used in the DRASTIC analysis are presented in Table 8.1 with some modifications for the study area and it is based on the availability and completion of data.

The general approach and procedure of the study is shown in flow chart (Fig 8.1).

8.2 DATA SOURCES

Both the secondary and primary data sources for the vulnerability assessment of the study area are collected and this summarized in Table 8.2.

Table 8.2 Major data sources for the study

Data	Data Source	Format	Scale
Drainage, topography	Digitized from topo map	Map Coverage / Vector Data	1:50,000
Well data and piezometric level	WWDSE, West Shewa Zone Water Resources Office, Alemgena Water Resources Office	Tables, reports	
Slope	Digitized contours	GRID	1:50,000
Meteorological data	National Meteorological Service Authority	Tables,	
Satellite image	Earth Sciences Dep't, AAU	Image	
Geological map	Oromia Mineral Resources Development Agency	Map (coverage)	1:50,000
Soil	MWR	Map, report	

8.3 MAPPING TOOL AND DATABASE CONSTRUCTIONS

To perform the overlay and mapping processes knowledge in GIS is essential. The DRASTIC system (Aller et al, 1987) subdivides an area into a regular square grid raster. For this research, all types of geographically-referenced data are spatially registered so that multiple themes of data can be compared and analyzed together.

The data that can be mapped or geographically referenced are digitized using ArcGIS 9.1 software and stored in the computer (Fig 8.1). The basic data on which vulnerability assessment and maps are based are introduced into a GIS in the form of values for point variables, point features, survey lines, and various maps, lines expressing relationships or linear features and remote sensing data.

Vector data are transformed into raster maps using interpolation function in spatial analyst tool of ArcGIS 9.1 software. The cell size used for every parameter is a square grid of 100 m per side which enables the corresponding values characterizing a cell to be calculated when modeled.

8.4 LIMITATIONS OF VULNERABILITY ASSESSMENT

There are certain limitations of vulnerability assessment that need to be mentioned. These include:

a) Lack of representative data – the amount and quality of data needed to construct a representative map are the biggest constraint. The maps are only as good as the information and data upon which they are based.

b) Inadequate description of the system – all hydrogeological maps have their limitations caused by our inability to accurately describe the complicated, heterogeneous physical world, our description of which is based on the extrapolation from a restricted number of observation points. Vulnerability maps are based on hydrogeological maps.

c) Vulnerability indexing involves rather subjective, not physically based, calculations, and therefore, it is unlikely that these methods are valid under different conditions.

d) The vulnerability maps are not used to substitute for site specific studies. They give only a first insight into vulnerability potential of an area, after which a detailed, on-site study must be done.

e) For the study area, the nitrate vulnerability mapping only considers the concentration of nitrate from boreholes, springs and hand dug wells. It does not take into account the behavior of the contaminant or the likelihood of the contaminant release.

8.5 INTRINSIC VULNERABILITY ASSESSMENT AND MAPPING

8.5.1 Input Data Analysis and Rating of the DRASTIC Parameters

The input data required in the intrinsic vulnerability assessment are depth to water table, net recharge, aquifer media, soil media, topography, vadose zone media and hydraulic conductivity. These parameters are described (explained), mapped, and rated for the study area as follows.

8.5.1.1 Depth to Water Table Mapping and Rating

Depth to water represents the depth of the water table from the surface and it determines the depth of material through which a contaminant must travel before reaching the aquifer. Further, it may help to determine the contact time with the surrounding media. The depth to water is also important because it provides the maximum opportunity for oxidation by atmospheric oxygen. Generally, there is a greater chance for attenuation of contaminants to occur as the depth to water increases since contaminants need to travel long paths.

The depth to the water for the study area is evaluated for unconfined aquifer and SWL data for hand dug wells are inventoried and lithological logs of shallow wells are analyzed. Very deep wells with high SWL are excluded from mapping the depth to water (Annex 1). For those areas in which no water depth data are not available, SWL is determined (computed) by conversion of the nearby wells water level observation data into water levels below the surface using the topographical inverse relationship to water depth (Fig 8.2).

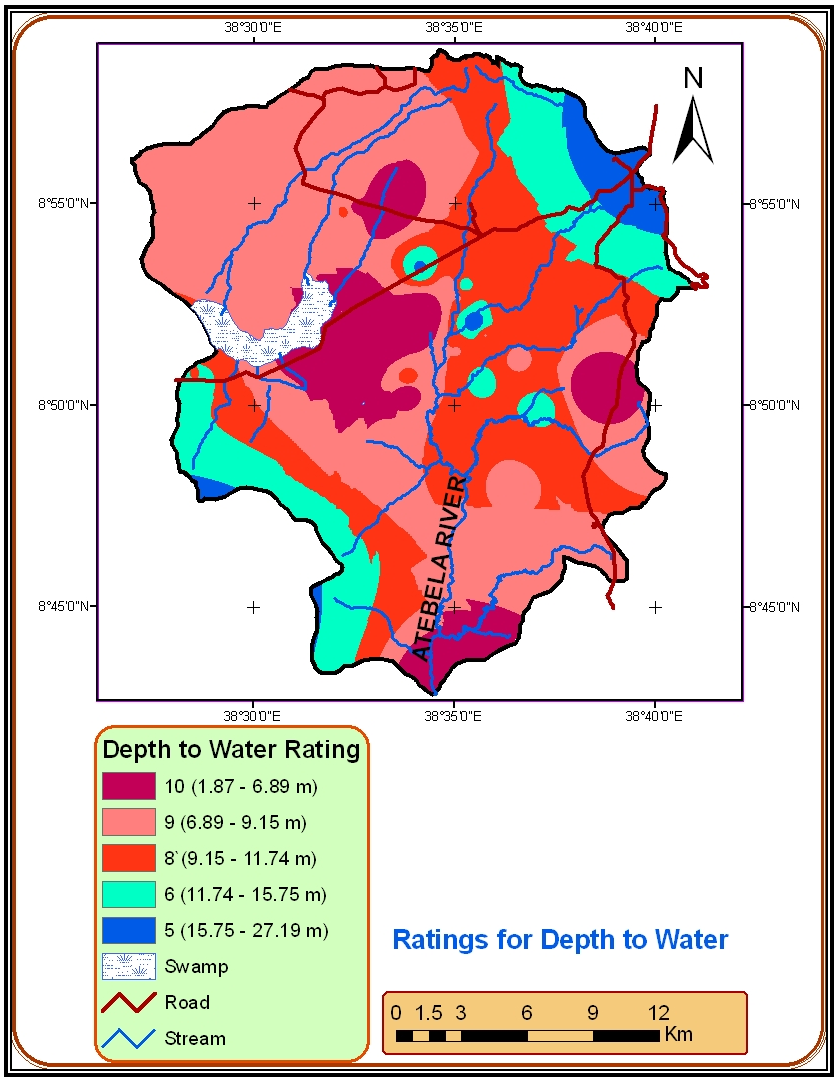

Fig 8.2 Depth to water rating map of the study area

8.5.1.2 Net Recharge Mapping and Rating

Net recharge represents the amount of water per unit area of land which penetrates the ground surface and reaches the water table. This recharge water is thus available to transport a contamination vertically to the water table and horizontally within the aquifer. Further, the quantity of water available for dispersion and dilution of the contaminant in the vadose zone and in the saturated zone is controlled by this parameter. Therefore, recharge water is a principal vehicle for leaching and transporting solid or liquid contaminants to the water table. High recharge into the groundwater implies high potential for groundwater pollution.

Net recharge map of the study area was obtained from the soil-water balance method which yielded only total recharge value (131.17 mm) of the catchment. In order to make net recharge map of the study area, the recharge value obtained using soil-water balance method was modified by accounting the effect of slope and soil thickness. Slope was given an importance weight of 40 % while the soil was given 60 % (Table 8.3). This was reclassified based on the rate given to slope and soil thickness in Table 8.1 and the recharge value is calculated in raster calculator function of ArcGIS 9.1 (Fig 8.3).

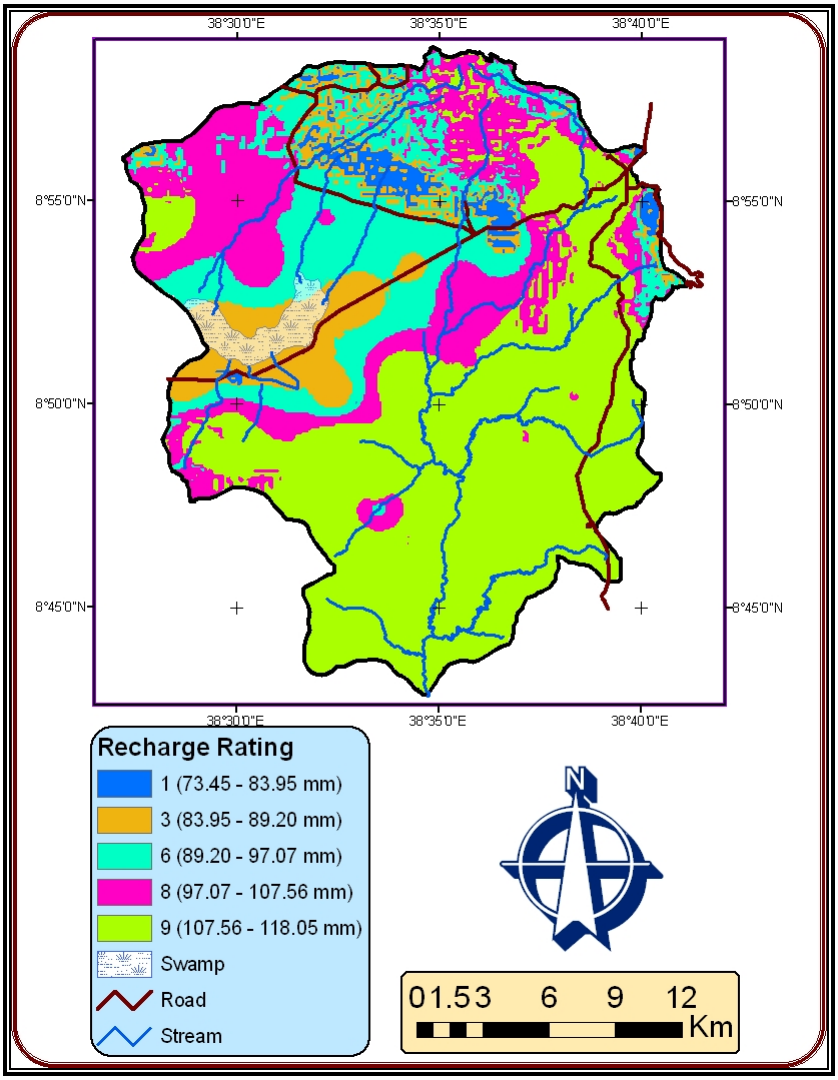

Fig 8.3 Recharge rating map of the study area

Table 8.3 Recharge controlling factors

I	II	III	IV	V	VI	VII
Total Recharge	Slope Rating	1-x/28	Reclassified slope rate for recharge	Soil Thickness Rating	1-x/30	Reclassified soil thickness rate for recharge
131.17 mm	1	0.964	9	2	0.933	9
	3	0.893	8	4	0.867	8
	5	0.821	7	6	0.800	7
	9	0.679	6	8	0.733	6
	10	0.643	5	10	0.667	5
	28			30		
Recharge = I * (0.04*IV + 0.06*VII)						

8.5.1.3 Aquifer Media Mapping and Rating

An aquifer media refers to the consolidated or unconsolidated rock which serves as an aquifer. Water is contained in aquifers within the pore spaces of granular and clastic rock and in the fractures and solution openings of non-clastic and non-granular rocks. The flow system within the aquifer is controlled by the aquifer medium which has either primary porosity or secondary porosity. This in turn controls the route and path length which a contaminant must follow. The path length controls the time available for attenuation processes such as sorption, reactivity and dispersion to occur. The aquifer medium also influences the amount of effective surface area of materials with which the contaminant may come in contact within the aquifer.

The aquifer media map for the study area is produced from the available borehole logs and the geological map is also used as a guide tool (Fig 8.4). Using the assumption of Vrba and Zaporozec (1994) that aquifer vulnerability analysis is conducted for the upper aquifer, the upper aquifer material was used in rating of aquifer media. Accordingly, rating of the media is based on the identification of the most significant media of the upper aquifer. The rating of the aquifer media assigned based on borehole data was transformed into polygon map and rated based on the characteristic fracturing and weathering of the units and as given by Aller et al (1987). Secondary processes such as fracturing and weathering of the media allowed the modification of the rating (Fig 8.4). Some of the media that are assigned the same rate

are reclassified to form the same value; especially the fractured and weathered basalt and ignimbrite are rated 9 while gravel and sand along the river bed are rated 8 and the weathered trachyte 5. The rhyolite is the least rated (Fig 8.4).

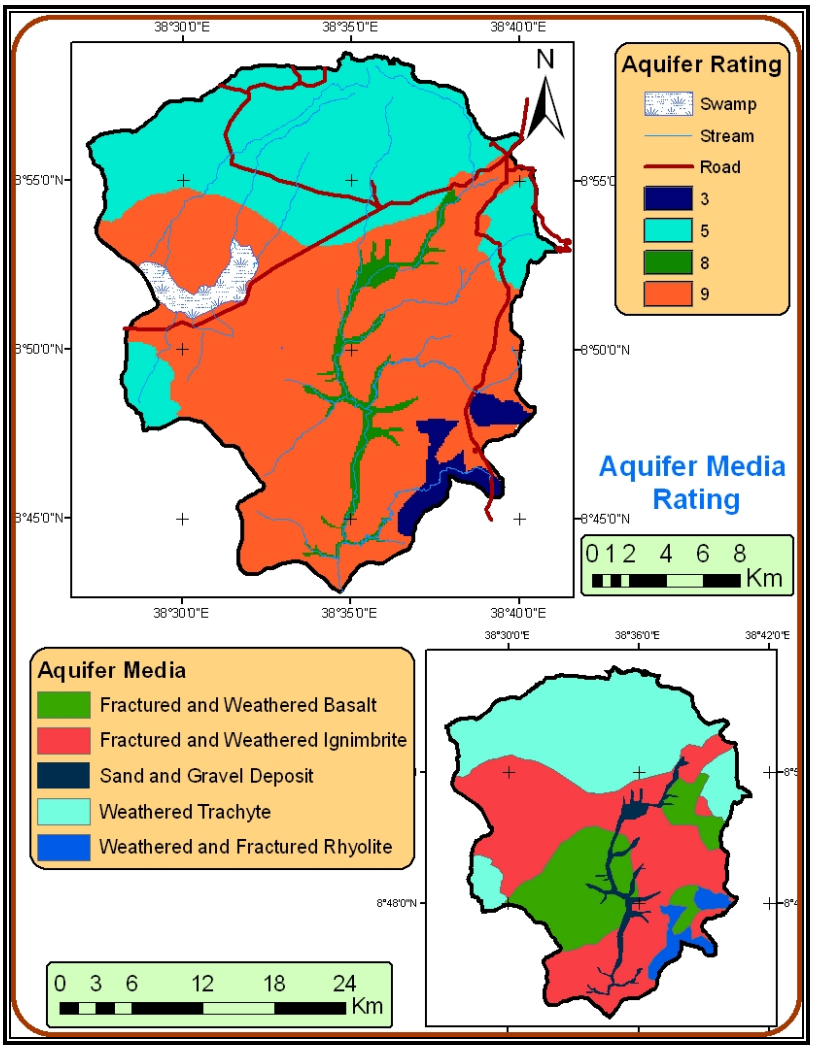

Fig 8.4 Aquifer media rating map of the study area

8.5.1.4 Soil Media Mapping and Rating

Soil media refers to the upper most portion of the vadose zone characterized biological activities. Soil has a significant impact on the amount of recharge which can infiltrate into the ground and hence on the ability of a contaminant to move vertically into the vadose zone. Soil texture and thickness have the influence on the rate of transport of contaminants and their life time in the soil. The presence of fine-textured

materials such as silts and clays can decrease the relative soil permeabilities and restrict contaminant migration. On the other hand, where the soil zone is very thick, the attenuation processes may be quite significant. The pollution potential of a soil is therefore largely affected by the type of clay present, the shrink/swell potential of the clay, and the grain size and thickness of the soil.

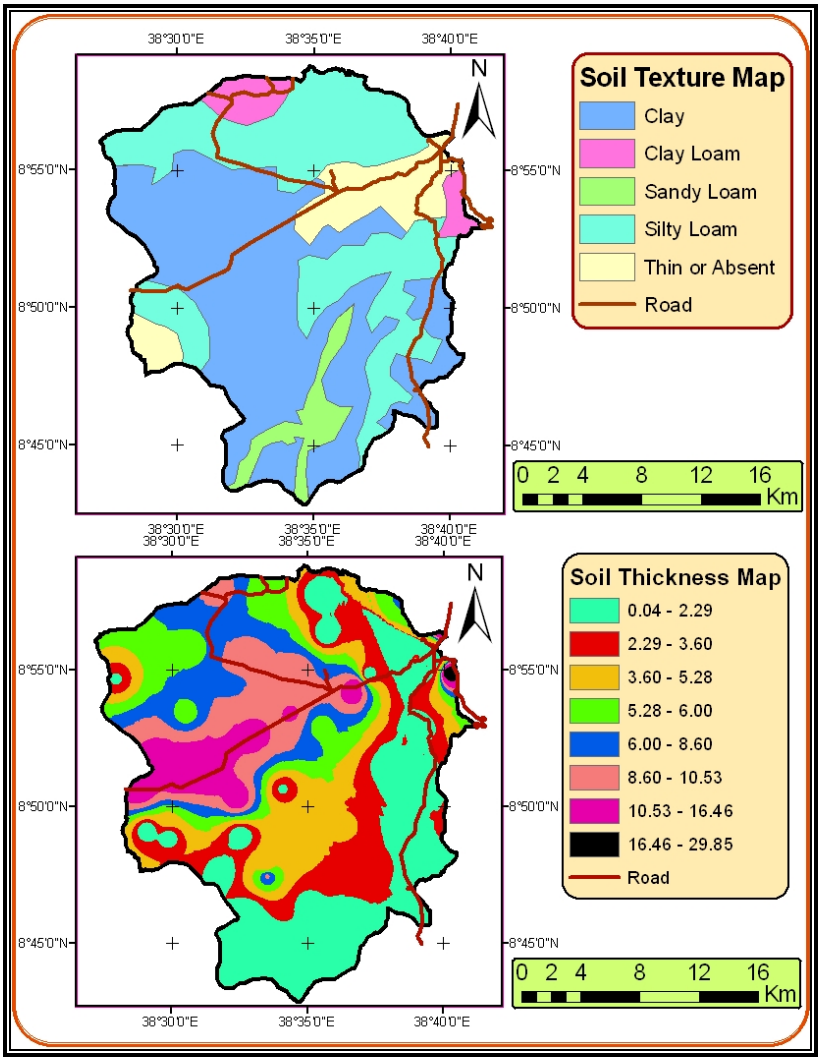

Fig 8.5 Soil texture and thickness maps of the study area

For the purpose of rating of the soil media, textural and thickness maps of the study area are prepared in Fig 8.5 above from borehole data, field observation thesis work of Abinet Gebremedhin on the Addis Ababa – Jimma (Annex 7, Annex 8 and Annex 9). Satellite image (Landsat 2000) with band combination of 5, 4, and 3 are used to map soil and field observation is also applied. For the thickness map, lithological logs

are used and information on hand dug wells is also applied. The maps are combined to produce an average rate using Modeler in Erdas 8.7 Software (Fig 8.6).

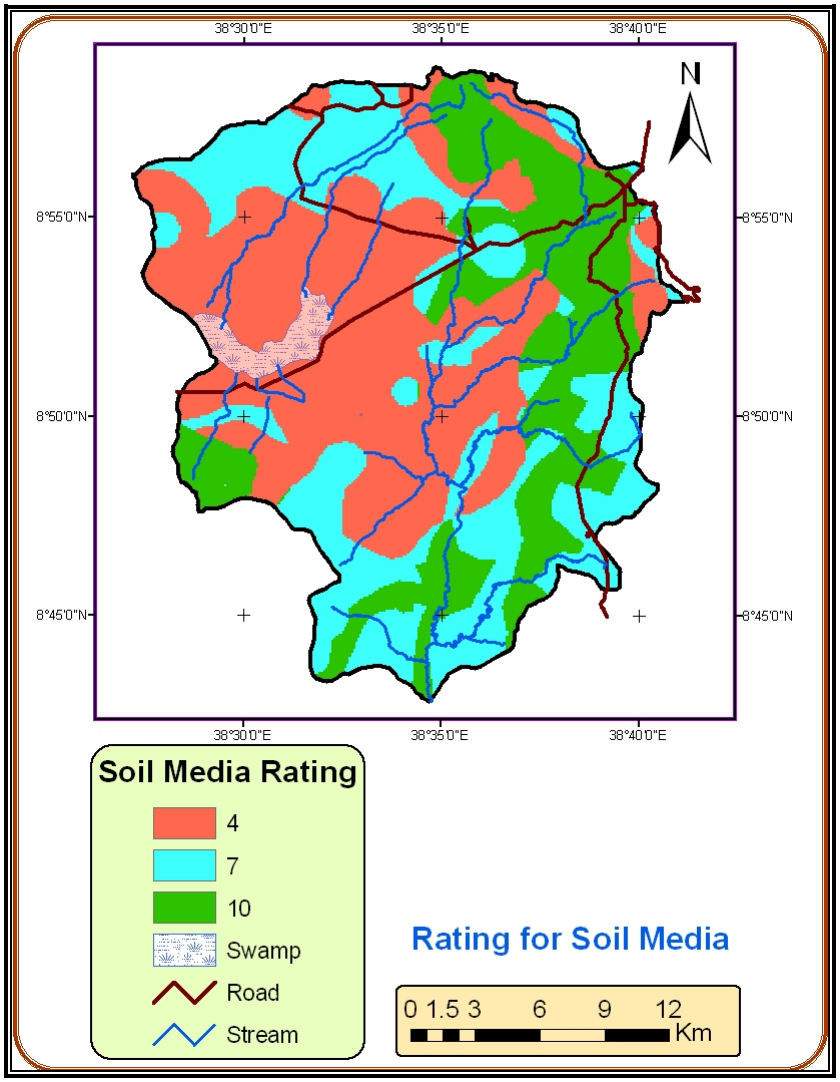

Fig 8.6 Soil rating map of the study area

8.5.1.5 Topography (Percent Slope) Mapping and Rating

Topography refers to the slope and slope variability of the land surface. It helps control the likelihood that a pollutant will run off or remain on the surface in one area long enough to infiltrate. It plays a role in soil development and therefore has an effect on contaminant attenuation. Slopes which provide a greater opportunity for contaminant to infiltrate will be associated with higher groundwater pollution potential.

Topography is also significant because gradient and direction of flow often can be inferred for water table conditions from the general slope of the land.

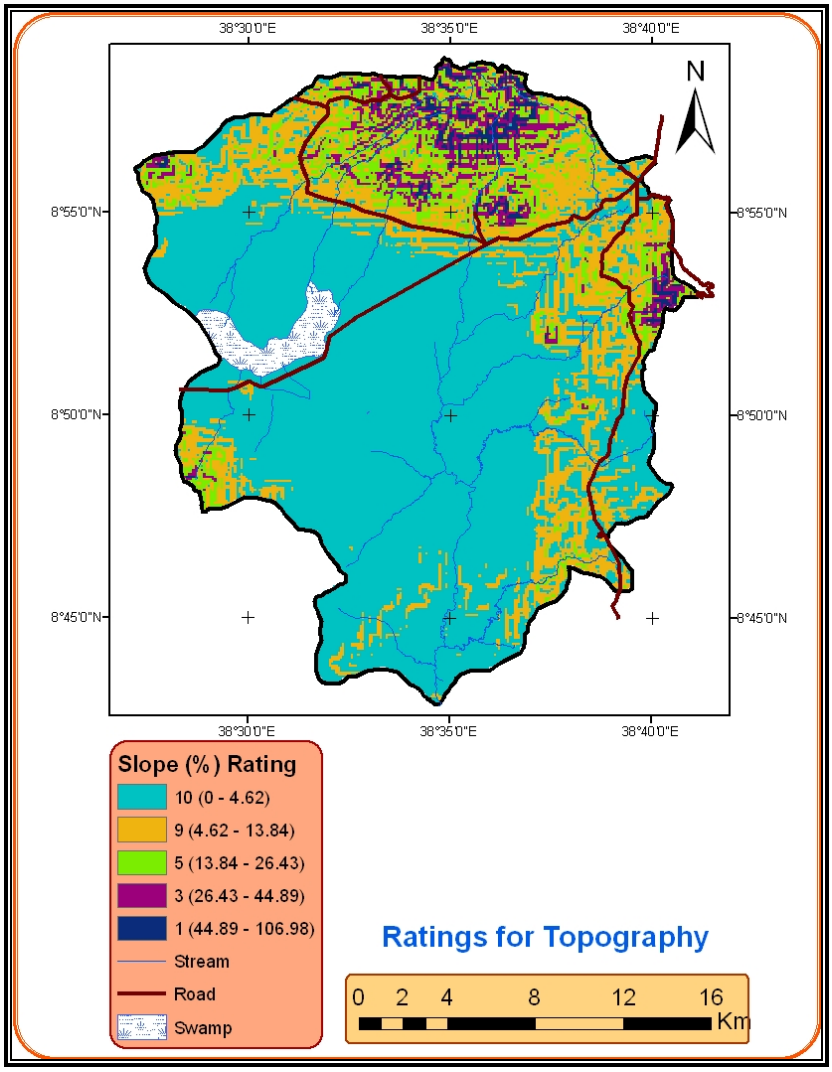

Fig 8.7 Topography rating map of the study area

Slope map of the study area (Fig 8.7) is produced from digitized contours of 1:50,000 topographic maps which are converted into TIN (Triangulated Irregular Network) on ArcGIS 9.1 using 3D Analyst and then rasterized. The raster is converted into slope percent of 100 x 100 grids using surface analysis function. The central, western and southern parts of the study area are characterized by flat to gentle topography and therefore take biggest portion of the slope map with the range 0 – 4.7% (lowest values of the slope). The slope percent increases to the north and east where there are hills and the highest values are of course found along the erosion gullies. Low rating

values are given to large percent slope ranges since they afford a high runoff capacity and a subsequent lower groundwater pollution potential, and the vice versa (Fig 8.7).

8.5.1.6 Vadose Zone Media Mapping and Rating

The vadose media is defined as the zone above the water table which is unsaturated or partially saturated. The type of vadose zone media determines the attenuation characteristics of the material below the soil horizon and above the water table. This media controls the path length and routing of the groundwater thereby that of the contaminant, thus affecting the time available for attenuation and the quantity of material encountered. The routing is of course strongly influenced by the presence of fracturing.

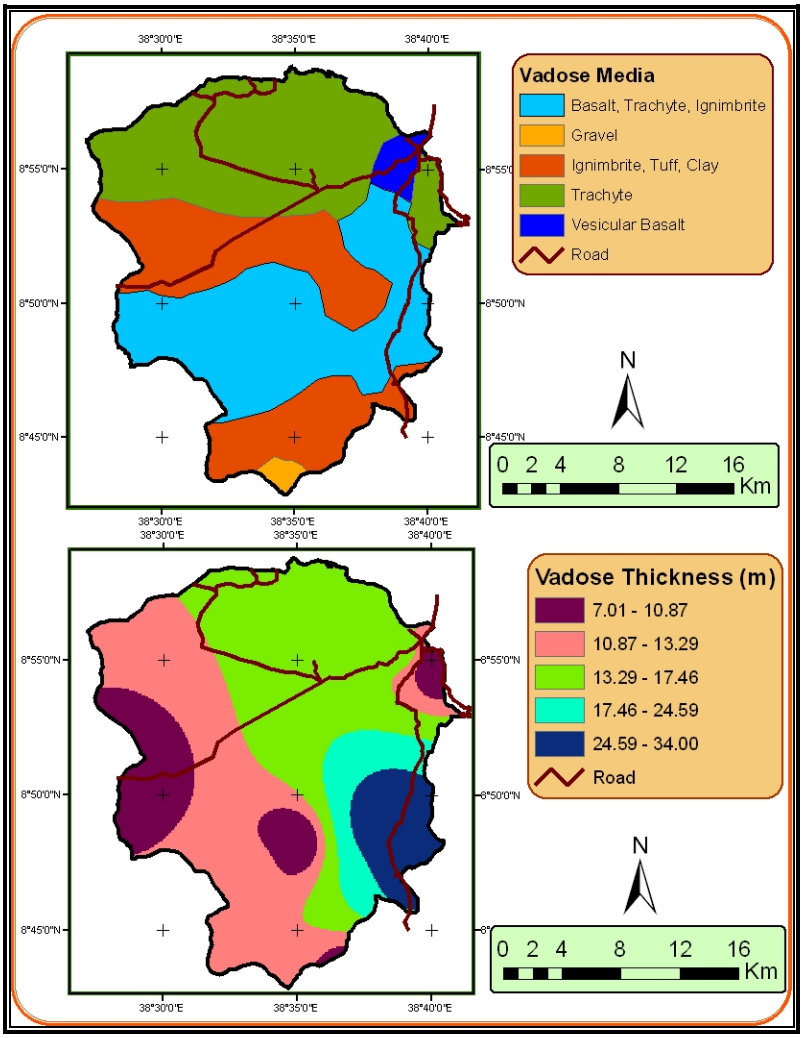

Fig 8.8 Vadose media and thickness map of the study area

The vadose media map for the study area is produced from borehole lithological logs. The selection of the vadose zone media is based on the static water level and the identification of whether the aquifer is unconfined. In order to produce the rating map for the impact of the vadose zone media, the maps of the vadose rock type and the thickness are made and rated separately (Fig 8.8).

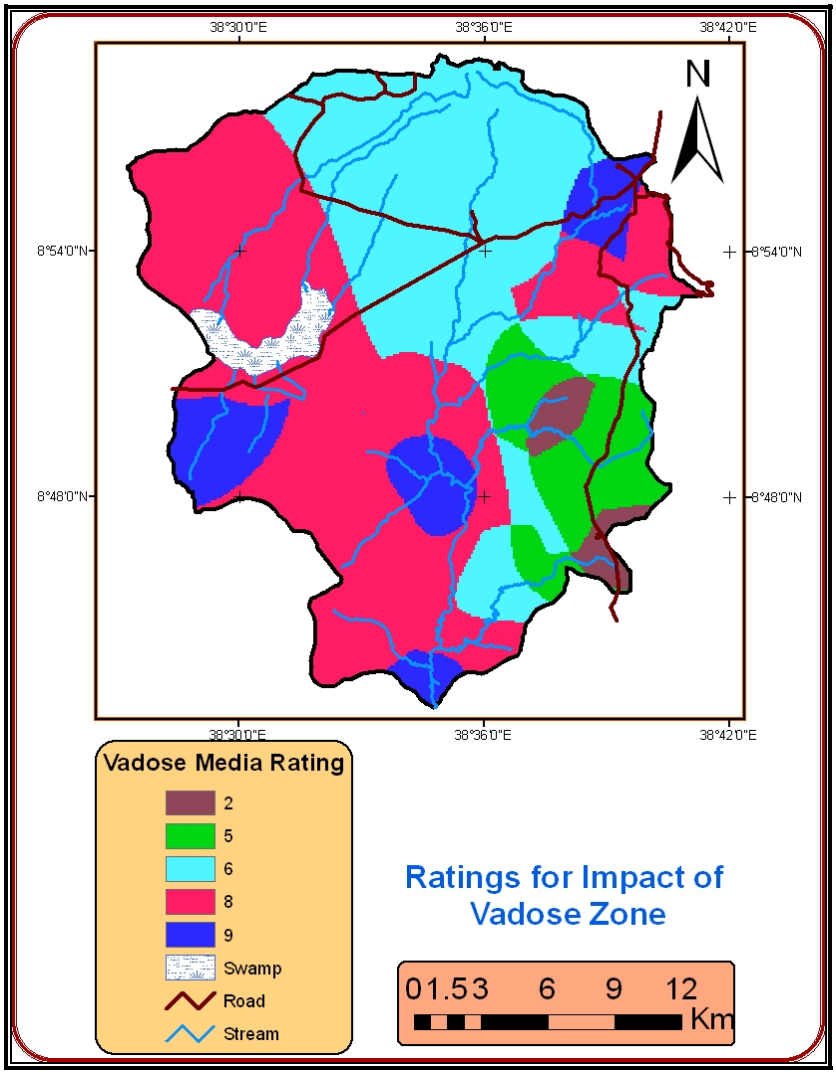

Fig 8.9 Impact of vadose zone rating map of the study area

The thickness of the vadose zone media for boreholes is obtained by considering those units which are above the static water level and below the soil media and interpolated for the catchment. The rate for the thickness is calculated by weighting the thickness of each unit constituting a borehole by the rate given according to Aller

et al (1987). Finally, both maps are combined to produce a raster map of average rate using Modeler in Erdas 8.6 Software (Fig 8.9).

8.5.1.7 Hydraulic Conductivity Mapping and Rating

Hydraulic conductivity refers to the ability of the aquifer materials to transmit water, which in turn, controls the rate at which groundwater will flow under a given hydraulic gradient. The groundwater flow rate controls the rate at which a contaminant moves away from the point at which it is incorporated into the aquifer. The hydraulic conductivity is governed by the amount of interconnection of void spaces within the aquifer which may occur as a consequence of intergranular porosity, fracturing and bedding planes.

Values of hydraulic conductivity are estimated from well yield which is not sufficient for mapping. Therefore, for areas where well yield values are not available, the values for hydraulic conductivity, which depend largely on the rock type and degree of weathering, are estimated based on Annex 6 as the ranges given by Freeze and Cherry, (1979) for geologic materials. The hydraulic conductivity map is shown in Fig 8.10 and the values are rated after reclassifying the map (Fig 8.10).

Very low hydraulic conductivities characterize the acidic rocks of rhyolite and trachyte and they are assigned the lowest rating value of 1 and 2. But the gravel deposit along the streams, recent basalts and pyroclastic materials of ignimbrite and tuff are characterized by high hydraulic conductivities and assigned rating values of 8 and 10.

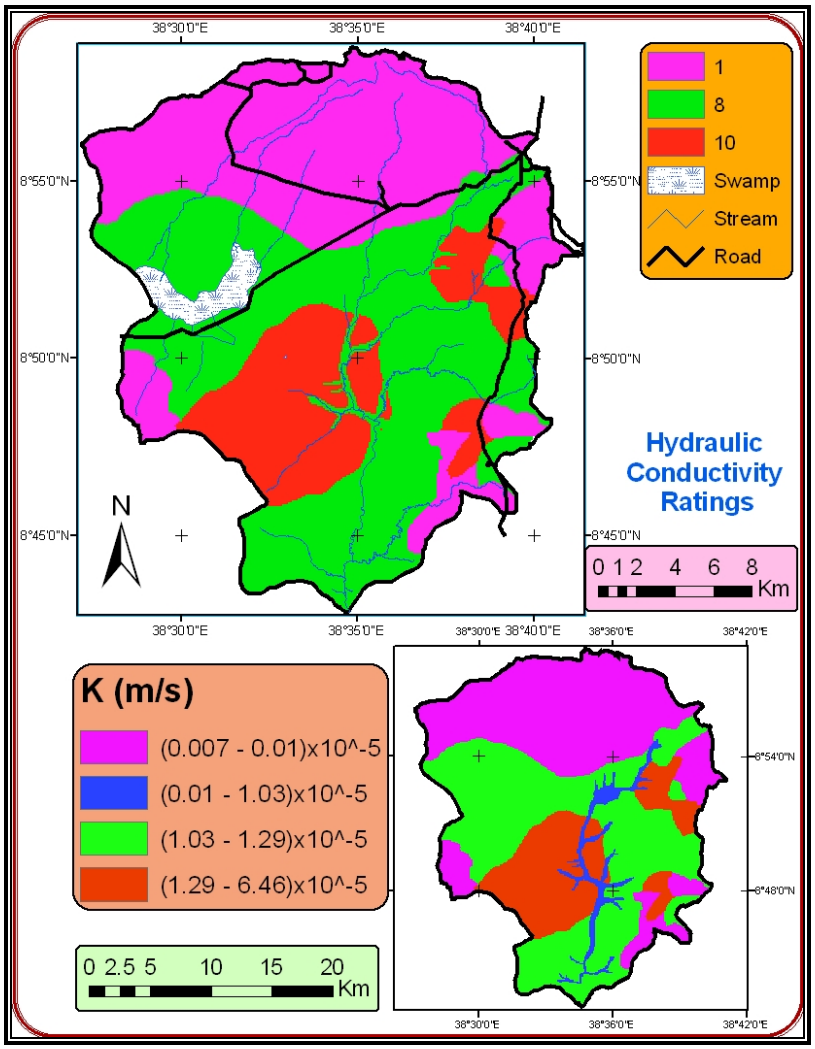

Fig 8.10 Hydraulic conductivity rating map of the study area

8.5.2 Model Outputs

8.5.2.1 Normal DRASTIC Map

The normal DRASTIC map or the intrinsic (natural) vulnerability map is produced by overlaying the seven parameters using the weights given in Table 8.1. This is done in ArcGIS 9.1 by raster calculator function. See Fig 8.11 for the normal DRASTIC map.

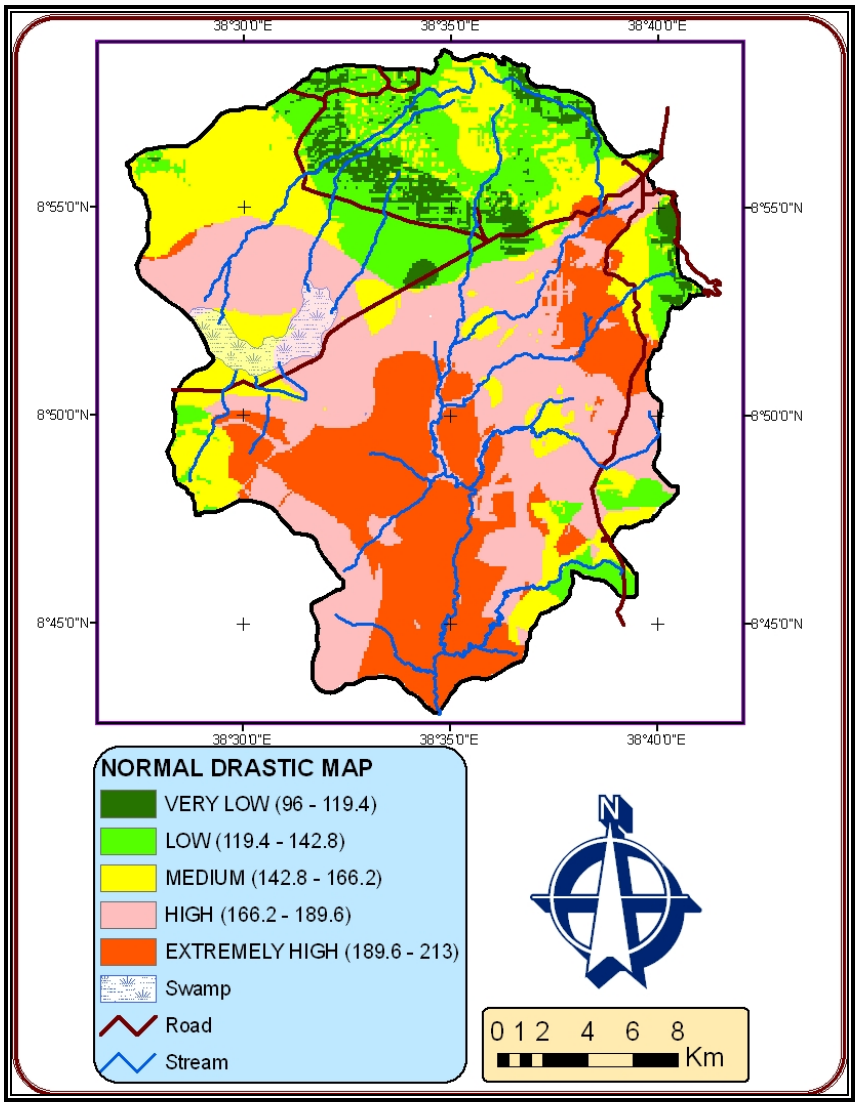

Fig 8.11 Normal intrinsic vulnerability map of the study area

8.5.2.1 Pesticide DRASTIC Map

The pesticide DRASTIC map on the other hand is designed to be used where the activity of concern is the application of pesticide to an area. It represents a special case of the DRASTIC Index. The only way in which it differs from the normal DRASTIC is in the assignment of relative weights for the seven DRASTIC parameters (Table 8.1). All other parts of the two indexes are identical; the ranges, ratings and instructions for use are the same (Fig 8.12).

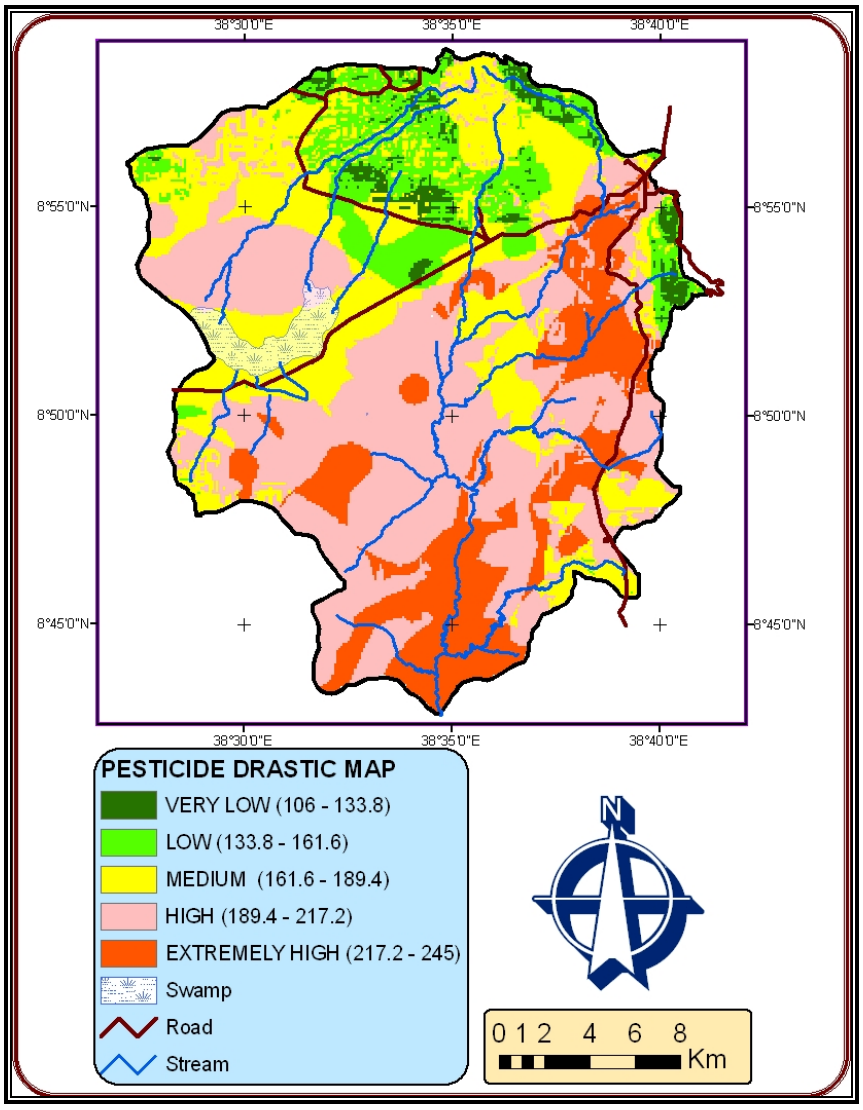

Fig 8.12 Pesticide intrinsic vulnerability map of the study area

8.6 SPECIFIC VULNERABILITY ASSESSMENT AND MAPPING

Specific vulnerability is assessed and mapped in terms of the danger of the groundwater system becoming exposed to certain contaminant load. The major attributes involved in assessing specific vulnerability include: nitrate and hazard centers such as industries and floricultures.

8.6.1 Nitrate

The general concept of specific vulnerability deals with the fact that different substances behave in a distinct way in the same geological and hydrogeological environment, due to their physical and chemical properties.

Nitrate may be naturally occurring, although its presence in drinking-water is more often associated with contamination by excessive use of fertilizers (both inorganic and organic), in combination with inappropriate farming practices and/or sewage. This chemical occurs widely throughout the world in both groundwater and surface water, and presents a particular problem in shallow wells. Nitrate is a major problem for bottle-fed infants, in whom the risk of methaemoglobinemia ("blue-baby syndrome") increases as the concentration of nitrate rises above 50 mg/l. The risk is increased by the presence of nitrite, which is a much more potent methaemoglobinemic agent than nitrate, and by the presence of microbial contamination, which can lead to gastric infections in infants (Meresa Kiros, 2006).

The groundwater nitrate content is derived from various point and non point sources, including cattle feed lots, septic tanks, sewage discharge and the oxidation of organically bound nitrogen in soils. Most of the aforementioned causes for nitrate pollution are applicable for the study area. The main sources of pollution in Sebeta-Alemgena area are multiple point sources, pit latrines and septic tanks and linear source pollution of industrial and domestic waste disposal along the river course.

The use of fertilizers is highly increasing from time to time to enhance productivity particularly in the study area. Moreover, urbanization and poor management of wastes cause a serious pollution problem to groundwater system. Hence nitrate is taken for specific vulnerability assessment to be conducted using the DRASTIC model (Fig 8.13).

The nitrate specific vulnerability map in Fig 8.13 is produced using the nitrate map in Fig 6.6. Since the nitrate concentration (0.23 – 27.85 mg/l) for the available data is

lower than the maximum permissible limit in drinking water according to WHO (45 mg/l), it is assigned weight of 3 while the normal DRASTIC is given weight of 5. The respective values of each map are multiplied by its weight and added using raster calculator in ArcGIS 9.1.

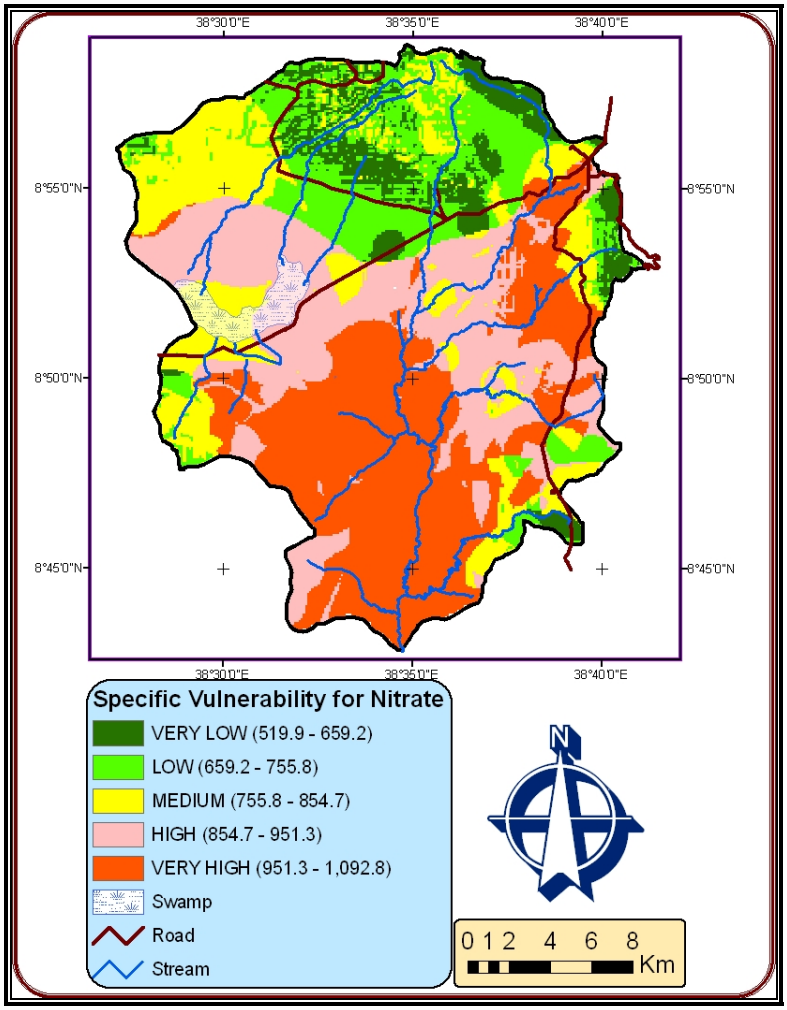

Fig 8.13 Specific vulnerability map for nitrate

8.6.2 Hazard Centers

The hazard centers considered for the other specific vulnerability mapping are tannery, alcohol factories, nursery, petrol station, municipal solid waste disposal site, soap factory, nursery and floricultures. Most of the hazard centers are located in Sebeta-Alemgena area especially along Sebeta River. They are falling on the high and medium vulnerable zone. Some of the floricultures are falling on high and

extremely vulnerable zone especially those located at the western part of the catchment (Fig 8.14).

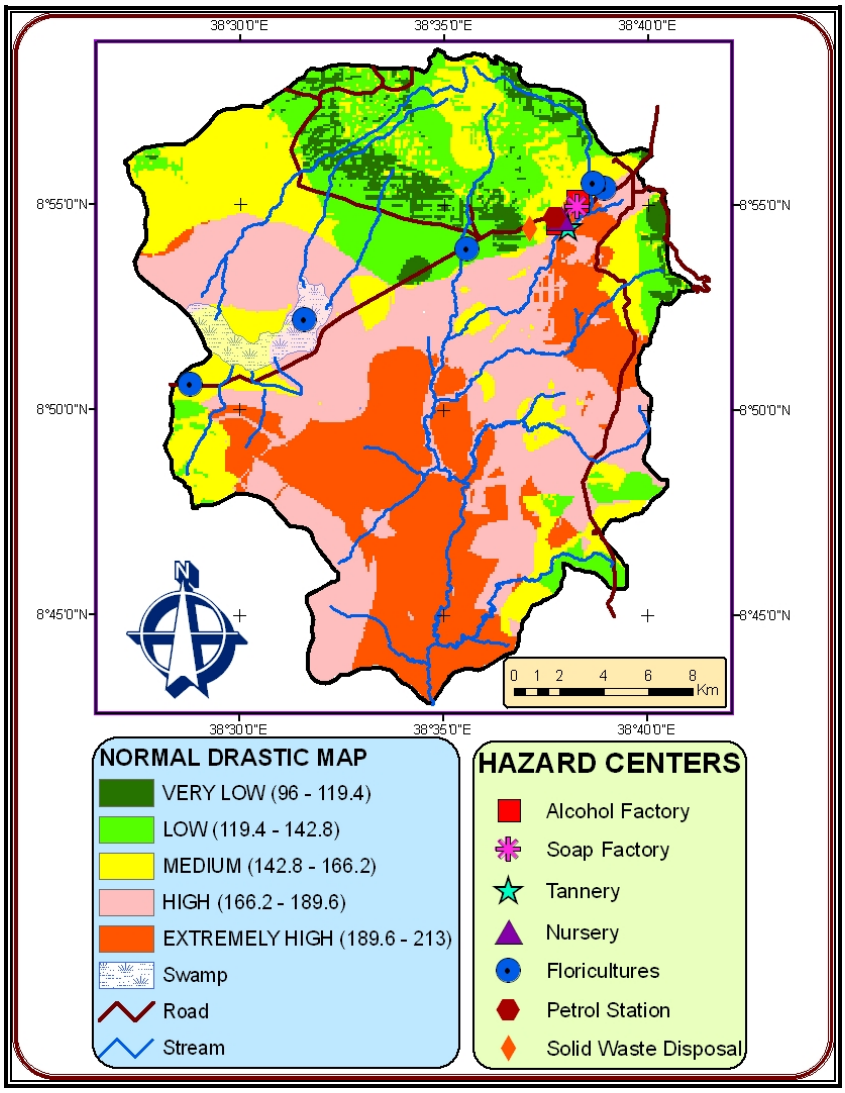

Fig 8.14 Specific vulnerability map for hazard centers

CHAPTER IX

9. RESULTS AND DISCUSSION

The result of the above analysis conducted for all the parameters are separately interpreted in this section and the final outputs in which the intrinsic vulnerability for normal DRASTIC and pesticide DRASTIC, specific vulnerability for nitrate and hazard centers produced are discussed.

Individual DRASTIC layer maps are prepared following the procedures of 1) collection of both secondary and primary data in the study area, 2) data base construction with the available data, 3) extraction of hydrogeologic factors from the database, and 4) carrying out overlay analysis of the factors.

Mapping of depth to water involved collection of data of 63 drilled wells, 18 hand-dug wells and 4 springs. Only 39 water points (Annex 1) are used to produce depth to water map of the catchment since most of the drilled wells do not have borehole information, especially lithological logs. On the other hand some of the boreholes are rejected as they are considered to be tapping from confined aquifers. The limitation with mapping of this parameter is the time difference in water level collected.

The maximum depth to water for the shallow groundwater considered is 27 m which is assigned rating of 5 while the minimum is 2 m assigned rating of 10. Very shallow groundwater is mostly found on the central and western flat part and southern part at the mouth of Atebela River. In addition, it is observed where springs are made into dug wells (Andode Spring) on the eastern portion along the road to Butajira. In contrast, the shallow groundwater becomes deeper on the hills (Fig 8.2).

Recharge estimation for the catchment is done by using the value obtained from the soil-water balance method which is distributed for the whole catchment based on the influence of the slope and soil on the recharge. Accordingly, the slope is given an

importance weight of 40 % and the soil thickness 60 %. Using the original rating assigned for slope soil thickness in Table 8.1, another rating values are given to each based on the principle that recharge is small on steep area and thick soil (See Table 8.3). The net recharge values over the area obtained using this method range between 73.45 – 118.05 mm. The recharge is high on the southern, southeastern and eastern part of the catchment and decreases towards the north. This can be attributed to the flat topography and coarser and small soil thickness. Recharge is observed to be low in the central and western part (on the swamp) may be due to the fine textured - montmorillonitic nature of the soil as well as its large thickness. Where the evaporation is high on the Suba Forest, the recharge is intermediate on the steep hillside the recharge is the lowest and a rating value of 1 is assigned. The highest rating value of 9 is assigned for the biggest recharge value (Fig 8.3).

Concerning the aquifer media, the highest rating value of 9 is assigned for both fractured and weathered ignimbrite and basalt which cover the largest portion of the catchment. Sand and gravel deposit found along the stream or river banks are assigned rating value of 8. The lowest rating value of 3 is assigned for the acidic rock of rhyolite found on the southeastern part of the study area. The rating values assigned is based on the available lithological logs and geological map of the study area and the exactness of the ratings depend on data density (Fig 8.4).

Soil media is the other DRASTIC parameter considered in the study area. For mapping of the soil media, borehole lithological logs, satellite image and field visual observation are applied. This involves of course mapping of both soil texture and soil thickness for the catchment which is separately rated (Table 8.1). The final rating map of the soil media is therefore the average of the two calculated in ERDAS Modeler. Accordingly, the result shows that the lowest rating value of 4 is falling on the central and western part of the catchment where the soil is texturally classified as clay (black cotton clay) and thick (Fig 8.5). The highest rating value of 10 is assigned where the soil is thin or absent and texturally sandy loam or silty loam found along stream banks and hills on the eastern and northeastern, southern and southwestern part of the

study area (Fig 8.6). Soil media is assigned only weight of 2 and its contribution in the final DRASTIC output becomes less.

There is big variation in the slope of the study area due to the presence of volcanic mountains and the flat area of deposition forming sharp slope angle. The mountains and hills are characterized by high slope where the erosion gullies are the highest. The rating value of 1 is assigned for the slope of 44 – 107 % while the highest rating of 10 is assigned for the slope of 0 – 5 % which is dominating the central, western and southern part of the catchment (Fig 8.7). Slope is assigned the least weight from the DRASTIC parameters and its influence in the final output will be undermined.

Rating of the vadose media is done in the same manner as applied in the soil media considering both the media and its thickness which are separately rated (Table 6.1). Borehole lithological logs and geological map of the study area are used in mapping the vadose media. The thickness did not consider the upper soil and each of the rock encountered is weighted for its thickness and rated accordingly (Fig 8.8). The average rate is calculated on ERDAS Modeler. Accordingly, the highest rating of 9 is falling on the vadose media characterized by vesicular basalt and basalt, trachyte and ignimbrite in the northeast and in the west, respectively where the thickness is lowest. The lowest rating of 2 on the other hand is assigned where vadose thickness is higher and the media is ignimbrite, tuff and clay (Fig 8.9).

The hydraulic conductivity on the other hand is determined based on the classification made by Freeze and Cherry (1979) which is cross-checked with well yields where available. The rating for hydraulic conductivity was therefore done from aquifer media in which the highest value is found in fractured and weathered basalt and it is assigned a rating value of 10. The weathered and fractured ignimbrite and the sand and gravel deposit are rated 8 while the weathered trachy-basalt and rhyolite are rated the least (Fig 8.10).

Finally, two DRASTIC vulnerability indexes, namely normal DRASTIC and pesticide DRASTIC were calculated and applied for the hydrogeologic catchment of Atebela River from the above DRASTIC parameters for which rating maps was produced in the objective of subdividing the area into several units showing differential potential for pollution (Fig 8.11 and Fig 8.12). The procedure followed to accomplish this based on Equation 2.1 and using spatial analysis function in ArcGIS 9.1 where all the values for the individual parameters are reclassified. This is followed by raster calculator function in which the parameters are multiplied by their respective weights and added to produce DRASTIC index. The cell size is equal for all input parameters which enable the corresponding cells representing different levels of vulnerability to be manipulated arithmetically. Therefore, the catchment was classified into five vulnerability groups based on the calculated indices which are presented in Table 9.1.

Table 9.1 Vulnerability classification and corresponding DRASTIC indices

No.	Normal DRASTIC Index	Pesticide DRASTIC Index	Vulnerability Classification	Color Assigned
1	96.0 – 119.4	106.0 – 133.8	VERY LOW	Dark olive green
2	119.4 – 142.8	133.8 – 161.6	LOW	Light olive green
3	142.8 – 166.2	161.6 – 189.4	MEDIUM	Yellow
4	166.2 – 189.6	189.4 – 217.2	HIGH	Rose
5	189.6 – 213.0	217.2 – 245.0	EXTREMELY HIGH	Red Orange

The groundwater intrinsic vulnerability map is displayed in Figure 8.11 and 8.12. The areas with very low or low vulnerability are shown in dark and light olive green, respectively; those with medium vulnerability are shown in yellow; and while those areas with high or extremely high vulnerability are shown in rose and red orange, respectively.

The normal DRASTIC map in Fig 8.11 shows extremely high vulnerability with DRASTIC Index of 189.6 – 213.0 is characterizing the southern flat part extending to the center of the catchment. It is also manifested along the road to Butajira southeast of Sebeta town. This area is characterized by the smallest slope percent and the aquifer is fractured and weathered basalt and gravel which have the highest rating

value. Further the soil thickness is varying between 0.04 – 6.00 m. High vulnerability with DRASTIC Index of 166.2 – 189.6 covers the major portion of the catchment extending from the east around Sebeta and Alemgena towns to the west beyond Tefki. The vulnerability index decreases towards the elevated area of the catchment where the percent slope increases and the recharge value decreases. The area around the swamp is classified as medium vulnerable zone including the area northwest of the catchment.

On the other hand, the pesticide DRASTIC in Fig 8.12 shows that extremely high vulnerability with DRASTIC Index of 217.2 – 245.0 is falling mostly following the stream channels characterized by sand and gravel deposit, along the road to Butajira southeast of Sebeta where jointed ignimbrite is expose and the soil is thin. In addition, it is manifested in some localities of weathered and fractured basalt in the southwest of the catchment. In the same manner, most of the catchment is classified as highly vulnerable characterized by the flat part of the catchment. The swampy are again is falling in medium vulnerable zone. The vulnerability values decrease still on the hillside (recharge areas) where the vadose media is characterized by large thickness of 17 – 34 m and trachyitic.

In general extremely high vulnerability zones are in limited areas following the rivers and flat areas of thin soil and high vulnerability zones are dominating the study area in both the intrinsic vulnerability DRASTIC cases.

The specific vulnerability map produced for nitrate in Fig 8.13 shows extremely high vulnerability in the central, southwestern and southern part of the catchment which is characterized by agricultural practices. In addition, the effect is observed along the road to Butajira. The major problem can be seen following the river course. High and medium vulnerability for nitrate is exhibited in down stream of the populated part and along the streams as well as the flat part of the catchment along the road to Jimma.

On the other hand, specific vulnerability mapped for hazard centers in Fig 8.14 shows that most of the pollutant sources in Sebeta-Alemgena area fall in medium to extremely high vulnerable zones. The effluents they are releasing are affecting the down stream settlers especially those found in the vicinity of the Atebela River. The impact of floricultures on groundwater is not yet detected but those which are located on the western part of the catchment around Tefki fall on medium vulnerable zone while those around the town of Sebeta are on high vulnerable zone.

CHAPTER X

10 SYNTHESIS

The objective of this chapter is to discuss the importance and contribution of each chapter for the overall current research and to each other. Mapping of groundwater vulnerability using the DRASTIC model involves seven parameters (depth to water, recharge, aquifer media, soil media, topography, vadose zone media and hydraulic conductivity), and in order to arrive to this ultimate goal one needs to consider many factors. These are: surface geologic properties, hydrogeological setting, soil properties, meteorological factors, land cover and land use, hydrochemistry, groundwater movement, and pollution sources.

Geological and hydrogeological investigations of the study area are conducted since there is no detail previous work done concerning it. Borehole data such as lithological logs, thickness of rocks, well yield, etc are used to infer these factors. Their importance for the research is considerable since, geology as a whole and hydrogeology in particular in the first place are the controlling factors for the fate and transport of contaminants. The surface geological cover determines the rate of infiltration of water and thereby that of the contaminant into the groundwater. That means the porosity and permeability property of the material control the entrance of water into the water bearing formations and the rate of transmission of the water and the contaminant through the groundwater, and the longer path it takes the more it is attenuated.

Groundwater movement is the other factor that needs to be worked out in the groundwater vulnerability assessment. It plays the role of controlling the movement (rate and direction) of contaminants within the soil, vadose or aquifer media. The attenuation of a contaminant depends on the rate at which the groundwater is being transporting the contaminant within the different media. The direction of groundwater movement (vertical or horizontal) of course is governed by the porosity and

permeability or the hydraulic conductivity of the material. Groundwater movement is higher and horizontal within materials of high hydraulic conductivity and therefore, contaminants can easily arrive to the groundwater before they are being attenuated.

The importance of soil mapping is a necessity since it is considered as the first defense line against the contamination of groundwater. It plays the role of attenuating the contaminants infiltrating downward through the soil together with water. The soil in general is characterized by many chemical processes going on in it. The textural and thickness classification of the soil in the study area becomes significant since it controls the rate of infiltration of the water and that of the contaminant. Contaminant migration is restricted by the presence of fine textured materials and these can decrease the overall permeability of the soil; in other word recharge into the groundwater is texture controlled. Soil thickness on the other hand determines the attenuation processes of filtration, biodegradation, sorption and volatilization and therefore needs to be mapped and rated separately.

The other important factor that needs to be analyzed to fulfill the goal of mapping the groundwater vulnerability to contamination is meteorological elements. This is a broad subject that involves the treatment of the elements (rainfall, temperature, wind speed, humidity, and sunshine) to determine the rainfall pattern and to obtain the actual evaporation rate of the study area. This ultimately leads us to obtaining the total recharge into the groundwater. The recharge obtained using the soil-water balance method well approximates the recharge value in the study area but this is only one recharge value obtained for the catchment and a different approach of distributing this value for the catchment based on the influence of the slope and soil on the recharge.

Land cover and land use mapping is done for the study area since it has the potential impact on groundwater quality. The effect of land cover and land use on the groundwater quality is resulting from alteration over time of the soil matrix and unsaturated zone media (Dereje Nigussa, 2003).

The importance of conducting hydrochemistry analysis for the available data of the study area is to make a comparison between the different zones obtained by applying vulnerability mapping. That is it is useful as a confirmation to tool for the research work. The natural groundwater chemistry is changing with time due to the increasing impact of human activities. Nitrate is one of the indicator ions and it has been applied to confirm the vulnerability mapping done in the study area. Bacteriological confirmation was also important but due to the shortage of data availability, it was not applied.

Lastly, analyzing the pollutant sources is important in order to identify those contributing to the deterioration of the groundwater quality. Several hazard centers are identified in the study area especially in the urbanized part where many factories are inventoried having the potential of contaminating the groundwater. The rural part on the other hand is experiencing modern farming practices of fertilizers and herbicides application and is also considered potential for polluting the groundwater. Currently, floricultures are known to use heavy metals for the production of metals and therefore they can be taken as point pollution sources.

CHAPTER XI

11 CONCLUSIONS AND RECOMMENDATIONS

11.1 CONCLUSIONS

The quality of groundwater is usually very good under natural conditions and normally requires less treatment to make it safe to drink than river water. But it is gradually and extensively being contaminated as time goes on and this can be attributed to the release of contaminants through several activities caused by human beings as well as natural factors. Groundwater vulnerability to contamination stems from land-based development and industry. Once this precious resource is contaminated, it is difficult, costly and sometimes impossible to reverse to the original condition. The best mechanism of sustainable utilization of groundwater is therefore the prevention of the resource through knowledge of the sensitivity of the hydrogeologic setting towards contamination scenarios.

Groundwater is at risk of pollution in Sebeta-Alemgena area due to the industrial and agricultural development as well population growth. The research is conducted in the overall objective of mapping the degree of groundwater vulnerability to contamination using hydrogeological data of the study area by applying DRASTIC model based on GIS. The model considers seven parameters like depth to water, recharge, aquifer media, soil media, topography, vadose zone media and hydraulic conductivity for which data base were produced are derived from meteorological data, soil data, borehole data, geology and land use.

The purpose of producing groundwater vulnerability map of the study area is to provide a guideline to the protection of the groundwater of the catchment and to help future land use planning within the catchment. Therefore, the following conclusions are drawn from the research work.

- The different lithologic unit in Sebeta-Alemgena area exhibit varying degree of intrinsic vulnerability classes as conducted by normal DRASTIC and pesticide DRASTIC methods. Those units which are classified as extremely high and high vulnerable class such as the river side sand and gravel deposits, the weathered and fractured basalt in the central, southern and southwestern part of the catchment and the weathered and fractured ignimbrite covering major part of the catchment need considerable attention.

- Although the central part of the catchment is characterized by thick clay soil, due to the other factors such as small percent slope, relatively higher recharge, shallow depth to water and fracturing and weathering properties of the aquifer media, the area has been grouped into high vulnerable zone.

- According to this research, the very low to low vulnerability areas are the elevated or the recharge areas of Wechecha Mountain in the north and Daleti Hill in the east which is attributed to high percent slope, deeper depth to water and thick vadose zone media. The medium vulnerability zone is relatively small in area coverage but it is manifested on the swampy area and northwest of the catchment.

- The specific vulnerability of nitrate prepared on normal DRASTIC vulnerability from the available nitrate data shows extremely high vulnerability in the central part of the catchment as well as the southern part following the river course. However, the nitrate vulnerability map of Atebela groundwater catchment does not reflect the contaminant transport and transformation behavior.

- The hazard centers located in Sebeta town are mostly located on extremely high and high vulnerable zones. Those industries found in Sebeta town are releasing their effluents into rivers which infiltrates into the groundwater through the stream bed characterized by jointed rocks and alluvial deposits. The odor of the effluents has disturbed the normal surface water utilization the downstream dwellers.

- The vulnerability maps are presenting various complex hydrogeological properties into an integrated and comprehensive way. A map showing areas of different color, symbolizing different degrees of vulnerability (or natural protection) and possible hazards to the groundwater pollution is easily interpreted and ultimately used to:

  - Provide useful information for designing and management of groundwater quality monitoring networks in the study area.

  - The graphical representation of vulnerable aquifers, combined with graphical representations of potential sources of contamination and public water supplies would allow decision makers to evaluate current land use practices and make recommendations for changes in land use regulations which would better prevent the groundwater from contamination.

  - Assist town planners and land use professionals in the development, settlement and housing expansion in relation to groundwater control within the study area,

  - They are useful for locating operation of facilities for waste disposal, treatment and reuse.

  - They can be useful tools for legislation, including zoning, regarding land-use alteration and practices in the context of protecting groundwater quality.

  - The maps are easily understandable even by non professionals, decision makers and managers.

  - They are generally practical tools for land-use planning, protection zoning and risk assessment

- Vulnerability mapping using model builder in ArcGIS 9.1 has the following advantages:
  - Very fast vector to raster map transformation, map overlay, reclassification and mapping results;
  - The established model is easy for correction, and the maps are easily corrected and reproduced;
  - All input data, intermediate and final mapping results can be displayed in one window by running the model once.

11.2 RECOMMENDATIONS

The following recommendations are synthesized from the research work in Atebela River catchment:

- The groundwater exploitation of Atebela catchment and that of the country as a whole which is restricted to water distribution, water use, operation and maintenance need to consider groundwater management and protection as one issue for its sustainable use.
- The highly vulnerable areas mapped by current research need attention and prevention of those aquifers falling within these zones are important. It is recommended to cautiously plan future land use practices within these zones.
- The specific vulnerability mapping for nitrate is not conducted using sufficient data from different sources of water and the reliability of the input data matters. It is highly recommended to conduct the validity of the maps applying different approaches such as seasonal water level data analysis, conducting bacteriological and other hydrochemical analysis of pollutant indicators, natural and artificial tracer test analysis.

- Assessment and mapping of vulnerability is conducted based on limited available data and is less detail. Hence, a detail investigation and mapping is highly recommended for a particular purpose and large scale considerations in order to include minor variations that can have major contribution towards the transport of contaminants.

- It is recommended to create public awareness about environmental protection and educate and inform planners, regulators, and decision makers about groundwater protection and contamination prevention.

- Those industries releasing effluents into the rivers are recommended and enforced to treat before disposing them for the well being of the society.

- I recommend detail soil mapping, hydrogeological investigation, recharge estimation and water level measurement for the study area.

REFERENCES

Abinet Gebremedhin, 2006. Engineering Geological Problems and Countermeasures for Flexible Pavement on Expansive Soils, thesis submitted to the School of Graduate Studies, Addis Ababa University, July, 2006.

Aller L., Bennet T., Lehr J.H., and Hackett G. 1987. DRASTIC: a standardized system for evaluating groundwater pollution potential using hydrogeologic settings. U.S. Environmental Protection Agency, Ada, OK, EPA/600/2-87-036,455 p.

Bachmat Y, and M. Collin (1987). Mapping to Assess Groundwater Vulnerability to Pollution, Proceedings of the International Conference on Vulnerability of Soil and Groundwater to Pollutants, March 30- April 3, 1987 at Nordwijk aan Zee / (ed. By W.van Duijven-booden and H.G.van Waegeningh)- The Hague. (p 297-307),

Civita, M., and De Maio M. (2000). SINTACS R5, a New Parametric System for the Assessment and Automating Mapping of Groundwater Vulnerability to Contamination, Pitagora Editor (Bologna).

Dereje Nigussa, 2003. GIS Based Groundwater Vulnerability Assessment in Akaki River Catchment, Addis Ababa, Central Ethiopia, MSc Thesis, School of Graduate Studies, Addis Ababa University, November 2003.

Di Paola, G.M., 1976. Geological Map of the Tulu Moya volcanic area CNR, Italy

Focazio, M.J., A.H. Welch, S.A. Watkins, D.R. Helsel, and M.A. Horn, 2000. A retrospective analysis on the occurrence of arsenic in ground-water resources of the United States and limitations in drinking-water supply characterizations. USGS Water Resources Investigations Report. 99-4279. Reston, Verginia.

Foster S.S.D. 1987. Fundamental concepts in aquifer vulnerability, pollution risk and protection strategy. In Vulnerability of soil and groundwater to pollutants (W. van Duijvenbooden and H.G. van Waegeningh, eds.), TNO Committee on Hydrological Research, The Hague, Proceedings and Information No. 38, p. 69-86.

Freeze R. and Cherry A. (1979). Groundwater. A Simon and Schuster Company Eaglewood Cliffs. New Jersey. USA.

Golwer A. 1983. Underground purification capacity. Groundwater in water resources planning, Proc. UNESCO Intl. Symp., Koblenz, Germany, Aug. 28-Sept. 3, 1983, UNESCO/IAH/IAHS, National Committee of the Federal Republic of Germany for the IHP, vol. II, p. 1063-1072.

GEODEV – AFREDS PLC Consortium, 1999. Final Report on Geology and Mineral Resources of Oromia, Oromia Mineral Resources Development Study Project, Oromia Economic Project Office, OMEB; Finfinne.

Hem, J.D. (1985). Study and Interpretation of the Chemical Characteristics of Natural Water, U.S. Geological Survey Water Supply Paper 2254, 263pp, 3rd ed.

Kazmin, V. 1979. Relationship between rifts and Precambrian basement in East Africa Annals of Geological Survey of Egypt V. 19 pp 54-60.

Kebede Tsheahyu, Solomon Waltenigus, Shiferaw Lulu, Abebe Gebrehiwot (2004). Groundwater management using groundwater modeling; Case study Akaki well field, Addis Ababa, Proceeding of the International Conference and Exhibition on Groundwater in Ethiopia.

Kukuric, N. (1999). Development of a Decision Support System for Groundwater Pollution Assessment, PHD dissertation, A.A. Balkema Publishers, Rotterdam, The Netherlands.

Manahan Stanleye (1991). Environmental Chemistry, 5th Edition, Lewis Publishers, USA.

Mengesha Teferra, Tadiwos Chernet and Werkineh Haro (compiler), 1996. Geological Map of Ethiopia, scale 1:2,000,000, 2nd edition and explanatory note, Bulletin No. 3, GSE.

Meresa Kiros (2006). GIS-based Vulnerability and Hazard Mapping for the Protection of Dire Dawa Groundwater Basin, Ethiopia, MSc Thesis (WSE-HY-06.03) UNESCO IHE Institute for Water Education, Delft, the Netherlands. March, 2006

Meyer W. Pilger A Rosler A and Stels J, 1975. Tectonic evolution of the northern part of the Main Ethiopian Rift in southern Ethiopia in Afar Depression of Ethiopia Eds A Pelger and A Rosler schweizerbart schverlag Stuttgart PP 375-360.

Morbedelli L. Nicoletti M. Petrucciani C. and Peclrillo E. M. 1975. Ethiopian southeastern plateau and related escarpment: K-Ar ages of the main volcanic events (Main Ethiopian Rift from 80 10'to 9. 00' lat N) In Afar Depression of Ethiopia Eds A plgert and A Roslet Schweizerbart schevErlag. Stuttgart, PP 362-369.

Morton, W. H., Mitchell J.G. Rex, D.C and Mohr P., 1979. Rift ward younging of volcanic units in the Addis Ababa region, Ethiopian Rift Valley, nature, 280, pp 284-288.

National Research Council (U.S). 1993. Groundwater vulnerability assessment—predicting relative contamination potential under conditions of uncertainty. Committee on Techniques for Assessing Groundwater Vulnerability, National Research Council, National Academy Press, Washington DC, 52 p.

Ogbanna, D.N., Ekeweozor I.K.E. and Igwe F.U. 2002. WasteManagement: A tool for Environmental Protection in Nigeria. Synopsis, Ambio, Vol. 31, No. 1, February2002.

Rao, P.S.C., and W.M. Alley, 1993. Pesticides. In W.M. alley (ed.). Regional groundwater quality. Van Nostrand Reinhold, New York.

Rao, C.S (1996). Environmental Pollution Control Engineering, Newage International (P) Limited, Publishers, New Delhi.

Robins, N.S. (1998). Groundwater pollution, Aquifer Recharge and Vulnerability, published Geological Society, Special Edition No. 130

Seifemichael Berhe and Kazmin V. 1978. Geological Map of Nazret map sheet (NB37-15) Eth Inst of Geological Survey. Addis Ababa.

Seifemichael Berhe and Kazmin V., 1987. Geology, Geochronology and Geodynamic implications of the Cainozoic Magmatic Province in west and southeastern Ethiopia, Journal of the Geol. Soc. of London, vol.144.

Shaw, E.M. 1988. Hydrology in Practice. Chapman and Hall London.

Tamiru Alemayehu, 2004. Assessment of Pollution Status and Groundwater Vulnerability mapping of the Addis Ababa Water Supply Aquifers, Ethiopia.

Tamiru Alemayehu, Dagnachew Legesse, Tenalem Ayenew, Yirga Tadesse, Solomon Waltenigus and Nuri Mohammed, 2005. Hydrogeology, Water Quality, and the Degree of Groundwater Vulnerability to Pollution in Addis Ababa, Ethiopia. UNEP/UNESCO/UN-HABITAT/ECA

Taye Alemayehu, 1988. Pollution of the Hydrogeologic system of Dire Dawa groundwater Basin,

Tesfaye Berhe, 1998. The Degradation of the Abo-Kebena River in Addis Ababa, Ethiopia. MSc Thesis, School of Graduate Studies, Addis Ababa University, June 1998.

Thornthwaite, C.W., 1944. Report of the committee on transpiration and evapotranspiration, 1943-1944. Transactions American Geophysical Union 25, 683-693.

Thornthwaite, C.W., 1948. An approach toward a rational classification of climate. Geographical Review, 38, 55-94, 1948

Thornthwaite, C.W. and Mather, J.R., 1957. Instructions and tables for computing potential evapotranspiration and the water balance, Publication 10, 185–311. Centeron, N.J.: Laboratory of Climatology

UK Groundwater Forum 2004. Groundwater Basics

Van Bavel, C.H.M., 1996. Potential evaporation: the combination concept and its experimental verification. Water Resources Res. 2: 19-31.

Vowinkel, E.F. and Clawges, R.M., 1996. Variables indicating nitrate contamination in bedrock aquifers, Newark Basin, New Jersey. Water Resources Bulletin 32: Vol. 32. N5. 1055-1066.

Vrba, J. and Zaporozec, A., 1994. Guidebook on Mapping Groundwater Vulnerability. International Contribution to Hydrogeology. IHP-IV, Project M-1.2 (a). Verlag Heinz Heise. Vol 16, 1994

Zaporozec, A. (ed.), 1985. Groundwater protection principles and alternatives for Rock County, Wisconsin. Wis. Geological and Natural History Survey, Madison, WI, Special Report 8, 73 p.

Zwahlen, F, 2003. Vulnerability and risk mapping for the protection of Carbonate (karst) Aquifers, European Approach, COST Action 620, Final Report.

ANNEXES

Annex 1 Water level database used for interpolation of depth to water map

Site	X_UTM	Y_UTM	Elev (m)	Depth to water	GW_Elev	Yield (l/s)
Boneya	460464	974637	2095	38.14	2056.86	3.5
Awash Melka	456740	962388	2000	3	1997	
Darge-Suq	464300	990600	2277	14.4	2262.6	
Gen.Gebre	463600	988200	2278	27.5	2250.5	
Fulaso (Harojila)	451518	985340	2141	2.45	2138.55	
Bole	450080	985388	2132	6	2126	
Qocha	449527	985178	2121	10	2111	
Makalo	448899	985053	2116	7.5	2108.5	
Hordofi	449558	986067	2149	9	2140	
Mt. View	453035	982639	2101	17	2084	
Haro Jila (HDW)	449434	980645	2075	7	2068	
Haro Jila2 (HDW)	449407	980765	2071	6	2065	
Dairy (Tefki)	447020	978672	2067	6	2061	
HDW (Tefki)	445254	978171	2066	9	2057	
Gora-1	452891	980250	2071	4.5	2066.5	
Gora-2	452924	980195	2069	3.5	2065.5	
Mango Gora	453268	980729	2076	1.8	2074.2	
Matali	451276	979174	2077	3.5	2073.5	
Gora Harkiso-1	452457	977565	2073	11	2062	
Gora Harkiso-2	452466	976970	2067	4.5	2062.5	
Mehal Atebela	455035	981813	2090	13	2077	
Andode Sp-HDW	461003	977106	2110	2	2108	
Cholo	441773	968943	2062	21	2041	
Lilu	441578	967182	2079	27	2052	
Gila	454714	978831	2062	9	2053	
Gombore	454683	975426	2064	11	2053	
Mehal Sefera	455784	977521	2059	13	2046	
Malima& Deti	455988	979556	2072	9	2063	
Bebeli	457439	978436	2077	8	2069	
Tiliqu Sefer	457922	974666	2073	10	2063	
Berga-1	455502	980145	2073	22	2051	
Berga-2	458390	976091	2075	14	2061	
Turo	457253	973055	2057	8	2049	
Koticha	456773	980613	2072	10	2062	
Dima Magno-1	454809	981251	2083	9	2074	
Dima Magno-2	454323	981723	2085	7	2078	
Bure	442993	968724	2082	28	2054	
Tafki Golden Rose-1	442842	977555	2074	14.15	2060	
Tefki Golden Rose-2	442811	977625	2073	9.9	2063	

Annex 2 Spring chemistry data

Site Name		Geme Spring	Debel Spring	Seb. WS Sp.	Sebeta WS	Meta Abo
Location	X_UTM	457023	459268	459268	459831	455287
	Y_UTM	981813	984313	985817	985582	985619
Elev (m)		2087	2164	2217	2227	2200
Temp (0C)		24.4	22.1	22.4		
pH		6.86	6.78	6.67	201	148
EC		467	513	306	138	18.8
TDS		303.55	333.45	198.9	21.5	
Alkal		240	210		6.56	
Na					201	148
K					138	18.8
Mg					9.1	
HCO_3		292.8	256.2		4.6	
CO_3					26.4	
SO_4		7	1		5	
Cl					122.98	
NO_3		40.92	3.96			
NO2-					0.26	
NH4		0.129	0.0387		9.6	
NH3		0.121	0.0363		3	
PO4		2.8	2.3			
B					0.025	
As					0.06	
Mn		0.03	0.2			
Fe		0.02	0.02			
Cu		Nil	0.01			
TH		180	188			
DO					86.3	

Annex 3 Chemistry and discharge data for boreholes and hand dug wells

Site Name	Location		Elev (m)	Temp (0C)	pH	EC	TDS	Alkal	Na	K	Ca	Mg	HCO_3
	X_UTM	Y_UTM											
Fulaso (Harojila)	451518	985340	2141	21.2	7.37	296	192.4	130					158.6
Bole	450080	985388	2132	21.8	6.94	364	236.6						
Makalo	448899	985053	2116	20.9	7.11	520	338	160					195.2
Hordofi	449558	986067	2149	21.4	7.22	610	396.5	260					195.2
Haro Jila (HDW)	449434	980645	2075	21	7.33	681	442.65						
Haro Jila2 (HDW)	449407	980765	2071	19.8	7.55	703	456.95						
Dairy (Tefki)	447020	978672	2067	19.5	7.79	805	523.25	316					385.52
HDW (Tefki)	445254	978171	2066	19.7	7.46	599	389.35						
Gora 1	452891	980250	2071	20.6	7.49	505	328.25						
Gora 2	452924	980195	2069	20.1	7.32	444	288.6	162					197.64
Mango Gora	453268	980729	2076	20.2	7.03	429	278.85						
Matali	451276	979174	2077	20.7	6.94	523	339.95						
Gora Harkiso 2	452466	976970	2067	20.6	7.48	733	476.45						
Mehal Atebela	455035	981813	2090	23.3	6.98	980	637						
Andode Sp-HDW	461003	977106	2110	23	7.26	488	317.2	192					234.24
Cholo	441773	968943	2062		6.6	294	174	144	9.4	2.8	41.5	7.02	175.7
Lilu	441578	967182	2079		6.7	440	270	187.2	22.5	4.2	56.45	8.64	228.4
Gila	454714	978831	2062		7.05	640	364	312	36	7.1	78.5	22.7	380.6
Gombore	454683	975426	2064		6.96	810	542	336	20	4.9	121.7	28.1	409.9
Mehal Sefera	455784	977521	2059		6.89	776	468	362.4	25	6.4	117.3	24.3	442.1
Malima& Deti	455988	979556	2072		6.75	837	500	285.6	34	5.7	99.7	28.1	348.4
Bebeli	457439	978436	2077		6.7	381	220	196.8	18	2.4	56.45	10.8	240.1
Tiliqu Sefer Adea)	457922	974666	2073		7.19	771	442	396	42	3.2	105.8	24.3	483.12
Berga #1	455502	980145	2073		6.84	386	226	148.8	16	4.2	49.4	11.9	181.5
Berga #2	458390	976091	2075		6.58	676	458	151.8	48	1.2	91.7	11.9	185.2
Turo	457253	973055	2057		7.2	523	294	249.6	30	3	74.1	12.42	304.5
Koticha	456773	980613	2072		7.18	523	302	268.8	22	5	70.56	19.44	327.9
Balchi Medianelem	458457	970573	2113		7.08	509	304	254.4	19	2.7	70.56	17.3	310.4
Gichichi	458061	971737	2080		7.18	606	354	312	18	3.5	84.7	23.76	380.64
Dima Magno_1	454809	981251	2083		6.86	338	214						
Dima Magno_2	454323	981723	2085		6.9	697	420	331.2	32	3.6	100.6	21.1	404.1
Kontoma	453850	973096	2060		7.23	632	303						
Dobi	451420	971692	2063			1327	645						
Boneya	460464	974637			7.1	376	236		15.5	1.8	46.98	13.8	226.5
Boneya (BH)	460464	974637		22.5			337.35	224					273.28
Awash Melka	456740	962388			7.19	510	350		42	9.8	62.8	9.4	333.1
Tefki	444624	978143			7.44	726	455		116	6.6	36.4	6.1	345.9
Tefki Golden 2	442811	977625	2066		7.94	653	313					44	
Daleti	460810	981473			6.97	344	222		15	4.8	43.7	13.2	217.8
Sebeta BH12	463742	985378			7.9				20.4	4	56.1	9.7	268.4
Meta Abo Bre	455000	985200			7.7	191	117		23.8		24.1	3.9	122
Alemg Jafar Tannery	459676	984947		20		291							
G. Gebre Kebede	463600	988200		19.7			220						
Sebeta Dragados	457030	984617			6.85	979	597		16	3.4	36	9	178
Healthy Water	463572	988693			6.92				8.6	11			
Geja Dera	461930	970844			7.37	507	243						
Seb Agro # 1	460850	985850			6.65	244	159		16	3.1	28.8	4.84	141.5
Seb Agro # 2	460500	986500		21.8	6	211	136						
Debel Yohanes	445643	973409			7.06	333	219		17	4.2	50	8.3	235.7
Meta A Bre BH5	455300	985250		21.6	7.3		139		14	6.6	20	46	122
Meta A Bre BH8	455525	984000		24.7			140						
Meta A Bre BH7	455350	985100		25			144						
Health Water Bottling	463572	988693			6.92	488	232		8.6	11			
A/G Hafde PLC	461412	986324		20		288							
Sebeta Tal Flow #2	455426	982736			6.7	422	273		17	4.2	68.3	9.4	218.4
Sebeta WS	459831	985582	2227	21.5	6.56	201	138		9.1	4.6	26.4	5	122.98
Meta Abo	455287	985619	2200			148	18.8						

Annex 3 – Continued

Site Name	Location		SO_4	Cl	NO_3	NH4	NH3	PO4	F	Mn	Fe	Q (l/s)
	X_UTM	Y_UTM										
Fulaso (Harojila)	451518	985340	13		13.64	10.449	9.801	1.75		0.45	1.18	
Bole	450080	985388										
Makalo	448899	985053	47		7.04	0.2064	0.936	2.8		0.1	0.03	
Hordofi	449558	986067	19		2.64	0.516	0.484	2.8		2.2	0.01	
Haro Jila (HDW)	449434	980645										
Haro Jila2 (HDW)	449407	980765										
Dairy (Tefki)	447020	978672	25		1.32	0.129	0.121	0.56		0.1	0.02	
HDW (Tefki)	445254	978171										
Gora 1	452891	980250										
Gora 2	452924	980195	12		7.04	2.064	1.936	1.71		0.01	0.08	
Mango Gora	453268	980729										
Matali	451276	979174										
Gora Harkiso 2	452466	976970										
Mehal Atebela	455035	981813										
Andode Sp-HDW	461003	977106	18		3.52	0.0645	0.605	0.84		0.1	0.06	
Cholo	441773	968943	8.99	1.92	13.2		0.532	0.158	0.7	0.05		
Lilu	441578	967182	17.9	17.3	1.5		0.311	0.327	0.3	0.05		
Gila	454714	978831	12.4	15.36	2.6		0.383	0.115	1.44	0.17		
Gombore	454683	975426	28.9	31.68	14.15		0.64	0.258	0.95	0.13		
Mehal Sefera	455784	977521	33.6	15.36	9.1		0.61	0.449	0.29	0.1		
Malima& Deti	455988	979556	18.6	81.6	0.62		1.1	0.122	0.94	0.07		
Bebeli	457439	978436	2	2.9	5.94		0.273	0.266	0.03	0.02		
Tiliqu Sefer Adea)	457922	974666	11.9	10.6	0.74		0.15	0.09	1	0.15		
Berga #1	455502	980145	15.1	12.5	11		0.02	0.413	0.6	0.02		
Berga #2	458390	976091	38.3	146.4	28		0.286	0.251		0.02		
Turo	457253	973055	10.5	6.72	4.09		0.409	0.348	1.15	0.02		
Koticha	456773	980613	2.2	3.84	4.78		0.617	0.19	1	0.1		
Balchi Medianalem	458457	970573	7	2.9	14.2		0.422	0.503	0.36			
Gichichi	458061	971737	4.65	4.8	8.31		0.526	0.334		0.02		
Dima Magno_1	454809	981251										
Dima Magno_2	454323	981723	25.8	11.5	4.29		0.331	0.122	0.58	0.15		

Kontoma	453850	973096	15.9	21	8.5	0.27		0.178	0.88			
Dobi	451420	971692	46.2	103	10.5	0.23		0.194	0.58	0.118		
Boneya	460464	974637	0.55	5.8	11.5	0.4		0.164	2.58	0		3.5
Boneya (BH)	460464	974637	2		131.12	Nil	Nil	3.7		0.1	0.06	
Awash Melka	456740	962388	2.64	6.7	7.5	0.06		0.18	1.25	0		6
Awash Sheba Fl	454852	962780										38
Tefki	444624	978143	15.6	56.6	4.8	0.113		0.29	3.6	0		0.75
Tefki Golden 2	442811	977625	4.7	5	0.26	0.0017		0.39	1.12	0.175		
Tefki Golden 1	442842	977555										3.4
Daleti	460810	981473	0	0	7.5	0.06		0.12	0.15	0		4
Sebeta BH12	463742	985378		7.1		0.46			0.67			
Meta Abo Brewery	455000	985200		14.2	9.3			0.12				
Alemg Jafar Tannery	459676	984947										
G. Gebre Kebede	463600	988200										
Sebeta Dragados	457030	984617	2.6	5	8.69				0.49			
Healthy Water	463572	988693	2.9					0.338	0.4	0.031		3.8
Sebeta Shooting	463599	988583										4
Geja Dera	461930	970844	0	0.9	0.008	0.0014		0.161	0.58	0.08		2.3
Sebeta Agro # 1	460850	985850	1.8	3.88	14							
Sebeta Agro # 2	460500	986500		3.5	1.1			0.35	0.65			
Debel Yohanes	445643	973409	0.53	2.9	7.5	0.025		0.31	0.8	0		
Debel Kajima	443843	969974										2
Meta Abo Bre BH5	455300	985250		7.1	0.1			0.04	0.65	0.2		
Meta Abo Bre BH8	455525	984000										
Meta A Bre BH7	455350	985100										
Health Water Bottling	463572	988693	2.9					0.338	0.4	0.031		
A/G Hafde PLC	461412	986324										4
A/G ODA Flow	460937	986565										19.5
Seb Tal Flow # 1	455450	983014										6
Seb Tal Flow #2	455426	982736	1.32	4.8	10.5	0.25		0.22	0.4	0		5.35
Sebeta WS	459831	985582	0.26	9.6	3	0.025		0.06	0.8			
Meta Abo	455287	985619										
Kelecha 1	445354	969451										3
Kelecha 2	445144	969045										3

Annex 4 Rainfall Data for Meteorological Stations

	Jan	Feb	Mar	Apr	May	Jun	Jul	Aug	Sep	Oct	Nov	Dec
		Teji Monthly RF (32 Years)					Geog coor	430440	972917		Elev	2110
Total	564.10	1156.00	1737.80	2520.00	2268.00	3881.40	7079.90	6902.00	3119.10	773.50	179.30	181.50
Mean	17.63	36.13	54.31	78.75	70.88	121.29	221.25	215.69	97.47	24.17	5.60	5.67
		Awash Melka Monthly RF (30 Years)					Geog coor	457501	962333		Elev	2070
Total	449.00	781.72	1806.01	2091.08	1778.30	3014.03	6922.04	6445.80	2587.56	675.78	79.80	108.90
Mean	14.97	26.06	60.20	69.70	59.28	100.47	230.73	214.86	86.25	22.53	2.66	3.63
		Sebeta Monthly RF (30 Years)					Geog coor	458824	985569		Elev	
Total	454.50	1907.35	2414.71	3259.38	3148.97	5601.93	9852.70	11096.00	4227.90	1195.50	259.90	193.70
Mean	15.15	63.58	80.49	108.65	104.97	186.73	328.42	369.87	140.93	39.85	8.66	6.46
		Addis Ababa (OBS) Monthly RF (31 Years)					Geog coor	472616	998662		Elev	2408
Total	573.00	1171.90	2046.50	2834.50	2689.00	4232.30	8217.80	8667.50	5196.80	1231.90	213.50	263.20
Mean	18.48	37.80	66.02	91.44	86.74	136.53	265.09	279.60	167.64	39.74	6.89	8.49
		Boneya Monthly RF (30 Years)					Geog coor	463447E	987614N		Elev	2310
Total	393.40	864.42	1379.43	1921.24	1701.21	3110.96	6248.46	6281.13	3427.76	471.46	102.00	152.60
Mean	12.69	27.88	44.50	61.98	54.88	100.35	201.56	202.62	110.57	15.21	3.29	4.92
		Asgori Monthly RF (32 Years)					Geog coor	426430	971756		Elev	
Total	541.51	989.74	1587.39	2636.69	2018.11	3852.65	7150.09	7203.50	3041.38	725.84	119.11	144.28
Mean	16.92	30.93	49.61	82.40	63.07	120.40	223.44	225.11	95.04	22.68	3.72	4.51
		Holeta RC Monthly RF (17 Years)					Geog coor	443219	1002171		Elev	2380
Total	230.9	744.8	1007.0	1296.7	1090.4	1760.5	3631.2	4149.1	2125.0	304.4	70.2	133.0
Mean	13.58	43.81	59.24	76.28	64.14	103.56	213.60	244.06	125.00	17.90	4.13	7.82
		Akaki Beseka RF (32 Years)					Geog coor	479841	980027		Elev	1999
Total	453.2	926.6	2014.5	2706.5	2326.4	3893.9	8344.1	8605.8	4091.2	761.4	124.7	97.3
Mean	14.16	28.96	62.95	84.58	72.70	121.68	260.75	268.93	127.85	23.79	3.90	3.04
		Ensilale RF (32 Years)					Geog coor	435870	987443		Elev	2205
Total	569.2	825.8	1601.5	2233.6	1801.2	3349.6	6384.7	6202.1	3046.0	689.3	278.9	88.5
Mean	17.79	25.81	50.05	69.80	56.29	104.68	199.52	193.82	95.19	21.54	8.72	2.77

Annex 5 Atebela River Discharge Measurements

Measurement coordinate and elevation

X_UTM	Y_UTM	Elev (m)
453614	963655	2009

Dimension- Cross-sectional distance = 1.4 m
Average depth = 0.4 m

v = 5.1091x + 0.2727

Date	Time	Rotor Rev.	Counts	Water Velocity (cm/s)	Water Velocity m/s	Area (m^2)	Q (m^3/s)	Remark
7/8/2007	9:37	14.33	143.33	732.56	7.33	0.564	4.133	Rain previous night
7/9/2007	9:20	8.90	89.00	454.98	4.55	0.546	2.484	
7/10/2007	9:20	10.33	103.33	528.21	5.28	0.5572	2.943	

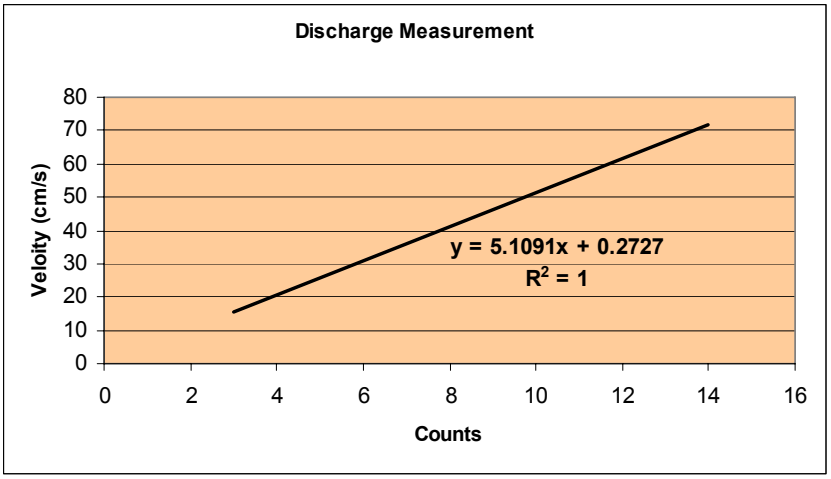

Annex 6 – Hydraulic conductivity ranges for of geological materials (Freeze and Cherry, 1979)

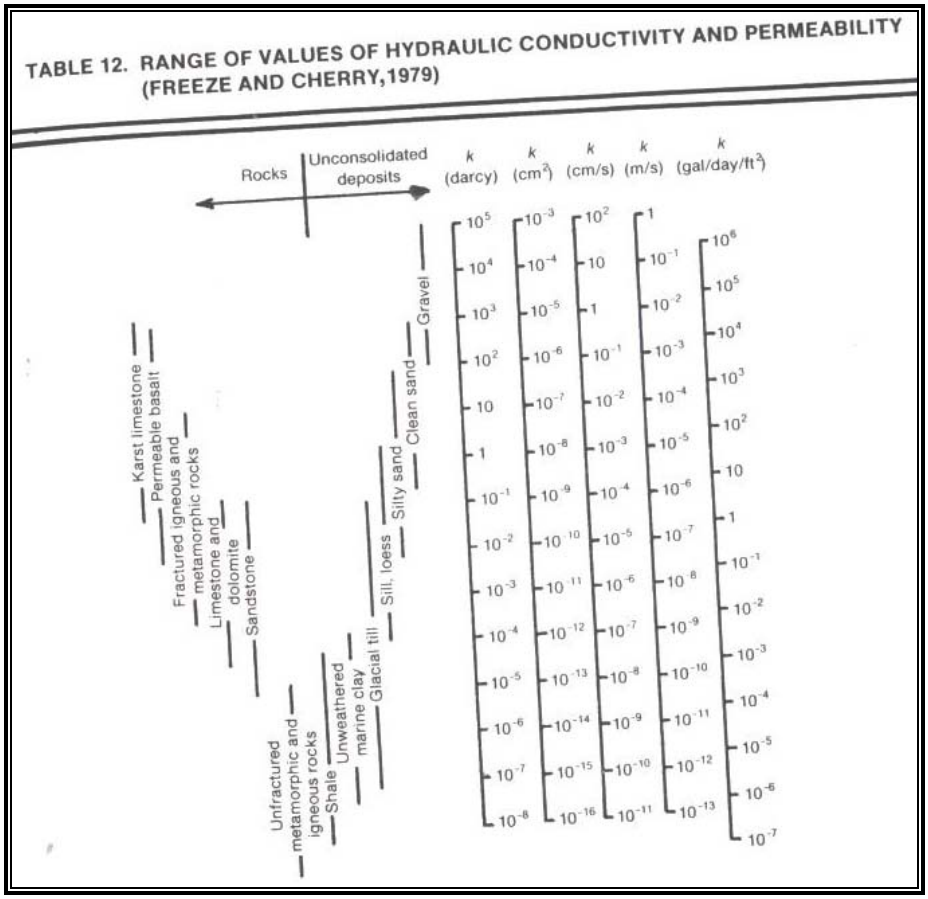

Annex 7 Soil textural classification chart (U.S. Soil Conservation Service, 1951)

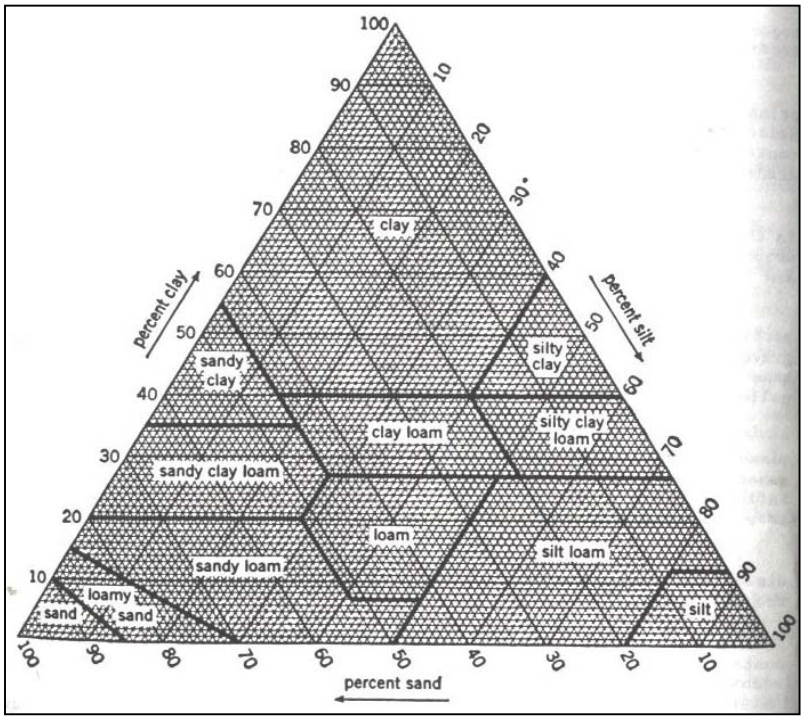

Annex 8 Soil thickness data from BHs, HDWs, and field collected

BH Name	UTM Coordinates X (m)	UTM Coordinates Y (m)	Elev. (m)	Depth (m)	Soil Thickness (m)	Soil Type
Geja Dera	461930	970844		183.2	2	
Awash Sheba Flower	454852	962780		56	4	
Alem Gena Hafde PLC	461412	986324		145	6	
Alem Gena ODA flowers	460937	986565		114	0	
Sebeta Shooting Station	463599	988583		130	32	
Sebeta BH12	463742	985378		125	30	
Geja Koye 1				165	2	
Geja Koye 2	458059	964012		112	4	
Daleti	467851	981886	2300	170	12	
Healthy Water	463572	988693	2296	100	29	
Dobi	451420	971692		60	9	
Kontoma	453850	973096		59	4	
Boneya	460464	974637		71	2	
Tefki Golden Rose#1	442842	977555	2073	100	42	
Tefki Golden Rose#2	442811	977625	2074	179	44	
	462436	986614	2284		0.4	BCC
	462564	986511	2277		1	BCC
	462480	986433	2276		0.3-0.5	gravely clay soil, grass covered
	462437	986336	2266		0.5-1	gravel mixed with black clay
	462445	986205	2271		1	BCC
	462391	986089	2270		Thin to few cm	BCC
	462177	985768	2255		>2	BCC
	462173	985668	2261		thin-absent	BCC, overlying weathered ignimbrite
	462117	985492	2275		1.5	boulder & gravel mixed with clay
Hora Food Complex	462004	985419	2275		1	
	452457	977565	2073		2	BCC
	458229	985257	2250		0.6	brown-red clay
	449090	985047	2110		7	
	449301	985534			10	

Annex 9 Soil texture data from thesis work of Abinet Gebremedhin, 2006

No.	X_UTM	Y_UTM	Cobble	Gravel	Sand	Silt	Clay	%Sand	%Silt	%Clay	Soil Texture Class
1	452456	982231			0.6	2	97.4	0.600	2.000	97.400	clay
2	451755	981825			0.4	1	98.6	0.400	1.000	98.600	clay
5	451479	981665			0	2	98	0.000	2.000	98.000	clay
6	451123	981452	0.9	1.5	1.8	3.7	92.1	1.844	3.791	94.365	clay
7	449598	980703	1.5	2.6	3.4	4.3	88.2	1.844	3.791	94.365	clay
8	448339	978932		6	15	25	54	15.957	26.596	57.447	clay
9	446374	978106	18.1	20.1	26.5	38.5		40.769	59.231	0.000	silt loam
10	445316	977812	1.8	2.3	2.3	11.9	81.7	2.398	12.409	85.193	clay
11	442731	977725	2.5	3.3	4	6.6	83.6	4.246	7.006	88.747	clay

Annex 10 Pollutants identified around Sebeta Town (after Deshu Mammo, 2004)

			Chemical Parameters									Bacteriological Parameters	
Station	X_UTM	Y_UTM	DO (mg/l)	COD (mg/l)	BOD (mg/l)	TN	NO3-N	NH3-N	PO4	SO4	S	T. Coli (CFU/ml)	F. Coli (CFU/ml)
S1	459650	986000	16.7	20	2.45	10.5	7.6	0.685	6.1	90	0.1	240000000	40000000
S2	459860	985700	0.39	38100	11064	1000	176.3	614.5	130.7	2093	2.2	29000	1400
S2a	459890	985550	0.46	28825	7266	600	21.4	350	63.6	4413	2.8	17000	5000
S2b	459690	985090	0.42	22962	5361	446	21.7	335	43.6	4060	2.2	1500	300
S3a	459640	984720	0.44	16873	5528	446	70.2	455	52.4	2626	1.1	90000	40000
S3b	459645	984800	0.41	17703	5818	414	62.5	355.2	52.1	3300	3.4	1900	300
S4a	459440	984500	0.43	13340	4414	363	90.2	230	38.6	2673	3.4	40000000	400000
S4b	459448	984600	0.37	13646	4334	433	64.4	185.8	43.1	2200	1.1	300000	2800
S5	459500	984350	2.09	1360	396	136	35	172.9	19.2	356	1.8	1000000	300000
S6	459380	984370	0.38	4703	1485	320	27.3	130.8	18.7	725	1	100000000	30000000
S7	459100	984100	0.22	5830	1871	250	26	140	19.9	1500	1.4	80000000	6000000
S8	458700	984998	0.43	3555	1183	153	0	112.25	21.4	1254	1.5	500000000	16000000
S9	458650	983100	0.39	3711	1186	220	0	128.1	11.9	1258	1.2	90000000	2000000
S10	458250	982840	0.41	4043	1289	163	0	93.83	10.3	1162	0.6	700000000	54000000

			Physical Parameters			Heavy Metals							
Station	X_UTM	Y_UTM	pH	Temp (^{0}C)	TDS (mg/l)	Cr (water)	Cr (sed)	Pb (water)	Pb (sed)	Cd (water)	Cd (water)	Zn (water)	Zn (sed)
S1	459650	986000	7.09	23.1	0			< 0.1				0.2	0.1
S2	459860	985700	5.13	32.7	69019	0.35	0.35	< 0.1	0.15			3.25	
S2a	459890	985550	5.58	25	78000	0.35	0.43	< 0.1	0.75			1.63	
S2b	459690	985090	5.84	22.6	42358	0.3	0.5	0.1	0.7			1.3	
S3a	459640	984720	5.46	23.6	35827	0.3	0.77	0.1				0.93	
S3b	459645	984800	5.99	23.3	36753	0.4	0.45	0.1	1.9			1.55	
S4a	459440	984500	5.48	22.5	32259	0.3	1.6	0.1				0.7	
S4b	459448	984600	5.38	23.2	30938	0.3	0.4	0.1	2.2			1.2	2.1
S5	459500	984350	8.4	21.6	6506	0.65	114.5	0.1	0.5			0.2	5.6
S6	459380	984370	6.98	22.1	11012	0.23	7.5	0.1	1.05				
S7	459100	984100	6.52	20.8	8099	0.3	1.97	0.1	0.7				
S8	458700	984998	8.16	23.8	9407	1.45	10.53	0.1	1.6				
S9	458650	983100	7.58	23	7000	0.2	1.7	0.1	2.8				
S10	458250	982840	8.49	23.3	7667	0.25	0.35	0.1					